Chem Soc Rev

REVIEW ARTICLE

View Article Online
View Journal | View Issue

Cite this: *Chem. Soc. Rev.*, 2021, **50**, 6871

Covalent organic frameworks (COFs) for electrochemical applications

Xiaojia Zhao, [ab] Pradip Pachfule*[b] and Arne Thomas *[b]

Covalent organic frameworks are a class of extended crystalline organic materials that possess unique architectures with high surface areas and tuneable pore sizes. Since the first discovery of the topological frameworks in 2005, COFs have been applied as promising materials in diverse areas such as separation and purification, sensing or catalysis. Considering the need for renewable and clean energy production, many research efforts have recently focused on the application of porous materials for electrochemical energy storage and conversion. In this respect, considerable efforts have been devoted to the design and synthesis of COF-based materials for electrochemical applications, including electrodes and membranes for fuel cells, supercapacitors and batteries. This review article highlights the design principles and strategies for the synthesis of COFs with a special focus on their potential for electrochemical applications. Recently suggested hybrid COF materials or COFs with hierarchical porosity will be discussed, which can alleviate the most challenging drawback of COFs for these applications. Finally, the major challenges and future trends of COF materials in electrochemical applications are outlined.

Received 17th December 2020

DOI: 10.1039/d0cs01569e

rsc.li/chem-soc-rev

[a] *Hebei Normal University, College of Chemistry and Materials Science, Hebei Key Laboratory of Inorganic Nano-materials, 20 South Second Ring East Road, Yuhua District, Shijiazhuang, 050024, Hebei, P. R. China*

[b] *Technische Universität Berlin, Department of Chemistry, Functional Materials, Hardenbergstr. 40, 10623 Berlin, Germany.*
E-mail: pradip.pachfule@campus.tu-berlin.de, arne.thomas@tu-berlin.de

1. Introduction

The crucial environmental problems related to the increased emission of greenhouse gases and pollutants (CO_x, NO_x, SO_x and fine particulates) and the growing global energy demand underpin the broad interest in clean energy technologies

Xiaojia Zhao

Dr Xiaojia Zhao received a bachelor's degree in polymer science from Hebei University of Science and Technology in 2012. Afterwards, he completed an MSc in polymer science and engineering at Beijing University of Chemical Technology. In 2015 he was awarded the China Scholarship Council (CSC) scholarship from the Chinese government to pursue his PhD in the group of Prof. Arne Thomas at Technische Universität Berlin, Germany. Currently, he is an associate professor at the College of Chemistry and Material Science at Hebei Normal University. His research is focused on the design and synthesis of porous materials and their potential applications in (photo)electrocatalysis.

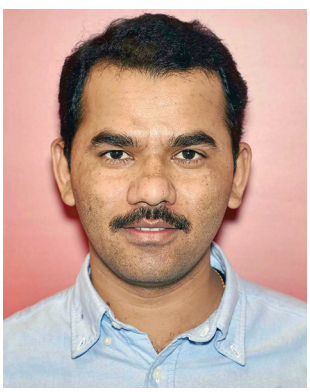

Pradip Pachfule

Dr Pradip Pachfule studied chemistry at Solapur University, India and graduated in 2008. He received his PhD at CSIR-National Chemical Laboratory, Pune, India under the supervision of Prof. Rahul Banerjee in 2014. Later, he worked as a JSPS postdoctoral research fellow in the laboratory of Prof. Qiang Xu at AIST, Kansai, Japan. This was followed by a further two years in the group of Prof. Arne Thomas as an Alexander von Humboldt postdoctoral fellow at the Technische Universität Berlin, Germany. Currently, he is working in the same laboratory of Prof. Thomas as a postdoctoral research fellow. His research is focused on covalent organic frameworks and their potential applications in (photo)catalysis, gas storage/separation and energy applications.

including *e.g.* electrochemical water splitting for hydrogen production, batteries/supercapacitors for clean energy storage and fuel cells for emission-free electricity generation.[1–6] To further advance such devices and processes needed for future sustainable energy production, conversion and storage, the development of novel materials is a key task. Chemical reactions occur on the surfaces of electrodes, while transport in membranes occurs through voids and thus it is obvious that porous and high surface area materials can play an important role in the development of such devices. The properties of porous materials have a close relationship with their performances in different electrochemical applications and these properties can vary with the size, structure and arrangement of the pores, the extent of porosity and composition of the materials themselves.[1,7–9] In particular, porous carbons have been widely investigated as electrode materials in energy conversion and storage devices, as they show high electrical conductivity, can exhibit very large surface areas and porosities to ensure a high number of active sites and sufficient mass transport and are furthermore often cheap and chemically stable.[7,10] However, as these materials are generally prepared by high temperature treatment, *i.e.* pyrolysis, their chemical and nano-/microstructure is hardly predictable and controllable.

Recently a range of novel porous materials has been developed, whose structures can be precisely manipulated and which are therefore interesting for several electrochemical processes,[9,11–17] particularly, metal organic frameworks (MOFs)[18–24] and covalent organic frameworks (COFs).[25–33] Through the modular nature of these materials, their pore structures and functional groups can be tailored independently, thus enabling the introduction of defined active sites onto the large permanent and accessible surfaces to promote or catalyse targeted electrochemical reactions.[34–36] Indeed, MOFs have been widely investigated as potential electrocatalysts in recent years. Chemical stability especially in reactions performed in strongly acidic or basic electrolyte solutions as well as low electrical conductivity are however issues that have to be considered when applying MOFs in electrochemical applications.

Arne Thomas

Prof. Arne Thomas studied chemistry in Giessen, Marburg and Edinburgh and received his PhD from the Max Planck Institute of Colloids and Interfaces (MPI-KGF) in Potsdam, Germany. After a postdoctoral stay at the University of California, Santa Barbara, as an AvH fellow, he rejoined the MPI-KGF as a group leader. In 2009, he became a professor at the Technische Universität Berlin, where he is leading the Department of Functional Materials.

COFs, a subclass of porous polymers, possess rigid backbones, long-range order and permanent porosity. 2D layered or 3D network structures can be constructed, determined by the geometry of the respective building units and the nature of the covalent linkage between them.[14,37–39] For the first time, COFs (COF-1 and COF-5) were reported by Yaghi and co-workers, who applied the topological design principles of MOFs in the synthesis and structural determinations of COFs.[16] As they are entirely built from organic building blocks connected by covalent bonds, many COFs show π-conjugated structures and thus at least a modest electronic conductivity. Indeed, many COFs are organic semiconductors with tuneable band gaps. Furthermore, the exclusive covalent connections can yield COFs with high chemical stability. In fact, while the first COFs reported were not even water stable, ongoing development has provided COFs with stability under harsh acidic and/or basic conditions.[40,41]

Although research efforts on COF applications in electrochemical devices are still in their infancy, these properties together with their large surface area, tuneable pore size, high crystallinity and tailorable architecture have made them promising candidates to promote electrochemical processes (Fig. 1). Several examples for the utilization of COFs in electrochemical applications have been demonstrated recently.[36,42–44] This review aims to discuss the principles of COF materials design and synthesis to introduce tailor-made properties useful for electrochemical applications. Furthermore, the challenges and future perspectives of COFs for clean energy conversion and storage are described. Finally, also the drawbacks of COFs in electrochemical applications will be discussed, for example their relatively small pores, which inhibit mass transport and

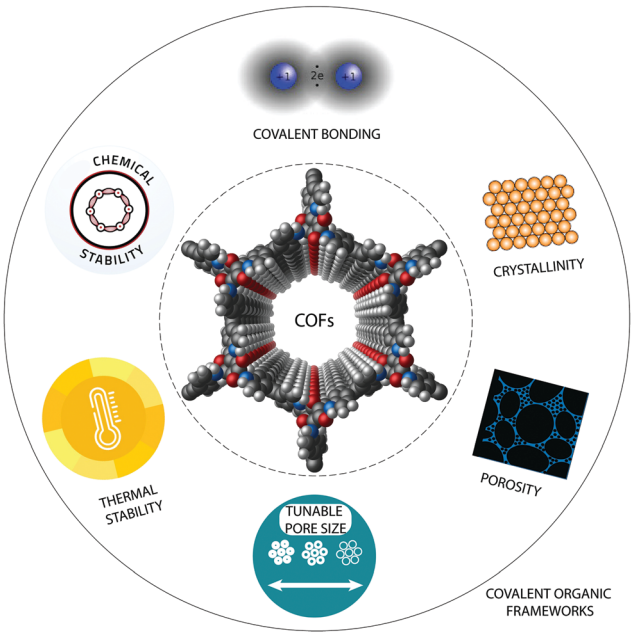

Fig. 1 The most important properties of covalent organic frameworks (COFs), which are decisive for the potential of these materials in electrochemical and other applications.

their relatively low conductivity, which yield low charge carrier mobility. To alleviate these drawbacks, a range of hybrid and/or hierarchical porous COFs has been suggested recently, which therefore receive a certain attention in this article.

2. Design and fabrication of COF-based materials for electrochemical applications

2.1 Requirements of electrode materials for electrochemical applications

Electrochemical reactions play an important role in the development of novel energy conversion and storage strategies. Some of them are electrocatalytic reactions, including the oxygen reduction reaction (ORR) in fuel cells,[45,46] oxygen evolution reaction (OER) in electrolytic water splitting and metal–air batteries,[47,48] hydrogen evolution reaction (HER) in water splitting,[5,49] and CO_2 reduction reaction (CO_2RR) in pollutant conversion.[50,51] Furthermore, challenging electrochemical reactions are found in energy storage devices such as lithium-ion batteries[6,42] and supercapacitors.[52,53] Thus, the design and synthesis of efficient electrode materials to gain suitable electrochemical performances are crucial for practical applications. There are some general requirements for electrode materials including high conductivity to promote electron transfer between electrode surface and electrolyte solution, large surface areas and pore volumes to ensure a high number of accessible catalytic sites and/or efficient mass transport to the electrodes, and high chemical stability to ensure a long lifetime of the device. Nevertheless, the detailed requirements on structure and properties of electrode materials are of course mainly dependent on the respective electrochemical application in focus.

COFs show some intriguing features, which make them interesting materials for electrochemical applications. There is at first the very good structural control. Indeed, by selection of appropriate linkage motifs and building blocks, the design principles of COFs enable the creation of materials with defined chemical structures in the backbone as well as tuneable pore sizes and pore geometries, which both help to modify the chemical and physical properties of the COFs.

COFs with well-defined active sites for electrocatalytic processes and controllable porosities for efficient mass transport have been developed.[54] Typically, nitrogen-containing ligands such as bipyridines and porphyrins could act as coordination sites for metal incorporation within COFs, providing single-atom metal catalysts in electrocatalytic reactions.[36,55] Besides, introduction of redox-active sites into COFs enables enhanced pseudocapacitive performance in supercapacitors as well as the reversable process in rechargeable batteries.[41,56] On the other hand, COF hybrid materials with controllable porosities for efficient mass transport and conducting materials for good electrical conductivity and mechanical stability have been developed to further improve their electrochemical performance.[57]

2.2 Design principles for COF-based materials for electrochemical applications

As the redox reactions in electrocatalysis and charge–discharge processes are accompanied by electrons, reactant/product and ion transport, several strategies to increase the mass transport and promote the electrical conductivity within the materials can be employed. For example, hierarchical porosities ensuring high surface areas but sufficient mass transport can be introduced in COF electrocatalysts.[36] Up to now, various strategies and methodologies have been developed to construct efficient COF-based electrodes (Fig. 2).

2.2.1 Chemical modifications. COFs enable scientists to control the composition and structure of crystalline and porous materials in terms of density and spatial arrangement of chemical functionalities. Depending on the desired application in electrocatalysis and energy storage, the chemical structure and thus number and nature of functional groups and active sites within COFs can be controlled by developing different approaches. Mostly, functional monomers, *e.g.* bearing redox-active or metal coordinating groups are directly applied in COF synthesis. If this is not directly possible, backbone modification and post-synthetic modifications are further pathways to tailor the chemical structure and functionality of COFs, which are described in more detail in the following (Fig. 3).

a. Backbone modification. The intrinsic electrocatalytic activity of COFs is related to the presence of functional groups or moieties within the backbone, which are generally introduced through appropriate monomers, called linkers. These linkers bear certain groups allowing them to form robust covalent linkages with other linkers to finally form the COFs. Functional moieties can be either present already in the linker molecules or they are formed during the COF-forming reaction. For the latter, especially triazines,[58] and imines[59] have been shown to be suitable for electrochemical reactions. These linkages thus introduce heteroatoms in an otherwise solely sp^2-carbon conjugated backbone structure, which can serve as binding sites for metals, basic sites or redox-active sites (Fig. 3a).

In addition to the aforementioned *de novo* synthesis strategies, the COF backbones can be further modified by post-synthetic modification, for example, by chemical reactions on the linkers or even entire building block exchange for framework-to-framework transformations.[60–62]

b. Functional group modifications. Constructing functional COFs with redox-active groups is of utmost significance, particularly for supercapacitor, Li-ion battery and proton conductivity applications.[63–65] However, because of the incompatibility with the building blocks or reaction conditions, it is difficult to directly incorporate such functional groups into COFs *via* the typical solvothermal and mechanochemical synthetic approaches. In this regard, introduction of functional moieties into COF skeletons through chemical transformation with the preservation of their topological structures enable the possibility of tuning the functional properties of COFs (Fig. 3b).[66–69]

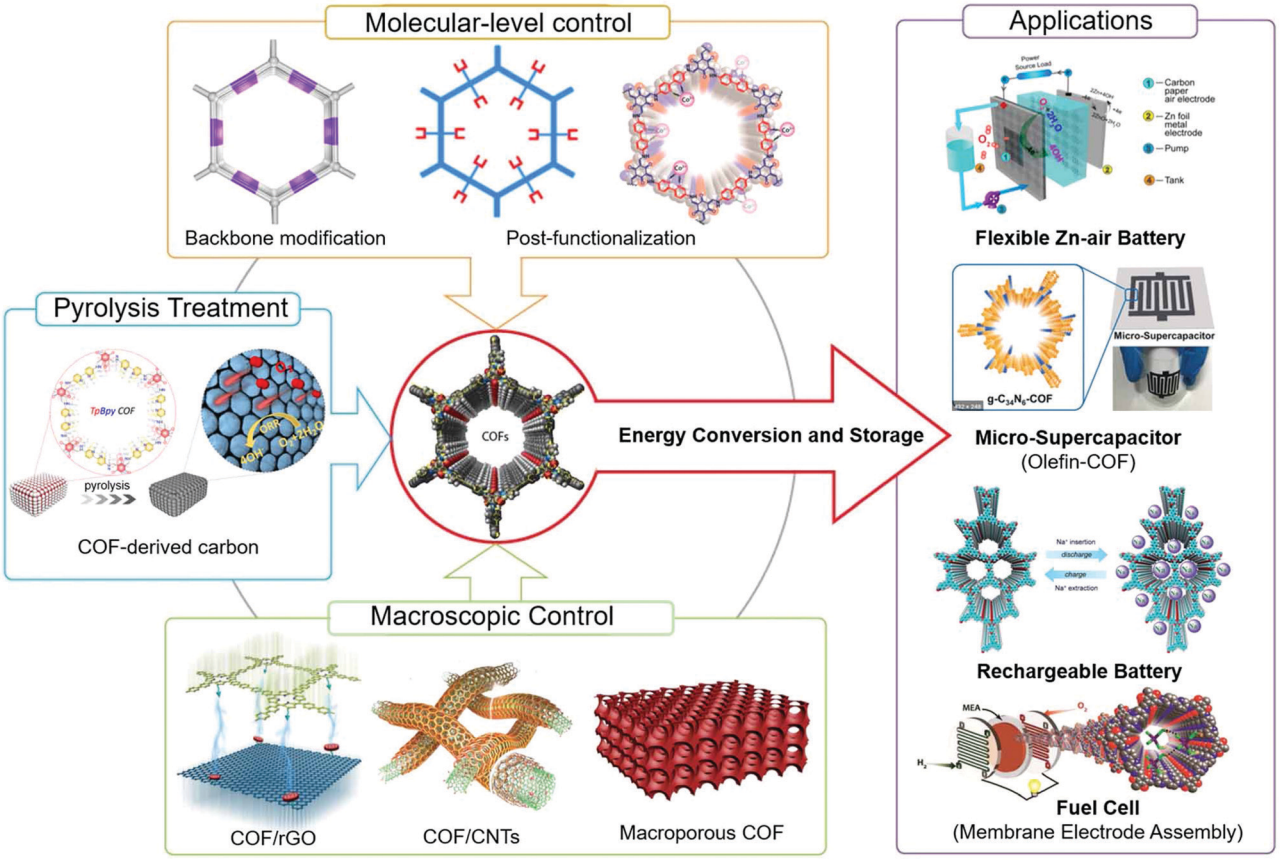

Fig. 2 Strategies for the design and fabrication of COF-based materials for energy conversion/storage applications.

By applying functional group modifications, it has been demonstrated that functional groups or moieties that cannot be incorporated using direct synthesis can be introduced into COF backbones.[70]

c. Post-synthetic metalation. Post-synthetic modification can also be applied to introduce metal atoms into COFs.[71] Heteroatoms in COF linkages, or functional groups attached to the linkers can be valuable to coordinate and bind metals introduced into the pore system. This can be extended to bind the metals to chelating moieties within the backbone. The presence of periodic and uniform porosity within COFs ensures that the adsorption sites for metals are fully accessible to metals added to the COFs. By applying this strategy, metal–organic complexes, probably already known for homogeneous catalytic reactions, can be immobilized as they act as maintaining part of the COF backbone (Fig. 3c).[36,43,72] In the meantime, this concept has been exploited many times, especially applying common nitrogen-containing ligands such as bipyridines,[36,55,73] or macrocyclic structures (*e.g.* porphyrin).[43,74–76] Incorporating metals within COFs *via* controlled bonding also provides a new approach to use single-atom metal catalysts with homogeneous dispersion in electrocatalytic reactions. Besides, the large surface areas and pore sizes in the small nanometre regime also allows the incorporation of small metal nanoparticles, which can also introduce new functionalities into COFs.

2.2.2 Controlling COF structures on all length scales. As mentioned, an intriguing advantage of COFs in electrochemical applications is that their chemical structure and nanostructure is, at least in principle, entirely known and can be tuned with high precision. However, regarding the microstructure, there are several further issues that have to be addressed. COFs are mostly observed in the form of bulk powders, which cannot be dissolved or melted, and thus can hardly be processed into bulk electrodes or films. Furthermore, reported charge carrier mobility in COFs is still very low, when compared to that of inorganic (semi)conductors and certainly does not get better when COFs are obtained as microcrystalline powders, as mentioned before. Finally, COFs possess mainly pores in the micropore or small mesopore regime, which impede mass transport through the material and thus the accessibility to the actually available abundant active sites on these large surface areas. In this regard, the design of COFs should not only focus on microscopic length scales (*i.e.* from angstrom to nanometres), but also include the engineering of COF materials on a macroscopic level *i.e.* from several nanometres to centimetres (Table 1). The challenge is to combine the chemical and crystalline structures of COFs with the possibility to design larger architectures with uniform sizes,

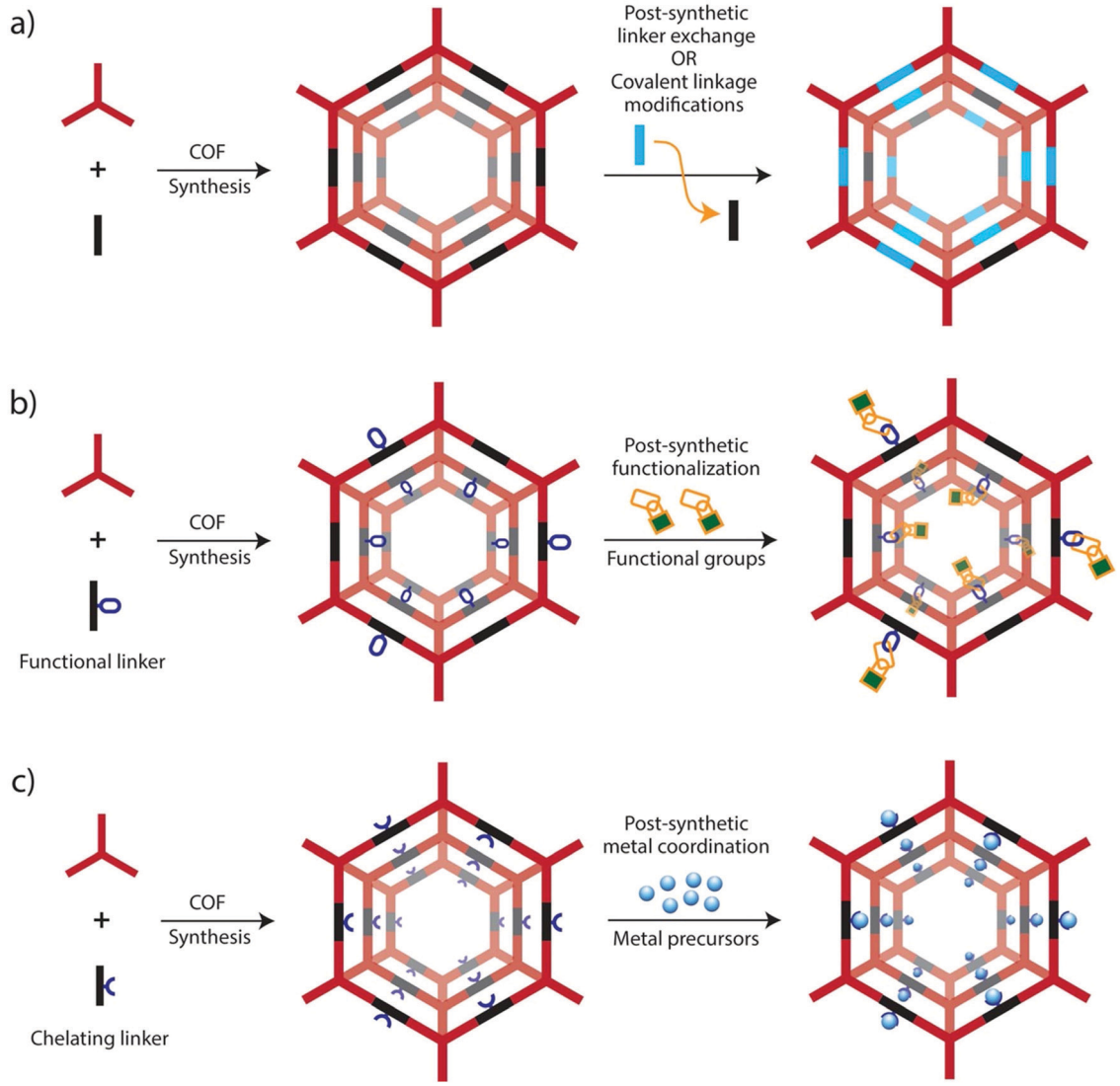

Fig. 3 Strategies for the preparation of functional COFs *via* post-synthetic modification (PSM) for their applications in electrocatalysis and energy conversion and storage.

well-defined morphologies and/or hybrid components to further enhance the properties of COFs. As an example, combining small and large pores, *i.e.* introducing hierarchical porosity into materials, can enhance ion and mass transfer, which will consequently improve the electrochemical performance, but will also be useful for other applications of COFs. Indeed, within recent years researchers have developed different strategies to control COF structures and morphologies at least on some length scales (Fig. 4).

a. Thin films and membranes. Beside the growth of COF films on typical electrode materials to achieve suitable electron transport and morphological control, growing of COF films can be important to construct other important compounds in electrochemical devices, namely the membranes, which separate the electrodes. Most prominent are probably the proton exchange membranes that are applied to separate the hydrogen and oxygen gases as an electronic insulator and a reactant barrier in fuel cells (Fig. 4a).[77,78] It has been demonstrated that COFs with well-defined pore structures could provide suitable space to accommodate proton carriers. Moreover, the versatile organic linkers for COF synthesis enable the anchoring of strong acid groups (*e.g.* sulfonic acid group) on the COF backbone to further improve the proton conductivity.[79]

To synthesize COF-based membranes, COFs were initially blended with polymers to create mixed matrix membranes.[80,81] With advanced COF synthesis methods, strategies such as *in situ* growth,[82] layer-by-layer stacking,[83] and interfacial polymerization[84] have been developed to construct even free-standing COF-based membranes. These membranes show promising applications in proton exchange in fuel cells as well as a huge potential in membrane technology for electrocatalysis.

b. Hierarchical porosities. The sole presence of micropores or small mesopores in COFs can lead to diffusion, *i.e.* mass transport limitations, which is problematic for many applications

Table 1 Selected properties of covalent organic frameworks for electrochemical applications. Early reports, controlling macroscopic level and most notable performances

Property	COF/hybrid	Year of report or achieved value	Ref.
Early report			
OER	$(CoP)_n$-MWCNTs	2015	120
ORR	Pt–CTF/CP	2014	121
HER	SB-PoRPy–COF	2017	101
CO_2RR	COF-366-Co	2015	43
Supercapacitor	DAAD-TFP-COF	2013	63
Battery	CTF-1/S@155 °C	2014	122
Fuel cell	TPB–DMTP-COF	2016	65
Controlling macroscopic level			
Terracotta process	TpOMe–DAQ-COF	Supercapacitor with specific capacitance (1600 mF cm^{-3} at 3.3 mA cm^{-2})	41
Film	DqTp	Supercapacitor with specific capacitance (154 F g^{-1} at 1.56 mA cm^{-2})	123
Macroporosity	Macro-COF	OER: overpotential of 380 mV at 10 mA cm^{-2}	36
Hollow sphere (D = 500–700 nm)	3D-Sp-COF	Supercapacitor with specific capacitance (251 F g^{-1} at 0.5 A g^{-1})	124
Hybrid composite	COF/rGO	Supercapacitor with specific capacitance (269 F g^{-1} at 0.5 A g^{-1})	57
Notable performance			
ORR	COF_{BTC} (0.1 M KOH)	E_0 = 0.965 V $E_{1/2}$ = 0.9 V	125
	PA@TAPT–DHTA–COF_{1000NH_3} (0.1 M KOH)	E_0 = 0.941 V $E_{1/2}$ = 0.83 V	112
OER	Co-TpBpy	Overpotential of ~520 mV at 10 mA cm^{-2} (phosphate buffer pH 7.0)	55
	Macro-TpBpy-Co	Overpotential of ~380 mV at 10 mA cm^{-2} (0.1 M KOH)	36
	Co-PDY/CF	Overpotential of ~270 mV at 10 mA cm^{-2} (1.0 M KOH)	126
HER	SB-PORPy COF	Overpotential of ~380 mV at 5 mA cm^{-2} (0.5 M H_2SO_4)	101
	CTF@MoS_2 composite	Overpotential of ~93 mV at 10 mA cm^{-2} (0.5 M H_2SO_4)	127
CO_2RR	COF-366-Co	Faradaic efficiency (FE_{CO}) of ~90% at −0.67 V	43
	COF-300-AR	Faradaic efficiency (FE_{CO}) of ~80% at −0.85 V	128
Supercapacitor	PEDOT/DAAQ–TFP	Specific capacitance (350 mF cm^{-3})	96
	TpOMe–DAQ-COF film	Specific capacitance (1600 mF cm^{-3} at 3.3 mA cm^{-2})	41
	COF/rGO	Specific capacitance (269 F g^{-1} at 0.5 A g^{-1})	57
Battery	COF-1/S	Cycling performance (DC/RC/DR/CN) 1628/770/0.5/200	129
	HCPT@COF/S	Cycling performance (DC/RC/DR/CN) 1224/1053/0.2/300	130
	PEDOT@DAPH-TFP	Cycling performance (DC/RC/DR/CN) 99.2/93.2/0.5/500	131
	Anionic COF (CD-COF)	Li-Ion conductivity of ~2.7 mS cm^{-1}	132
Proton conductivity	im@TPB–DMTP-COF	1.79 × 10^{-3} S cm^{-1} (373 K)	65

Note: DC (discharge capacity, mA h g^{-1}), RC (reversible capacity, mA h g^{-1}), DR (discharge rate, C), and CN (cycle number).

and also for chemical reactions on electrodes. It has been demonstrated that introduction of larger pores (*i.e.* meso- and macropores) can provide unhindered mass transport to and from the electrode surface.[85,86] Such a secondary porosity can be useful as the micropores in crystalline COFs already offer large surface areas to enable fast surface reactions. Currently, several synthetic strategies to generate hierarchical porosities (two or more defined pore sizes in one material) in COFs have been explored (Fig. 4b), including the preparation of hollow micro- and meso-tubular porous COFs,[87,88] hollow spherical COFs,[89] and macro/microporous COFs.[36] Such hierarchical porous systems, showing large surface areas, good mass transport and distribution of active sites, should facilitate applications in electrocatalysis, supercapacitors, batteries, *etc.*[90]

c. Hybrid nanostructures. For electrochemical applications, the low electric conductivity of COFs is one of the major drawbacks. Considering the presence of active sites in the COF backbone, a certain charge-transport pathway within the COF matrix is necessary for good electrocatalytic activities. Generally, the intrinsic bulk conductivity of COFs can be leveraged by through-bond and through-space charge transport characteristics by applying proper building units and synthetic routes such as full annulation of building blocks through aromatic linkages and maximizing orbital overlap through a strategic choice of building blocks.[91–94] Nonetheless, the electrical conductivities of COFs are still inferior to those of other typical electrode materials. Intriguingly, formation of COF hybrid materials promise to not only yield morphology control but also to circumvent the conductivity problem, especially when conducting materials such as carbon nanotubes (CNTs), graphene and conductive polymers are applied as a second compound in the composite (Fig. 4c).[74,95,96] To ensure close contact between COFs and these conducting materials, direct growth of COFs on the substrate as crystalline thin films seems to be the way to go for achieving good electric conductivity and mechanical stability.

d. Terracotta process. Considering the polycrystalline nature of COFs, the processing of COF powders into desired geometrical shapes without using any binder or plasticizer is very difficult. To process the COFs into definite shapes and induce the hierarchical

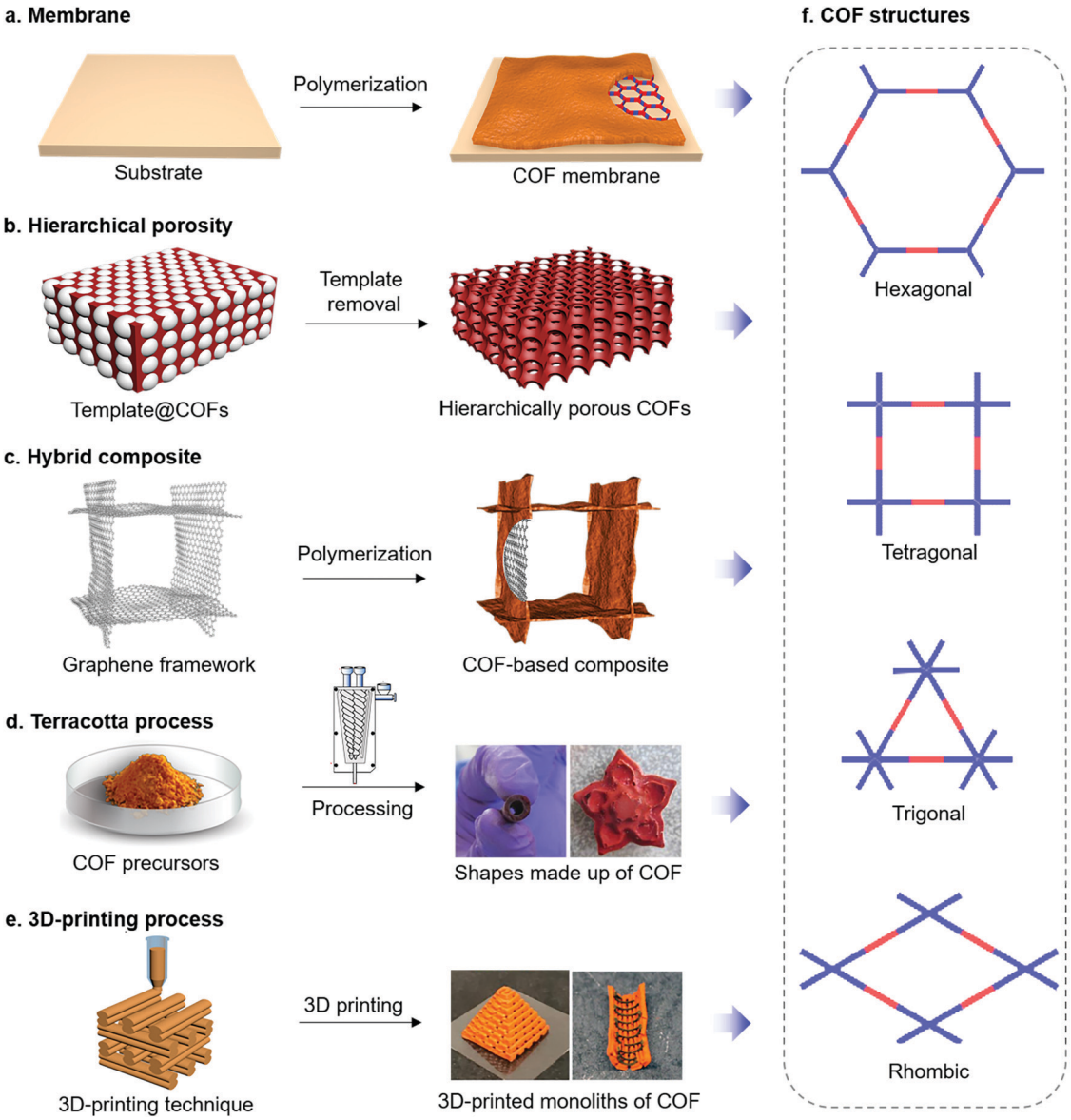

Fig. 4 (a–e) Strategies for the synthesis of COFs through macroscopically controlled engineering. (f) Types of topologically distinct COF structures. Reproduced from ref. 97 (4d) and ref. 99 (4e) with permission from American Chemical Society, copyright 2017 and copyright 2019.

porosity in the COF matrix, recently, a so-called Terracotta process has been employed.[97] In this method, grinding of diamine linkers together with *p*-toluenesulfonic acid (PTSA), water and multitopic aldehydes, followed by heating for a few minutes yielded β-ketoenamine COFs in large quantities and with enhanced porosity. As the reagent mixture holds the consistent properties as dough, it is possible to process COFs into various shapes without any additives and binders, thus achieving the construction of different COF sculptures (Fig. 4d). By introducing the use of baking soda during the terracotta process for COF synthesis, even hierarchical porosity with an interconnected pore network has been incorporated in the COF matrix.[98]

e. 3D-printing. To form COF-based macroarchitectures as well as to introduce the macro- and mesoporosity, 3D-printing methods are another possibility (Fig. 4e). In one example, imine-based polymers were initially co-assembled with Pluronic F127 in an aqueous solution.[99] By limiting the degree of imine polycondensation, the co-assembled amorphous imine polymer and F127 were used as hydrogels for 3D-printing. Subsequent removal of F127 followed by an amorphous-to-crystalline transformation resulted in the formation of 3D COF monoliths possessing hierarchical porosities and robust mechanical stability. Similarly, graphene oxide (GO) was chosen as a foaming agent, successfully engineering the crystalline COF foams into 3D-printed geometrical forms, for efficient mass transport and adsorption.[100]

2.2.3 Construction of COF-based electrodes. To achieve high electrochemical performance, it is critical to construct efficient and durable COF-based electrodes. Since COFs are mostly prepared as the bulk powders that cannot be dissolved

or melted, generally, COF powders are physically dispersed in ethanol solution with additives acting as a binder (*e.g.* Nafion) and conductor (*e.g.* activated carbons), to form a homogeneous mixed solution.[36,101] Then the resulting "ink" can be dropped or spin-coated on different substrates such as a rotating disk electrode (RDE), carbon cloth and nickel foam to form the working electrodes for further applications.[44] Even though this method enables the construction of COF electrodes, it entails some inherent problems that have to be considered. Thus, partial aggregation or embedding of COF particles, weak interactions between the COF and the substrates or pore blockage by additives can reduce the accessibility of active sites within COFs for substrates or charge carriers. COF electrodes produced in this way are usually compared to bare carbon or other reference electrodes and, when published, logically exhibit an enhanced performance, which is related to the COF material. However, due to the above-mentioned points this kind of electrode manufacturing does not guarantee that the potential of the COF is indeed fully exploited.

In situ growth of COF materials on substrates can in contrast yield a uniform distribution of COF films on conductive substrates without any additives, ensuring close contact between COFs and conducting materials. The substrates can be commercial current collectors such as nickel foams, carbon cloths, FTO, ITO, *etc.*[102,103] or other conductive substrates such as graphene aerogels.[57] It can be supposed that such *in situ* grown COF electrodes not only display better mechanical stability and durability than traditional ones prepared by deposition of COF inks, but also exhibit more open and regular pore structures, providing sufficient active sites for electrochemical applications. Furthermore, strategies controlling the COF morphologies at a macroscopic level enable the construction of COFs as self-standing electrodes. For example, COF membranes have been suggested as flexible electrodes in wearable electronic devices.[77] On the other hand, considering the low conductivity of self-standing COF electrodes, the conducting materials (*e.g.* graphene, CNTs)[100] can be mixed and processed *via* 3D printing and Terracotta processes for constructing COF architectures with desirable shapes, sizes and conductivities.

2.2.4 Pyrolysis of COFs to carbon materials. Beside metals, carbonaceous materials are the most used materials in energy conversion and storage because of their large surface area and pore volume, high electrical conductivity and good chemical stability.[7,8,104–107] A plethora of organic precursors have been applied to synthesize carbonaceous electrode materials. As they are able to create high surface areas or introduce heteroatoms into the carbon materials, such precursors should obviously be (extremely) cheap, easily available and abundant for applications in real-life, *i.e.*, large-scale devices. COFs are hardly fulfilling these latter requirements and seem therefore not to be ideal precursors for carbon materials. Nevertheless, crystalline porous materials have received increasing interest recently as carbon precursors, mainly because it was claimed that their crystalline structure with organized carbon sheets or atoms and metal species in well-defined frameworks could be a promising platform to guide the carbonization process.[108–111]

In this respect, COFs as two dimensional carbon-rich materials with abundant heteroatoms might be used as precursors for heteroatom-doped carbons.[110,112–115] Furthermore, COFs with implemented coordination sites (*e.g.* bipyridine and porphyrin structures) for metal ions allow the construction of metal incorporated/heteroatom-doped carbons. The periodical feature of COFs with distributed and separated metal coordination sites is a possible pathway to create single atom catalysts in the final carbon materials.

As the structure of COFs usually collapses when carbonized, which seriously questions the often made statement, that the crystalline structure acts as a scaffold for the carbon materials, templates are normally required for the generation of porous carbonaceous materials from COFs.[110,116] Indeed, the question can be asked, why should the advantages of a highly ordered material with precise chemical structure be sacrificed to form materials with rather ill-defined structures and unknown active sites, especially if related carbonaceous materials can be prepared from much cheaper precursors. However, it has been shown a number of times that carbon materials prepared from COFs show superior performances compared to carbons prepared from the respective monomers.[110] Thus, it seems that the periodic structure of COFs indeed brings benefits as a carbon precursor. In this review, carbon materials from COFs will just be discussed if such a beneficial effect of the defined COF structure on the later carbon materials has been proven.

3. Applications of COF-based materials

As mentioned in the introduction section, COFs exhibit unique properties including large surface areas, ultrahigh porosity, tuneable pore sizes, a relatively high chemical/thermal stability combined with a tailorable architecture. Because of these appealing properties, in recent years, vast research has been witnessed on COF-based materials for various applications, with an increasing interest in their utilization for electrocatalysis as well as electrochemical energy storage.[117–119] Early reports of COF materials for electrochemical applications as well as some notable performances of later reported COFs in the different electrochemical applications discussed in this review are summarized in Table 1. This review intends to timely summarize the recent progress in this field and to act as an inspiration for further development and utilization of COF materials in electrochemical applications.

3.1 Energy conversion and electrocatalysis

The transformation of energy from one form (chemical energy, heat, electricity, light, motion, *etc.*) to another is called energy conversion. In history, many devices and systems have been developed to achieve energy conversion. Very early examples of energy conversion systems are applied in windmills, where the kinetic energy of the wind was transformed into mechanical energy for pumping water or grinding grains. Nowadays, windmills are widely disseminated to convert wind

into electrical energy, which is the most needed form of energy for our communities.

Indeed, wind and sun energy are the most sustainable sources of energy and consequently their contribution to the energy mix is rising constantly, while resources like fossil or nuclear fuels are slowly but steadily depleting. However, in direct energy conversion devices, such as the named windmills or solar cells, the electrical energy produced must be stored so that it can be used independently from peak wind and sun hours. Electricity can be stored in electrical devices such as batteries or supercapacitors, but can also be converted into chemical energy, for example in an electrolyser, by using the electrical energy to split water into hydrogen and oxygen as storable chemical fuels. When needed, these fuels can be converted back into electrical energy using fuel cells. For all these devices and the processes occurring therein the breaking and formation of chemical bonds take place, which can be achieved by choosing the right electrode materials and electrocatalysts.

Herein, the applications of COFs as electrocatalysts and/or electrode materials in energy-conversion technologies are summarized, highlighting the advantages, limitations and current status of these materials for such applications.

3.1.1 Hydrogen evolution reaction (HER). As one of the most promising renewable energy sources, hydrogen possesses the highest gravimetric energy density compared to other fuels and produces only water as a by-product when used in fuel cells.[3] Currently, the world's leading automotive manufactures are engaged in the development of fuel cell vehicles (FCVs) for a sustainable future mobility. It can be expected that the demand for hydrogen will increase sharply, if such hydrogen-powered vehicles enter the market to a large extent. To enable large-scale H_2 production in an environmentally-friendly way, water splitting has become an efficient process as the existing methods (*e.g.* steam reforming) used for hydrogen production are also produce large amounts of carbon dioxide as byproduct.

Water splitting is composed of two half reactions, namely the hydrogen evolution and oxygen evolution reactions, which in many cases are investigated and optimized separately. In principal, a thermodynamic voltage of 1.23 V (25 °C) is required to split water into hydrogen and oxygen. However, due to the existing resistances (*e.g.* solution and contact resistances) and the intrinsic activation barriers present on electrodes, a much higher voltage than the thermodynamic potential is generally required. The excess potential needed is known as the overpotential. The reduction of this overpotential by applying efficient and stable catalysts is the central issue to achieving effective water splitting. Apart from the overpotential, the indicators to appraise the performance of a given HER electrocatalyst can be readily described by current density, Tafel slope, stability and faradaic efficiency. (i) The current density is defined to determine the electrocatalytic activity of a catalyst. Currents are measured at different applied voltages and normalized to the sample mass (mA mg^{-1}) or geometric electrode area (mA cm^{-2}). In general, the specific overpotential at a current density of 10 mA cm^{-2} (which is the current density expected for a 12.3% efficient solar water-splitting device) in HER is deliberately provided to compare the activities between the electrocatalysts. (ii) The Tafel plot depicts the relationship between current density (j) and overpotential (η), and the Tafel equation ($\eta = b\log(j) + a$) is deduced to describe the linear portion of the Tafel plot where the linear slope b is defined as the Tafel slope and the values of b indicate the different catalytic mechanisms for the electrode reaction (Table 2). (iii) Stability testing is conducted to evaluate the practical applicability of a HER catalyst. Two methods are used to characterize the electrocatalytic stability, namely chronoamperometry and chronopotentiometry. (iv) Faradaic efficiency is calculated from the ratio of the experimental hydrogen production to the theoretical hydrogen production,[5] describing the charge efficiency by which electrons are utilized to form hydrogen.

The H_2 evolution process is a multistep reaction on the catalyst surface involving adsorption, reduction and desorption processes of protons/water, dihydrogen and the formed intermediates. As shown in Table 2, the mechanism of HER includes three steps in both acidic and alkaline solutions. The "Volmer step" indicates the hydrogen adsorption on the catalyst surface (H*, where * is defined as an active site on the catalyst surface) during the reduction of protons. Molecular hydrogen is then formed through the combination of H* *via* either a Heyrovsky or Tafel step. DFT calculations show that the free energy of hydrogen adsorption (ΔG_{H^*}) could be a suitable descriptor for the reaction kinetics of HER, where a nearly zero ΔG_{H^*} indicates an optimal HER catalyst. Based on theoretical and experimental studies, the most efficient electrocatalysts for HER are platinum-based materials. Nevertheless, the price and scarcity of platinum hinders its widespread and practical use. Thus, it is quite desirable to develop efficient and affordable HER electrocatalysts composed of earth-abundant elements to achieve cost-efficient hydrogen production.[133–135] For example, transition metal dichalcogenides,[136–138] carbon-based materials,[139,140] single metal atom-doped materials[141–143] and polymeric materials[144,145] have been widely studied and applied as candidates for H_2 production. In this section, recent progress in the design of COF-based HER electrocatalysts is described.

Table 2 HER mechanisms under acidic and alkaline conditions

	Acid	Alkaline	Tafel slope
Volmer	$* + H^+ + e^- \rightarrow H^*$	$* + H_2O + e^- \rightarrow H^* + OH^-$	$b \approx 120$ mV dec^{-1}
Heyrovsky	$H^+ + e^- + H^* \rightarrow H_2 + *$	$H_2O + e^- + H^* \rightarrow H_2 + OH^- + *$	$b \approx 40$ mV dec^{-1}
Tafel	$2H^* \rightarrow H_2 + 2*$	$2H^* \rightarrow H_2 + 2*$	$b \approx 30$ mV dec^{-1}
Overall	$2H^+ + 2e^- \rightarrow H_2$	$2H_2O + 2e^- \rightarrow H_2 + 2OH^-$	

where * is defined as an active site on the catalyst surface.

As discussed above, COFs provide several opportunities to design new HER catalysts. However, the intrinsic properties of polymeric materials, *i.e.* the low conductivity and the moderate stability of COFs in the electrocatalysis process, must also be considered. Starting with an important contribution from Pradhan and co-workers, a crystalline 2D COF (SB-PORPy) was exploited for hydrogen production. The COF was formed through Schiff based condensation between 5,10,15,20-tetrakis-(4-aminophenyl)porphyrin (TAP) and 1,3,6,8-tetrakis(4-formylphenyl)pyrene (TFFPy) (Fig. 5a and b).[101] The synthesized COF with a surface area of 869 m^2 g^{-1} (Fig. 5c) was mechanically ground with carbon black in a 1 : 1 weight ratio. When investigated as a HER electrocatalyst in 0.5 M H_2SO_4 aqueous solution, the SB-PORPy COF exhibits a lower onset potential of 50 mV compared to that of Vulcan and bare glassy carbon, demonstrating its electrocatalytic activity for HER (Fig. 5d). As no metals were added or involved during synthesis, it was speculated that the imine nitrogens (–N=) were protonated as free docking sites for HER, forming hyperporphyrinic structures with positive charge. On the other hand, by taking advantage of the conducting channels derived from the π electronic conjugation between pyrene and porphyrin, the H–H combination could occur with the help of other adjacent imine nitrogen sites, which indicates a Volmer–Heyrovsky mechanism on the SB-PORPy COF surface for the HER. As the first of its kind, this work demonstrated the potential application of COFs for hydrogen production, even though carbon black was applied as a conductive additive to promote the conductivity of the system.

Inspired by the catalytic activities of porphyrin and metalloporphyrins in biological systems and chemical catalysis,[146,147] similarly, Bhaumik's group reported a metal-free porphyrin-based microporous organic polymer (TpPAM) as a HER electrocatalyst for hydrogen production.[144] Even though the as-synthesized covalent organic polymer was found to be amorphous, its HER performance underlined the potential applications of porphyrin-based polymers for HER catalysis, with a low overpotential (250 mV at 10 mA cm^{-2}) and a small Tafel slope (106 mV dev^{-1}). However, based on DFT calculations, the authors concluded that the origin of HER activity of TpPAM was derived from the porphyrin cores, which is contradictory to the above explanation. Thus there is certainly an interest to create more COF-based electrocatalysts with varying molecular architectures to clarify the HER mechanism of such metal-free systems.

Furthermore, metal atoms have been incorporated into porphyrin-based networks to promote the performance for HER. For example, a cobalt porphyrin-based COF was reported by Villagrán and co-workers for electrocatalytic hydrogen generation in strong acidic media.[148] The crystalline polymer exhibits a large surface area and its catalytic HER performance (deposited on FTO glass slides by using silver glue) can be ascribed to the existence of porous channels and exposed active sites derived from metalloporphyrins. In addition, the enhanced HER performance in comparison to the cobalt porphyrin monomer gives

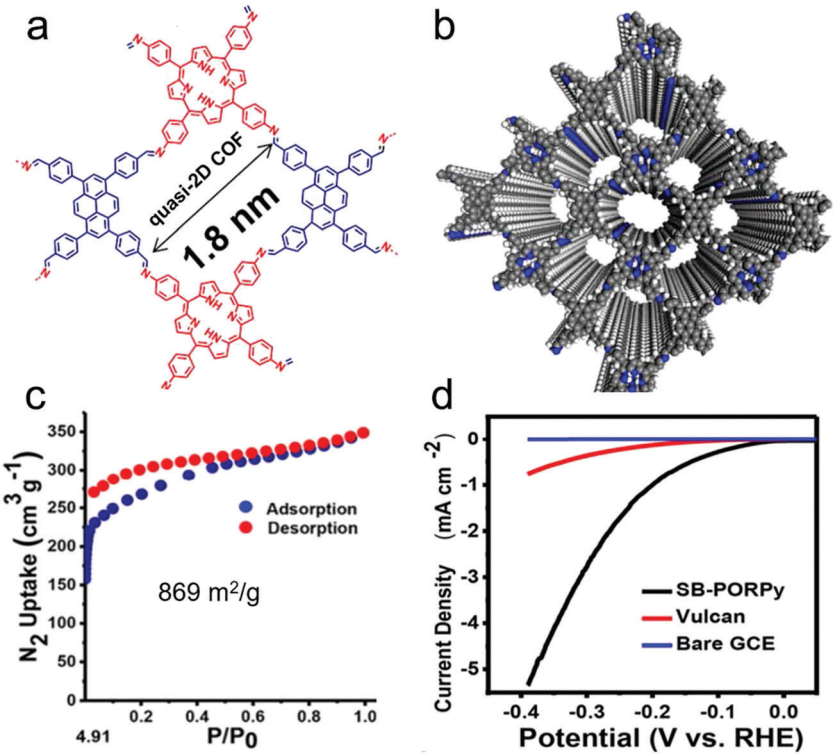

Fig. 5 (a) Topological structure of SB-PORPy COF; (b) simulated structure of SB-PORPy COF; (c) N_2 sorption isotherm at 77 K of SB-PORPy COF; (d) linear sweep voltammetry (LSV) profile of the SB-PORPy COF electrode compared to those of the bare glassy carbon electrode (GCE) and Vulcan. Reproduced from ref. 101 with permission from the American Chemical Society, copyright 2017.

strong evidence that the construction of an extended conjugated system can promote the electrocatalytic efficiency and confirms the role of crystallinity and well-ordered channels present in COFs for enhancing the HER performance.

Furthermore, COFs can be used as support to immobilize and stabilize small nanoparticles with HER catalytic activity.[127,149] Covalent triazine frameworks (CTFs) are a chemically stable class of COFs synthesized using triazine (C_3N_3) units as cross-linkers.[58,127,150–152] Hu and co-workers reported a CTF@MoS_2 composite by *in situ* growing MoS_2 nanoparticles into the 1D channel arrays of CTFs (Fig. 6a).[127] The influence of the amount of MoS_2 was studied, and it was demonstrated that the CTF@MoS_2-5 (where 5 represents the mass ratio of CTFs : MoS_2) exhibited catalytic kinetics with an overpotential of 93 mV at 10 mA cm^{-2}, which is close to that of the benchmark catalyst (20% Pt/C) and lower than those of the pure CTFs or MoS_2 and CTFs@MoS_2-*X* with different mass ratios (Fig. 6b). It was suggested that the crystalline 1D channel arrays formed by the stacking of 2D in-plane porous layers could promote the electron transmission, mass diffusion as well as the accessibility of MoS_2 active sites in the H_2 evolution process (Fig. 6c). While these are promising examples for COF-based, non-noble metal or even metal-free HER catalysts, the so far presented electrocatalytic performances are still lower than those for Pt-based systems but also for many other non-noble metal HER catalysts. So far, the poor conductivity of COFs and their lower stability, especially under a strong electrolyte environment seem to be the major bottlenecks to achieving practical application for large-scale H_2 production. Future work should therefore also concentrate on the development of COFs with enhanced stability and new approaches to ensure an intimate contact with conducting supports to promote the HER performance of COF-based electrocatalysts.

3.1.2 Oxygen evolution reaction (OER). The other half reaction in water splitting, the OER, involves a $4e^-$ transfer step and suffers from sluggish kinetics and a high overpotential, thus is actually considered as the main bottleneck of overall water splitting and consequently sustainable hydrogen production. The proposed mechanisms of OER include several intermediate species (OH*, OOH* and O*) that are produced in the process of OER and subsequently react to give O_2 (Table 3).[153] Their binding energies exhibit a strong correlation, and thus form a scaling relation between OOH* and OH*. As a result, in OER more critical steps have to be considered than in HER either in acidic or alkaline solution, involving the breaking of O–H bonds and the subsequent formation of O=O double bonds.

Similar to HER, indicators such as overpotential, Tafel slope, faradaic efficiency and stability are normally applied for elucidating the electrocatalytic performance of a given OER catalyst, which are also important to gain insight into the OER mechanism.[47] For example, the overpotential at a catalytic current density of 10 mA cm^{-2} is commonly compared to judge the performance of different electrocatalysts. As for HER, the Tafel slope is another crucial indicator for an OER catalyst in characterizing the relationship between current density and overpotential. Typically, a smaller Tafel slope is expected to imply good electrocatalytic kinetics of an OER catalyst, which means that the current density can increase faster with a smaller change in overpotential. As OER is operated at a high applied voltage (*V*), the chemical stability is another important factor to evaluate the degradation of OER catalysts. Descriptors such as the chemical composition, crystallinity, micro- and macro-scale morphology and of course electrochemical performance over time are usually considered to evaluate the stability of electrocatalysts. Currently, noble metal oxides

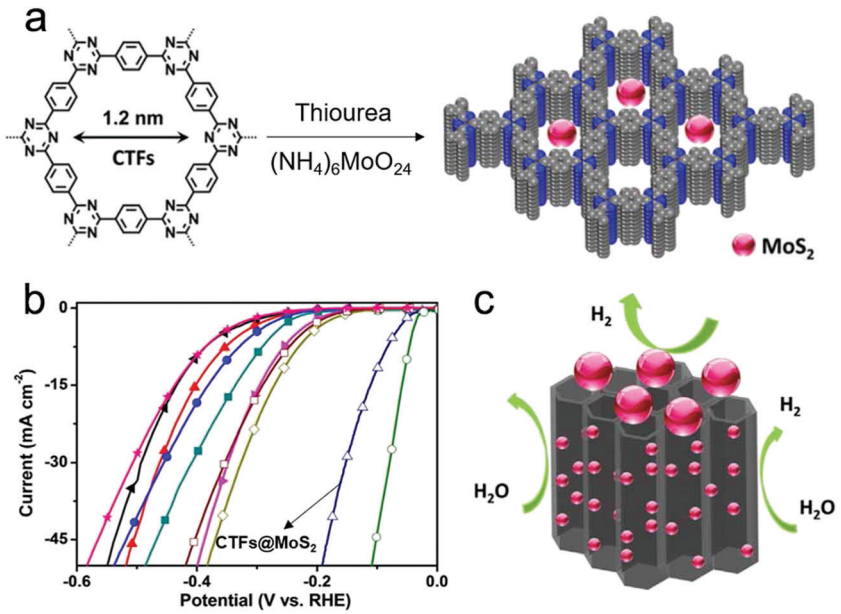

Fig. 6 (a) The formation process of CTF@MoS_2; (b) polarization curve of CTF@MoS_2 for HER catalysis in 0.5 M H_2SO_4, compared to those of other materials such as Pt/C (green), pure CTFs (black), MoS_2 (rose red) and CTF@MoS_2-*X* with different mass ratios; (c) schematic structure of crystal 1D channel arrays derived from 2D in-plane porous layer stacking. Reproduced from ref. 127 with permission from John Wiley and Sons, copyright 2019.

Table 3 OER mechanisms in acid and alkaline conditions

	In acidic solution	In alkaline solution
Anode reaction	$2H_2O \rightarrow O_2 + 4H^+ + 4e^-$	$4OH^- \rightarrow 2O_2 + 2H_2O + 4e^-$
Mechanisms	$* + H_2O \rightarrow OH^* + H^+ + e^-$ $OH^* \rightarrow O^* + H^+ + e^-$ $2O^* \rightarrow 2^* + O_2$ $O^* + H_2O \rightarrow OOH^* + H^+ + e^-$ $OOH^* \rightarrow * + O_2 + H^+ + e^-$	$* + OH^- \rightarrow OH^* + e^-$ $OH^* + OH^- \rightarrow O^* + H_2O + e^-$ $2O^* \rightarrow 2^* + O_2$ $O^* + OH^- \rightarrow OOH^* + e^-$ $OOH^* + OH^- \rightarrow * + O_2 + H_2O + e^-$

where * is defined as an active site on the catalyst surface.

(*e.g.* RuO_2 and IrO_2) are still considered as the best OER catalysts, even though they have drawbacks such as high-cost, and scarcity. In this regard, many efforts have been devoted to search for active and low-cost alternatives, including transition metal oxides and their derivatives,[154–158] carbon-based materials[159,160] and single-atom systems.[161,162]

To gain a better understanding of the mechanism of this multielectron reaction, OER catalysts with well-defined active sites and structures are preferentially designed, making COFs an interesting option. Probably the most often used approach is the incorporation of metal-coordinating units (*e.g.* bipyridine and porphyrin structures) into the COF skeletons to finally achieve the immobilization of metal-complexes within the framework. Such metalated COFs might be promising OER catalysts by taking advantage of a high amount of accessible metal active sites on the high surface areas and the mass-transfer channels provided by the pores. For example, Banerjee's group synthesized a bipyridine-COF by reacting 1,3,5-trifomylphloroglucinol (Tp) and 2,2′-bipyridine-5,5′-diamine (Bpy) *via* the Schiff base reaction.[55] Bipyridine moieties were used for cobalt ion coordination, yielding abundant Co–N active sites, mimicking metal–bipyridine molecular systems (Fig. 7a).[163,164] The obtained bipyridine-COF with Co incorporation (Co-TpBpy) possesses an accessible surface area of ~450 $m^2\ g^{-1}$ (Fig. 7b) and a reasonable OER performance with an overpotential of 400 mV at 1 mA cm^{-2} (a calculated overpotential of ~520 mV at 10 mA cm^{-2}) under neutral pH conditions (Fig. 7c). In addition, Co-TpBpy exhibits good stability with a similar polarization curve retention after 1000 scans from 0.6 V to 1.8 V (*vs.* RHE). It should be noted that acetylene black was applied as a conductive additive to enhance the conductivity of the system with a mass ratio of 9 : 1 for Co-TpBpy to acetylene black.

Metal porphyrins with their four-coordinated (metal–N_4) structures were one of the first molecules tested for noble metal-free OER.[165,166] In particular, the porphyrin structure with high/low-valent metal ion incorporation was preferentially designed for oxidizing/reducing catalytic cycles.[167,168] Consequently, porphyrin-based COFs have been designed as

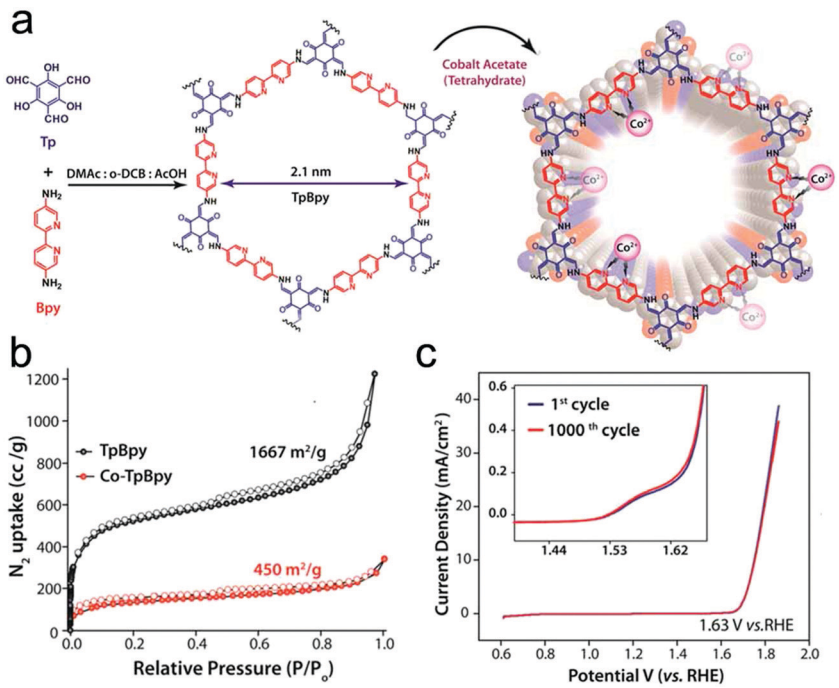

Fig. 7 (a) Schematic illustration of TpBpy and Co-TpBpy with Co incorporation; (b) N_2 sorption isotherms of TpBpy (black) and Co-TpBpy (red); (c) LSV profiles of Co-TpBpy before and after 1000 cycles from 0.6 V to 1.8 V in a phosphate buffer (pH 7.0). Inset: An enlarged view of the LSV profile. Reproduced from ref. 55 with permission from the American Chemical Society, copyright 2016.

an OER electrocatalyst. For instance, Chen's group described a metalloporphyrin-based graphdiyne analogue (Co-PDY) by using Co-coordinated 5,10,15,20-(tetra-4-ethynylphenyl)porphyrin (Co-TEPP) as the monomer to fabricate a novel graphdiyne analogue (Fig. 8a).[126] Notably, graphdiyne is composed of two acetylene (butadiyne) linkages (–C≡C–C≡C–) between the aromatic rings and possesses a unique electronic structure.[169,170] Consequently, the formed Co-PDY, even though just low crystallinity was reported, shows a uniform distribution of Co–N_4 moieties, serving as active sites for OER. Meanwhile, the conjugated structure of porphyrin and the butadiyne linkage could promote the electron transfer in the OER process, achieving the consecutive activity. To further improve the OER electrocatalytic activity and stability, copper foam (CF) was applied as a substrate for polymer growth, serving as a robust 3D porous conductive network (Fig. 8b and c). When used as a working electrode in an alkaline electrolyte (1.0 M KOH), Co-PDY/CF provided an enhanced OER activity with an overpotential of 270 mV at 10 mA cm^{-2}, in comparison to those of bare CF substrate (442 mV) and PDY/CF (381 mV) (Fig. 8d). A chronopotentiometry measurement was further performed to confirm the chemical stability of Co-PDY/CF for OER (Fig. 8e).

Mass transport (of electrolyte molecules, ions, gas molecules *etc.*) is a crucial factor for any electrocatalytic process. The micro- or small mesopores of COFs on one hand increase their surface area but can be too small to ensure unhindered mass transport throughout the pore system. The construction of hierarchical porosities, which is the introduction of additional mesopores or macropores into COFs is supposed to be an effective way to facilitate mass transport through COFs. COFs with hierarchical pore structures have been prepared by applying polystyrene spheres (PSs) as a hard template (Fig. 8f).[36] The macroporous COFs preserve their crystalline structure and high surface area (Fig. 8g and h). The benefit of additional macroporosity was proven by applying macro/microporous co-coordinated bipyridine-COFs (macro-TpBpy-Co) as OER catalysts. A low overpotential (380 mV) was required to reach a current density of 10 mA cm^{-2}, which is superior to that of a

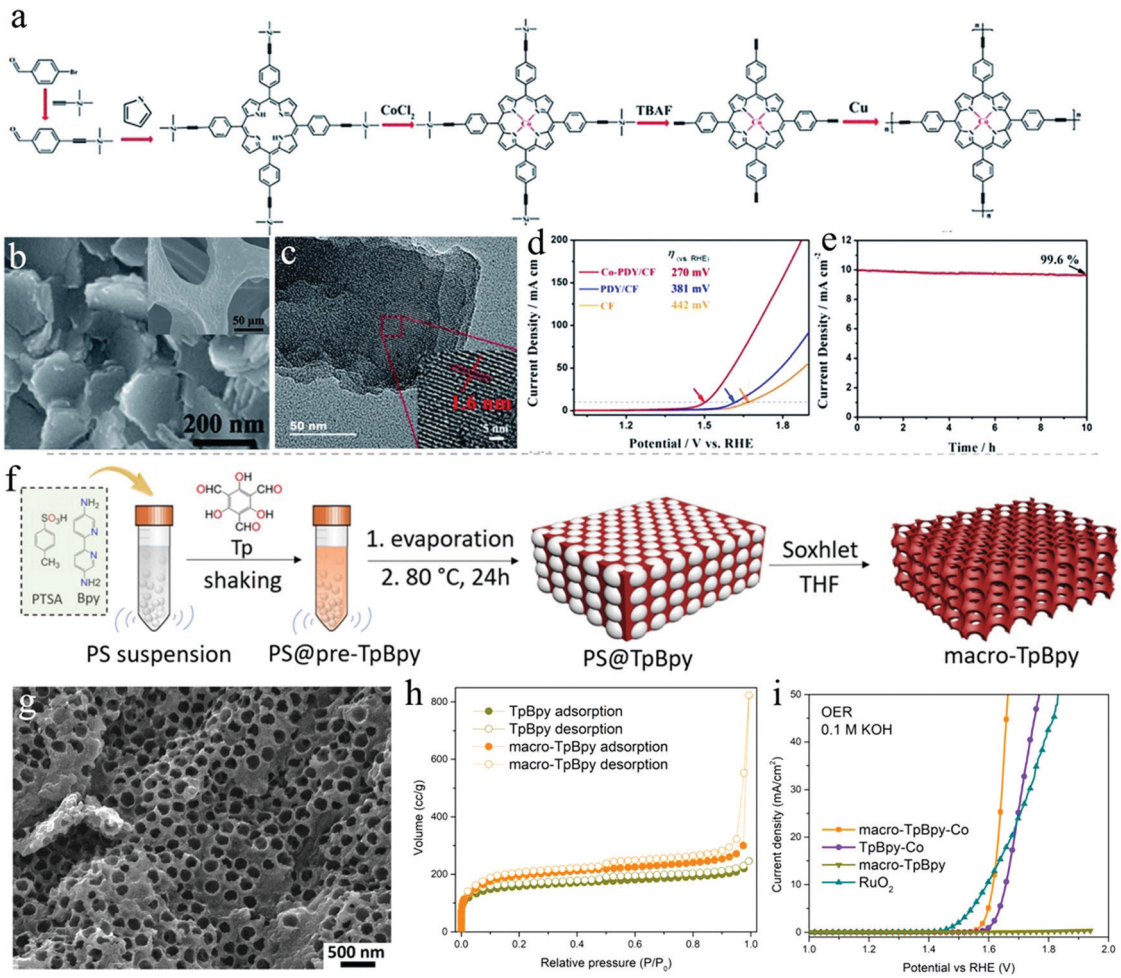

Fig. 8 (a) Schematic representation of the synthesis of Co-PDY. (b) SEM image of Co-PDY/CF, inset: SEM image of copper foam (CF); (c) TEM image of Co-PDY/CF; (d) LSV profiles of Co-PDY/CF, PDY/CF, and CF; (e) chronopotentiometry curve of Co-PDY/CF for OER at 1.50 V (*vs.* RHE); (f) schematic illustration of the synthesis of macro-TpBpy COF with macroporous structure; (g) SEM image of macro-TpBpy; (h) N_2 sorption isotherms of macro-TpBpy and TpBpy; (i) polarization curves of macro-TpBpy-Co. Reproduced from ref. 126 with permission from The Royal Society of Chemistry, copyright 2019; and ref. 36 with permission from the American Chemical Society, copyright 2019.

COF without hierarchical porosity (TpBpy-Co) (Fig. 8i), thus demonstrating the improvement regarding mass diffusion and accessibility of active sites in the electrocatalytic process.

3.1.3 Oxygen reduction reaction (ORR). Oxygen reduction is a fundamental reaction related to the energy conversion devices including fuel cells and metal–air batteries. As for OER, the oxygen reduction process is composed of multistep reactions, involving multiple adsorbed intermediate species such as O*, OH* and OOH*.[171] Depending on the number of electrons transferred, the oxygen reduction process could be divided into two pathways: the direct $4e^-$ transfer pathway from O_2 to H_2O; and the $2e^-$ transfer pathway from O_2 to H_2O_2 (Table 4).

Typically, to obtain a high efficiency in the oxygen reduction process, the $4e^-$ transfer pathway is required. For an ORR catalyst, the selectivity of the $2e^-$ or $4e^-$ pathway is determined by the adsorption energetics of the aforementioned intermediates (O*, OH* and OOH*) and the reaction barriers on the catalyst surface. Currently, the most suitable ORR electrocatalysts are based on the precious Pt metal and its alloys, as evidenced by the volcano plot that counts experimental ORR activity as a function of hydroxyl binding energy.[46,172] However, also many non-noble metal ORR electrocatalysts, including carbon-based catalysts,[173,174] MOFs and their derivatives,[175,176] as well as transition metal oxides[177] have been reported to promote the ORR performance.

To evaluate the performance of ORR catalysts, the most frequently used technique is steady-state polarization on a rotating disk electrode (RDE) or a rotating ring-disk electrode (RRDE). Typically, on an RDE, the indicators such as onset potential, half-wave potential and limiting current density could be calculated as the standard criteria to evaluate the ORR performance for different electrocatalysts. Besides, the total electron transfer number (n) is another important indicator to demonstrate the progress of ORR, which can be calculated by the Koutecky–Levich (K–L) equation on an RDE or directly measured on an RRDE through the equation.

It is known that a $2e^-$ transfer pathway of ORR can produce H_2O_2 (in acidic medium) or HO_2^- (in alkaline medium), whereas it is still unclear whether to define it as a key intermediate of the dominant ORR mechanism or a side product.[46] It is essential to further study the interaction of intermediates with catalyst surfaces to understand the ORR mechanism and develop advanced catalysts to promote the ORR performance. Currently, COFs in their pristine state exhibit promising potential for ORR.[178–180] In particular, inspired by the naturally available biocatalysts such as cytochrome *c* oxidase in mitochondria, which contain as active center an iron(II)–porphyrin structure serving as the "ORR" catalyst in cellular organelles, COFs have been prepared using macrocyclic clusters such as porphyrin, phthalocyanine and tetraazannulene. This provides a biomimetic strategy for designing ORR catalysts by mimicking their homogeneous metal-complex counterparts.[181] The activity of metalloporphyrin COFs for ORR has been evaluated by DFT calculations. Similar to the results of metalloporphyrin COFs for OER, metal–porphyrin structures with Co, Rh and Ir incorporation could be potential candidates for ORR catalysis considering their intermediate free energies close to those of an ideal catalyst.[75]

Recently, Xiang's group synthesized a 2D COF material (COF_{BTC}) where the phthalocyanine iron centres were arranged into rigid networks and endowed the COF_{BTC} with positively charged centres (Fig. 9a).[125] The XRD pattern confirms the crystal structure of the as-synthesized COF_{BTC} (Fig. 9b). Notably, at alkaline conditions, the COF_{BTC} layers can be exfoliated and solvated to form a stable dispersion, which is ascribed to the insertion and absorption of negative hydroxyl groups onto the positively charged centres within the COF_{BTC} stacks (Fig. 9c). When applied for ORR with carbon paper as the working electrode in 0.1 M KOH aqueous electrolyte, the COF_{BTC} catalyst with ordered N-coordinated Fe centres and conjugated structures provides a half-wave potential of 0.9 V *vs.* RHE and an onset potential of 0.965 V *vs.* RHE at a COF_{BTC} concentration of 1.25 g mL^{-1} (Fig. 9d), which compare well to those of some reported metal–nitrogen–carbon based catalysts.[182] When further applied in a zinc–air battery with O_2/OH^- and Zn^{2+}/Zn as redox couples, this COF can be directly used as the catalyst for ORR, due to its solubility in the electrolyte. As such, the COF_{BTC} could provide more accessible active sites compared with the conventional air electrodes such as catalyst-coated carbon paper. Expectedly, the COF_{BTC} catalyst exhibits practical applications in zinc–air flow batteries with voltage gaps (0.77 V at 5 mA cm^{-2}, 0.83 V at 10 mA cm^{-2}, and 0.96 V at 20 mA cm^{-2}) and high energy efficiencies (60.7% at 5 mA cm^{-2}, 59.0% at 10 mA cm^{-2}, and 52.6% at 20 mA cm^{-2}) (Fig. 9e and f).

To improve the electron transport during the electrocatalytic process, the hybridization of COFs with conducting additives such as graphene and CNTs has been achieved by *in situ* polymerization.[95,183] For instance, Xiang's group reported a hybridized covalent organic polymer/graphene (COP/rGO) by self-assembling highly ordered porphyrin COPs with graphene.[95]

Table 4 ORR mechanisms under acid and alkaline conditions

	Mechanism	
Alkaline media	$O_2 + 2H_2O + 4e^- \rightarrow 4OH^-$	(Four-electron process)
	$O_2 + H_2O + 2e^- \rightarrow HO_2^- + OH^-$	(Two-electron process)
	$HO_2^- + H_2O + 2e^- \rightarrow 3OH^-$	
Acidic media	$O_2 + 4H^+ + 4e^- \rightarrow 2H_2O$	(Four-electron process)
	$O_2 + 2H^+ + 2e^- \rightarrow H_2O_2$	(Two-electron process)
	$H_2O_2 + 2H^+ + 2e^- \rightarrow 2H_2O$	

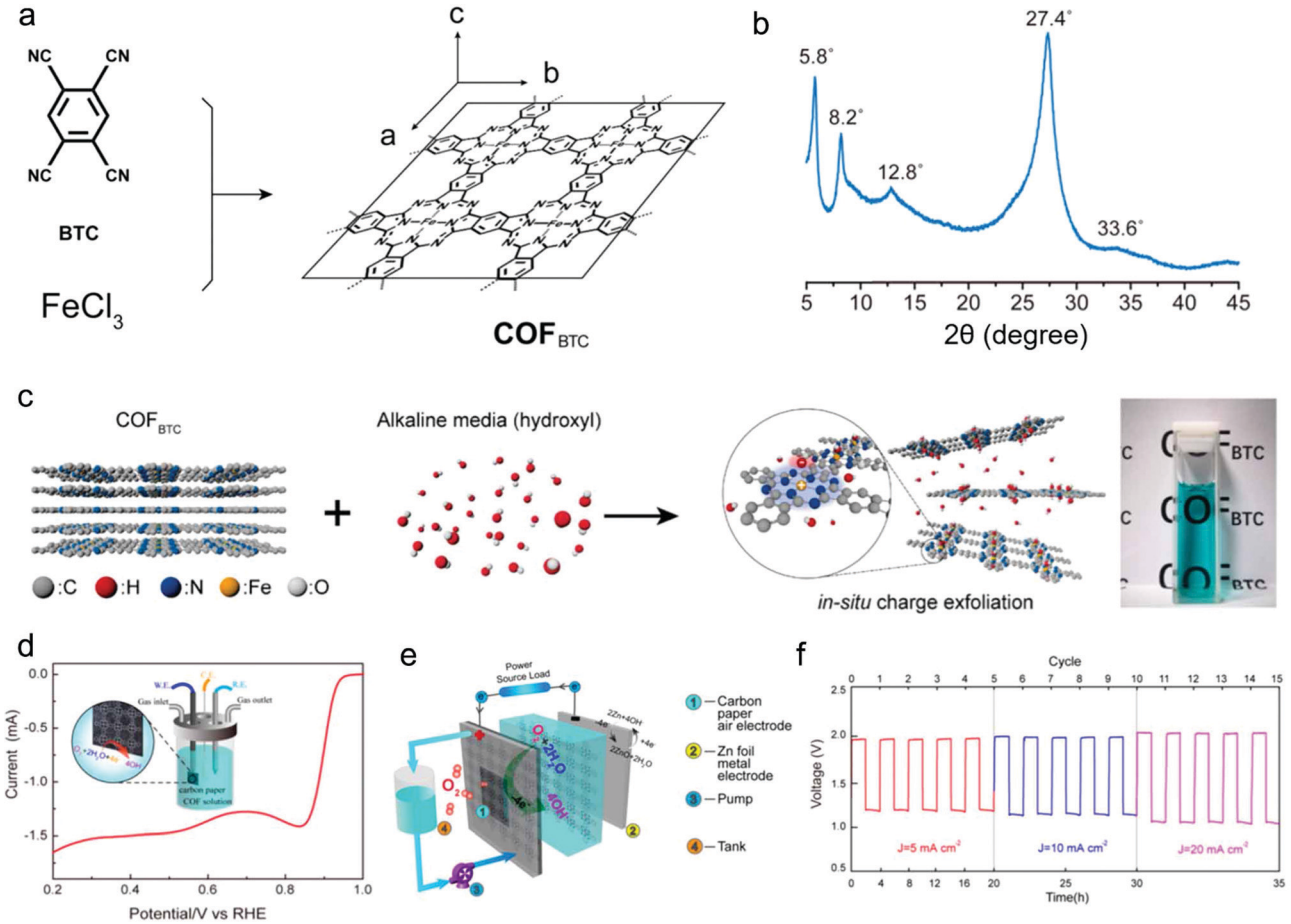

Fig. 9 (a) Schematic representation of the synthesis process for COF_{BTC}; (b) XRD pattern of COF_{BTC}; (c) schematic illustration of the exfoliation and dissolution processes of COF_{BTC} in an alkaline solution; (d) LSV profile of the COF_{BTC} in O_2-saturated 0.1 M KOH. Inset: Scheme for the detailed operation of the measurement with carbon paper as electrodes. (e) Schematic configuration of rechargeable Zn–air batteries; (f) galvanostatic discharge–charge cycling curves of Zn–air batteries at different current densities of 5, 10, and 20 mA cm^{-2}. Reproduced from ref. 125 with permission from the American Chemical Society, copyright 2019.

As a result, the conductivity showed a significant increase (from 3.06×10^{-9} to 2.56×10^{-1} S m^{-1}) compared to pure COPs. It is assumed that the synergetic effects between active COP and high electrical conductivity of rGO are responsible for the high ORR activities and long-term stability.

COF materials have been recently used as precursors to construct carbon-based electrocatalysts for ORR, such as metal-free carbon,[112] single-atom doped carbon[110] as well as metal–carbon composites.[184–187] Nevertheless, the direct pyrolysis of COFs destroys their inherent porous structure forming bulk carbons with hardly controllable structures. With this in consideration, Jiang's group applied phytic acid (PA) as a template to guide the pyrolysis, which successfully converted a traditional COF (TAPT-DHTA-COF) into nanosized 2D carbons (Fig. 10a).[112] It was demonstrated that PA can enter the 1D channels of COFs, acting as templating and directing agents during the pyrolysis process of COFs at 1000 °C under N_2 (Fig. 10b). As a result, the resulting 2D COF (PA@TAPT–DHTA–COF_{1000}) possesses good conductivity, hierarchical porosity and abundant catalytic edges with phosphorus and nitrogen doping. Later on, the PA@TAPT–DHTA–COF_{1000} was pyrolyzed under NH_3 at 900 °C for 0.5 h, to further improve its specific surface area (1160 m^2 g^{-1}), pore volume (0.59 m^3 g^{-1}) and ORR catalytic activity (Fig. 10c and d). PA@TAPT–DHTA–$COF_{1000NH3}$ as a metal-free ORR electrocatalyst achieved a half-wave potential of 0.831 V (*vs.* RHE), an onset potential of 0.941 V (*vs.* RHE), and a limiting current density of 7.2 mA cm^{-2}, superior to those of Pt/C (Fig. 10e).

Recently, our group applied silica nanoparticles as a hard template to convert a bipyridine-COF (TpBpy) into mesoporous carbon *via* carbonization.[110] A molecular organizer (*p*-toluenesulfonic acid, PTSA) was used for COF growth and enabled the formation of SiO_2@TpBpy composites *via* a grinding approach. Bipyridine moieties (2,2′-bipyridine-5,5′-diamine, Bpy) were chosen and incorporated within the COF backbone to coordinate metal, here Fe ions. When taken as a carbon precursor with a pyrolysis process followed by suitable treatment with HCl and NaOH, the bipyridine-COF with Fe incorporation was successfully converted into mesoporous carbon (mC-TpBpy-Fe) with a surface area of 362 m^2 g^{-1} and abundant Fe–N_x active sites.

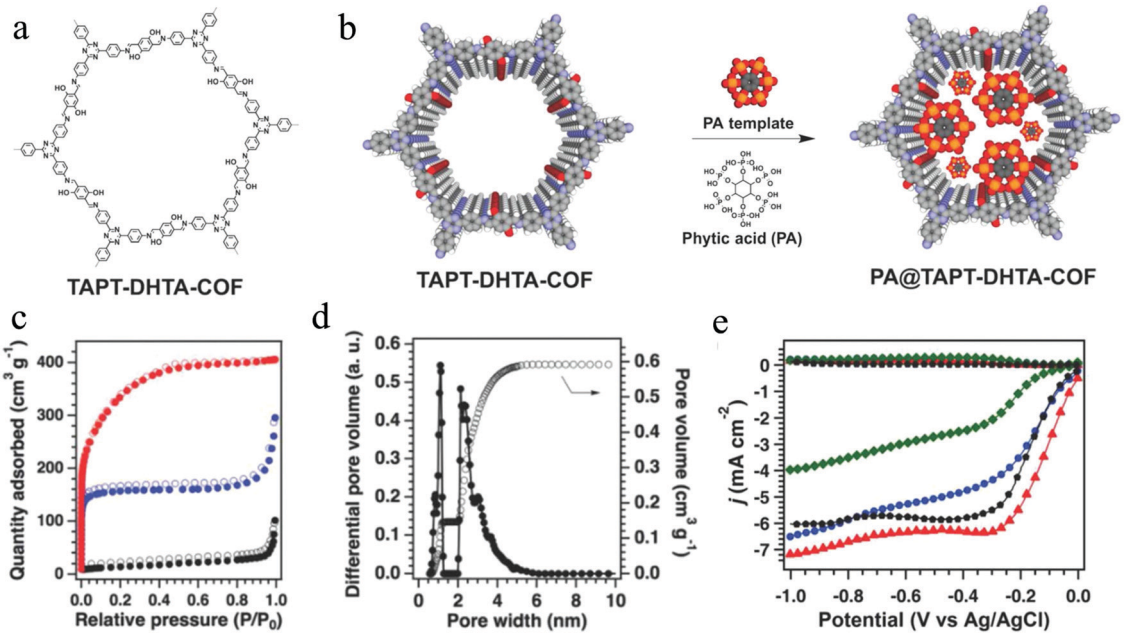

Fig. 10 (a) Structure of TAPT-DHTA-COF; (b) PA-templated synthesis of PA@TAPT–DHTA–COF; (c) N_2 sorption isotherms of PA@TAPT–DHTA–$COF_{1000NH3}$ (red), PA@TAPT–DHTA–COF_{1000} (blue) and TAPT–DHTA–COF_{1000} (black); (d) pore size distribution of PA@TAPT–DHTA–$COF_{1000NH3}$; (e) ORR performances of PA@TAPT–DHTA–$COF_{1000NH3}$ (red), PA@TAPT–DHTA–COF_{1000} (blue), TAPT–DHTA–COF_{1000} (green), and Pt/C (black) in 0.1 M O_2-saturated KOH aqueous solutions at 1600 rpm. Reproduced from ref. 112 with permission from John Wiley and Sons, copyright 2018.

Electrocatalytic studies show that mC-TpBpy-Fe exhibits an onset potential of 0.92 V (*vs.* RHE) and half-wave potential of 0.845 V (*vs.* RHE), which are comparable to those of commercial Pt/C in oxygen-saturated 0.1 M KOH. In addition, the performance was superior to carbonaceous materials derived from the carbonisation of the pure monomers or an amorphous polymer network with similar chemical structure. It can thus be suggested that the periodicity of the COF precursor yield a more homogenous distribution of functional groups within the carbon framework, *i.e.* that the formation of a crystalline COF precursor is indeed beneficial for the preparation of highly active and porous Fe–N–C catalysts.

3.1.4 Bifunctional OER/ORR catalysts. As mentioned above, OER and ORR are key processes in renewable energy conversion. To design efficient bifunctional electrocatalysts both for ORR and OER is of significance in the commercialization of renewable energy devices such as Zn–air batteries. Typically, the rechargeable Zn–air battery consists of a Zn anode, a separator soaked in an aqueous alkaline electrolyte and an air cathode. In a discharge process, the Zn anode is oxidized, while O_2 from air diffuses through the cathode electrode and is then reduced by electrons to form OH^-. This process reverses during charging, where the Zn recovers at the anode electrode and O_2 is regenerated, evolving at the cathode electrode. For a rechargeable battery, indicators including discharge/charge potentials, power density and galvanostatic discharge–charge cycling are generally considered to evaluate its performance such as rechargeability and energy efficiency.

Recently, many research efforts have been dedicated to the development of efficient bifunctional electrocatalysts for the OER and ORR.[188,189] Based on density functional theory (DFT) calculations, Promarak and co-workers studied the free energy changes of intermediates both for ORR and OER on metalloporphyrins in a 2D framework.[75] The metalloporphyrin frameworks with 14 different metal sites were applied to investigate the free energies of the reaction intermediates, including OH*, OOH* and O*. As a result, especially the metalloporphyrin frameworks with Co, Ir and Rh incorporation could be potential candidates for both the OER and ORR. In this regard, Zhang's group reported a porphyrin framework ("POF") through dehydration polymerization between pyrrole and benzene-1,4-dialdehyde (BDA) (Fig. 11a).[190] Molecular dynamic (MD) simulations and XRD measurements were performed to confirm that the constructed POFs possess a slightly ordered structures distinguished from those of fully amorphous polymers. After adding cobalt ions, the Co-coordinated POF exhibited electrocatalytic performances both for OER and ORR, demonstrating its potential application as a bifunctional electrocatalyst.

Considering the limitation of electronic transport of such crystalline materials, the authors applied carbon nanotubes (CNTs) as scaffolds to fabricate a CNT@POF hybrid material and explored its practical application in zinc–air batteries. It was found that the POF was uniformly coated on CNTs as thin layers with a calculated thickness of ~4 nm, thus fully exposing the porphyrin active sites to reactants (Fig. 11b).[74] When applied as the cathode in a Zn–air battery (Fig. 11c), the CNT@POF hybrid exhibits a superior current density than that of a reference Pt/C + Ir/C cathode, while the discharge and charge potentials for CNT@POF are 1.21 V and 1.99 V at a required current density of 20.0 mA cm^{-2} (0.95 V and 2.02 V for

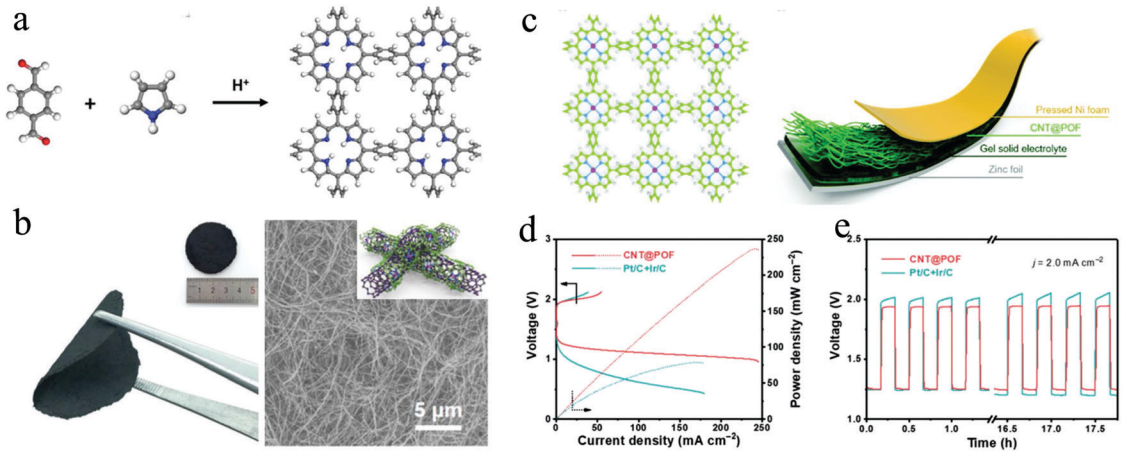

Fig. 11 (a) Schematic illustration of the synthesis of POF; (b) Photographs and SEM image of CNT@POF. (Inset shows a schemtic drawing of the POF-CNT composite); (c) left: chemical structure of POF with Co incorporation. The hydrogen (white), carbon (green), nitrogen (blue) and cobalt (pink) atoms are marked in different colours. Right: Schematic illustration of a flexible Zn–air battery; (d) polarization curves of CNT@POF in the rechargeable Zn–air battery; (e) charge/discharge cycling of CNT@POF and Pt/C + Ir/C at 2.0 mA cm^{-2}. Reproduced from ref. 190 with permission from John Wiley and Sons, copyright 2019; and ref. 74 with permission from the Royal Society of Chemistry, copyright 2018.

Pt/C + Ir/C) (Fig. 11d). The peak power density of CNT@POF (237 mW cm^{-2}) is much higher than that of the reference Pt/C + Ir/C cathode (78 mW cm^{-2}). Besides, the galvanostatic discharge–charge cycling curves were conducted at 2.0 mA cm^{-2} to investigate the cycling performance of CNT@POF in a rechargeable Zn–air battery, where the CNT@POF hybrid shows a smaller voltage gap of 0.71 V than that of Pt/C + Ir/C (0.77 V), demonstrating its impressive performance in rechargeable flexible Zn–air batteries (Fig. 11e).

3.1.5 Carbon dioxide reduction reaction (CO_2RR). Carbon dioxide (CO_2) emission from the utilization of fossil fuels constitutes a potential threat to the global climate. Transforming CO_2 into a valuable carbon feedstock is therefore an important goal for a sustainable economy.[191–193] However, because of the competitive side reactions (for example: HER) and the stable C═O double bond, the CO_2RR is kinetically challenging. The reaction process of CO_2RR mainly involves three steps: (1) adsorption of CO_2 molecules on a catalyst surface; (2) the breaking of C–O bonds and/or the forming of C–H bonds; (3) the rearrangement and desorption processes of products. In particular, the second step is a complex process with multielectron transfer pathways producing different products. Depending on the number of migrated protons and electrons, CO_2 can be converted into different products, including formic acid, methane, methanol, ethanol, ethylene, carbon monoxide and many others.[191] In most cases, the products are multiple species rather than a single product. The type and amount of species mainly depend on the surface properties of electrocatalysts and the applied electrode potentials. Consequently, electrocatalysts with various sizes, morphologies, crystal structures and chemical states have been designed to increase the CO_2RR kinetics and selectivity.[194,195] To evaluate the performance of a CO_2RR electrocatalyst, the indicators generally include onset potential, overpotential and current density. Besides, due to the formation of multiple products in the CO_2RR process, the faradaic efficiency is required to evaluate the conversion efficiency and selectivity of catalysts. Typically, faradaic efficiency (FE) is defined through the following equation for a certain product:

$$\mathrm{FE} = \frac{\alpha n F}{Q}$$

where α is the electron transfer number to form a certain product; F is the Faraday constant; Q is the total charge during the reduction process; n is the number of moles of the product produced.

Currently, the most widely employed electrocatalysts for CO_2 conversion are traditional bulk metals and metal-containing inorganic materials.[51,196,197] However, these metal-based catalysts are generally poisoned by impurities or some strongly bound intermediates, showing limited active sites. In this regard, various advanced catalysts have been studied to further enhance CO_2RR,[194,198,199] and recently COFs have also been applied to this reaction.[44,73,200,201]

Starting with an important contribution from Yaghi and co-workers, two Co-based COFs (*i.e.* COF-366-Co and COF-367-Co) were synthesized through the imine condensation of 5,10,15,20-tetrakis(4-aminophenyl)porphinato cobalt [Co(TAP)] with 1,4-benzenedicarboxaldehyde (BDA) and biphenyl-4,4′-dicarboxaldehyde (BPDA), respectively, serving as electrocatalysts to convert CO_2 into carbon monoxide (CO) (Fig. 12a).[43] The as-synthesized Co-COFs exhibit high crystallinity and large surface areas (1360 m^2 g^{-1} for COF-366-Co and 1470 m^2 g^{-1} for COF-367-Co), enabling abundant active sites for CO_2RR. The faradaic efficiency (FE_{CO}) of the COF-366-Co is 90% at −0.67 V, showing a superior catalytic performance compared to that of the molecular cobalt complex Co-(TAP). At standard temperature and pressure (STP), COF-366-Co could yield more than 36 mL of carbon monoxide per mg of COF during a 24 hour period. When the framework is expanded through the replacement of BDA with

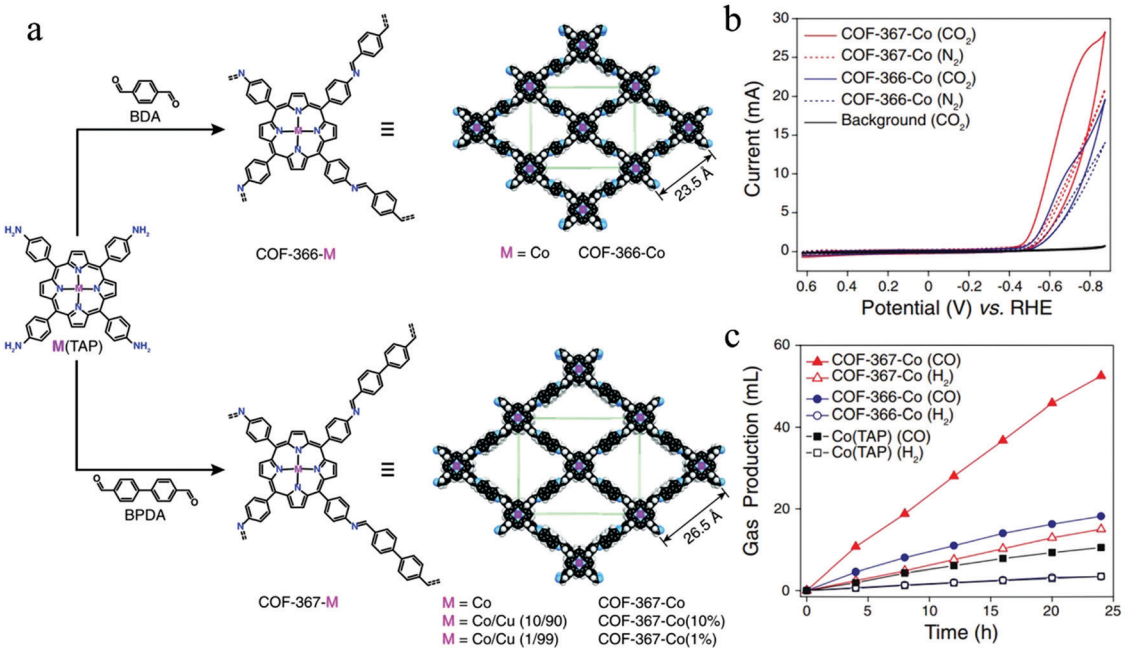

Fig. 12 (a) Schematic illustration of metalloporphyrin-derived COFs (COF-366-Co and COF-367-Co); (b) cyclic voltammograms (CVs) of COF-366-Co and COF-367-Co in a CO_2-or N_2-saturated medium. A bare carbon electrode was applied as the background (black solid line). (c) Long-term bulk electrolysis at 0.67 V (*vs.* RHE), showing the volumes of CO_2 (H_2) produced by COF-367-Co, COF-366-Co, and Co(TAP). Reproduced from ref. 43 with permission from AAAS, copyright 2015.

BPDA, the expanded COF-367-Co with larger pore size provides a greater number of active cobalt-porphyrin moieties and thus possesses an improved capacity of CO_2 adsorption within the framework. Consequently, the COF-367-Co exhibits enhanced catalytic performance compared to that of the COF-366-Co (Fig. 12b and c), where the faradaic efficiency of COF-367-Co is 91% and the production of carbon monoxide per milligram is more than 100 mL at −0.67 V during a 24 hour period. X-ray absorption spectra show that the COF structure is of importance in modulating the electronic properties of molecular centers. This demonstrates that because of the interaction between the COF lattice and cobalt atoms, the cobalt centers within COFs could possess a more delocalized electronic structure, which is responsible for the high activity and selectivity of the reduction process from CO_2 to CO. This work thus clearly proves the advantages of ordered and porous COF materials for carbon dioxide reduction.

Given the unique features such as a fully conjugated skeleton, high chemical stability and the abundant presence of heteroatoms, CTFs exhibit strong affinity to CO_2 and can be considered as promising candidates for CO_2RR.[202] Zhuang and co-workers designed a Ni-coordinated porphyrin-based covalent triazine framework (NiPor-CTF).[203] The formed NiN_4 centres are uniformly dispersed within the frameworks. When applied as electrocatalyst for CO_2RR, the NiPor-CTF possesses a superior selectivity for CO conversion with a faradaic efficiency of >90%. DFT calculations indicated that the NiN_4 active sites could decrease the kinetic energy barriers of the transition from $*CO_2$ to *COOH, thus improving the performance of CO_2RR. Similarly, Nakanishi's group reported CTF-based materials with incorporation of 3d metal atoms (Co, Ni or Cu) as electrocatalysts for CO_2RR.[204] They proved that the CTFs with Co and Ni incorporation (Co-CTF and Ni-CTF) could effectively provide reductive activity from CO_2 to CO at −0.5 *vs.* RHE. Particularly, the Ni-CTF possesses a superior faradaic efficiency of 90% at −0.8 V during CO formation, in contrast to the corresponding Ni–porphyrin (using tetraphenylporphyrin, TPP). It is evidenced by the aid of first principles calculation that because of the low-coordination environment in the Ni-CTF, the intermediates could be stabilized on the metal atoms, which means the free energy barriers for the formation of intermediate species (adsorbed COOH) on the metal atoms in CTF is lower than those on the TPP supports.

Due to the opposite properties of the strength of a linkage and its reversibility required for the crystallization process of COFs, it is a challenge to synthesize COF materials with high chemical stability in general and of course also for electrocatalysis application. In this regard, the attempts to build chemically strong COFs *via* keto–enol tautomerism enabled the synthetic possibilities of imine-based COFs.[40] From such an imine COF, Deng's group synthesized an amine COF (COF-300-AR, "after reduction") by direct reduction of the corresponding imine COF (COF-300) (Fig. 13a).[128] The amine COF maintains the crystalline structure of the parent COF-300 and exhibits a satisfactory chemical stability both in acidic and alkaline solutions. Notably, the COF-300-AR here is not the electrocatalyst but is deposited on a silver electrode to form a molecularly defined interface for the catalytic CO_2RR. It is demonstrated that the COF with amine linkages provides chemically sorptive sites to concentrate CO_2 molecules to form carbamates close to the electrode surface, and then the silver

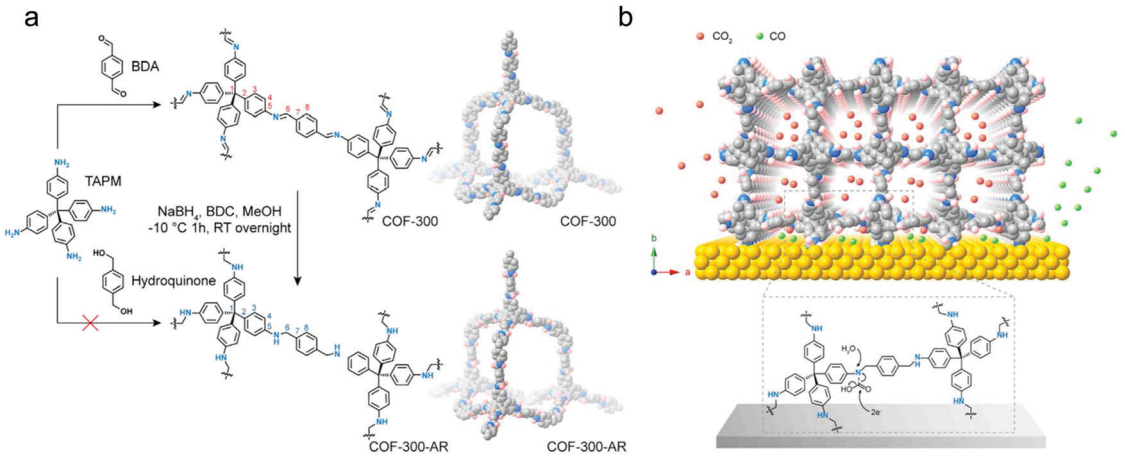

Fig. 13 (a) Reduction process of COF-300 to COF-300-AR; (b) schematic representation of the molecularly defined interface between the COF-300-AR and silver electrode. Reproduced from ref. 128 with permission from Elsevier Inc., copyright 2018.

surface with sufficient electrons could activate the carbamates, leading to the selective generation of CO (Fig. 13b). This work provides a novel approach by using COFs to achieve the construction of ordered porous structures on the surface of silver electrodes. Forming the molecularly defined interface achieves the favourable diffusion of CO_2 molecules and good CO_2RR selectivity.

3.2 Energy storage

The process of capturing energy produced at one time for later use is called energy storage. Devices used for energy storage are supercapacitors, accumulators or batteries. With the discovery of electricity, there was a search for effective approaches for storing the electricity for use on demand. In the past decades, the change in renewable energy requirements and the development of nanotechnology has enabled the energy storage industry to continue to develop, adapt and transform. To build more sustainable energy infrastructures and achieve the economic utilization of electric energy, there is a need for sustainable and large-scale energy storage devices or systems.

3.2.1 Supercapacitors. Supercapacitors with high power density and long cycling life are considered as promising energy storage devices. Depending on the energy storage mechanism and the nature of the electrode material, supercapacitors exhibit two distinct processes for storing electricity: the non-faradaic processes related to the electrochemical double layer and the faradaic processes derived from reversible redox processes on the electrode (*i.e.* pseudocapacitance).[52,205,206] Supercapacitors are generally related to the electrochemical process occurring at the interface of the electrolyte and electrode. In the non-faradaic process, found in electrochemical double layer supercapacitors, the electrical energy is stored through the adsorption of ions onto electrode surfaces. Consequently, electrodes with high surface areas (*e.g.* porous carbons) provide maximum energy storage.[207,208] Meanwhile, the faradaic processes in pseudocapacitors are characterised by reversible chemical reactions, *i.e.* oxidation/reduction reactions occurring on the electrode surfaces, which usually provide higher supercapacitor performance in contrast to those of electric double layer formation only.[206] Electrochemical parameters, such as capacitance, power density, energy density and cycling stability, are applied to characterize the performance of a supercapacitor.[209] The capacitance is one of the key parameters, which is defined by the ratio of the change in electrical charge to the corresponding change in electrical potential. In particular, the specific capacitance is calculated as the most significant indicator to compare the ability of charge storage for supercapacitor materials. When normalized by the surface area, volume, and mass of the active materials, the obtained specific capacitance is correspondingly defined as the areal capacitance (F cm^{-2}), volumetric capacitance (F cm^{-3}) and gravimetric capacitance (F g^{-1}), respectively. Similarly, the power density and energy density of a supercapacitor can be gravimetrical or volumetrical, where the power density indicates the efficiency of energy delivery and uptake by W kg^{-1} or W m^{-3} and the energy density demonstrates the amount of stored and deliverable electrical energy by W h kg^{-1} or W h m^{-3}. Cycling stability is another important parameter, which is usually estimated in the form of capacitance retention rate, which is obtained in a galvanostatic charge–discharge (GCD) test through comparison of the capacitance before and after thousands of cycles.

For electrochemical double layer supercapacitors, the most widely used electrode materials are porous carbons with high surface area because of their low cost and enormous availability, whereas the electrode materials for pseudocapacitors depend on metal oxides, redox-active polymers and functionalized porous carbons that conduct the electrostatic and pseudocapacitive processes simultaneously. Even though pseudocapacitors possess superior specific capacitance compared to electrochemical double layer supercapacitors, the fast-redox reactions in pseudocapacitors usually lead to swelling and shrinkage of the electrodes, resulting in poor mechanical stability and inaccessible active sites. In this regard, the design of advanced electrode materials with stable and controllable porous structures, high surface areas and integrated redox-active groups, is crucially required to achieve an efficient redox process in supercapacitors.

COFs can be promising electrode materials for electrochemical capacitors due to their unique advantages such as large surface areas, tuneable pore sizes and shapes as well as the adjustable redox-active groups within the frameworks.[210–217] It can be supposed that the long-range ordered structure with high surface area could promote the ion transport at the interface of the electrode and electrolyte. In addition, the tuneable building units enable COFs to be functionalized by the incorporation of redox-active sites, suitable for pseudocapacitive energy storage.[218] In this section, the development of COF-based electrode materials applied in supercapacitors is summarized.

In 2013, Dichtel's group firstly applied COFs as electrode materials for pseudocapacitors by introducing redox-active anthraquinone moieties from 2,6-diaminoanthraquinone (DAAQ) into the crystalline framework (DAAQ–TFP COF) that was synthesized by condensing DAAQ and 1,3,5-triformylphloroglucinol (TFP).[63] However, due to the poor conductivity, the DAAQ–TFP COF exhibited only 40 F g^{-1} capacitance after 5000 charge–discharge cycles. To address the conductivity issues, DAAQ–TFP COF thin films were fabricated on Au substrates through the slow reaction of the TFP monomer with DAAQ (Fig. 14a and b).[219] The thin films enable many more redox-active sites to be accessible and an order of magnitude higher capacitance was obtained compared to the bulk COFs that were synthesized as randomly oriented microcrystalline powder. Thus, this work not only demonstrated the possibility to apply redox-active COFs in pseudocapacitors but also the impact of regulating the morphology and microstructure of the COFs to enhance their electrochemical performance.

Furthermore, to enhance the electrical conductivity of redox-active COF films, conductive polymers were integrated into the ordered channels within the COF matrix. Dichtel and co-workers applied the above DAAQ–TFP COF as a scaffold to achieve the infiltration of the conductive poly(3,4-ethylenedioxythiophene) (PEDOT) into the channels of COFs (Fig. 15a).[96] The as-fabricated PEDOT-infiltrated COF (PEDOT-modified DAAQ–TFP) exhibited greatly enhanced electrochemical activities with good accessibility of the redox-active groups within DAAQ–TFP COF. It is supposed that the PEDOT chains could act as electron transfer channels to the redox-active groups, achieving a high efficiency of electron transfer between electrodes and redox-active groups. Consequently, the galvanostatic charge–discharge process was conducted to evaluate the capacitance of samples at different charging rates, where the PEDOT-modified DAAQ–TFP COF film exhibited superior capacitance in comparison to the DAAQ–TFP COF film, with a maximum capacitance of 350 F cm^{-3} at a charging rate of 10C and 50% of the capacitance was maintained even at 1600C (Fig. 15b). Moreover, the PEDOT-infiltrated COF shows good chemical stability after 10 000 cycles, where the capacitance shows no significant changes at the charging rates of 10C and 100C (Fig. 15c).

Subsequently, a chemically stable and redox active COF (TpOMe–DAQ COF) was developed by Banerjee's group through the condensation of 2,4,6-trimethoxy-1,3,5-benzenetricarbaldehyde (TpOMe) and 2,6-diaminoanthraquinone (DAQ) (Fig. 16a).[41] The chemical stability of TpOMe–DAQ COF was derived from the effect of both steric and hydrophobic protection of imine (C═N) bonds by the neighbouring-OCH_3 functionalities and the interlayer C–H···N H-bonding (Fig. 16b). By applying a mechanochemical grinding approach, TpOMe–DAQ COF was processed as thin film and applied as a free-standing electrode material for supercapacitors in 3.0 M H_2SO_4 solution. Given the good porosity of the COF and redox activity of the quinone/hydroquinone couple, the as-synthesized TpOMe–DAQ

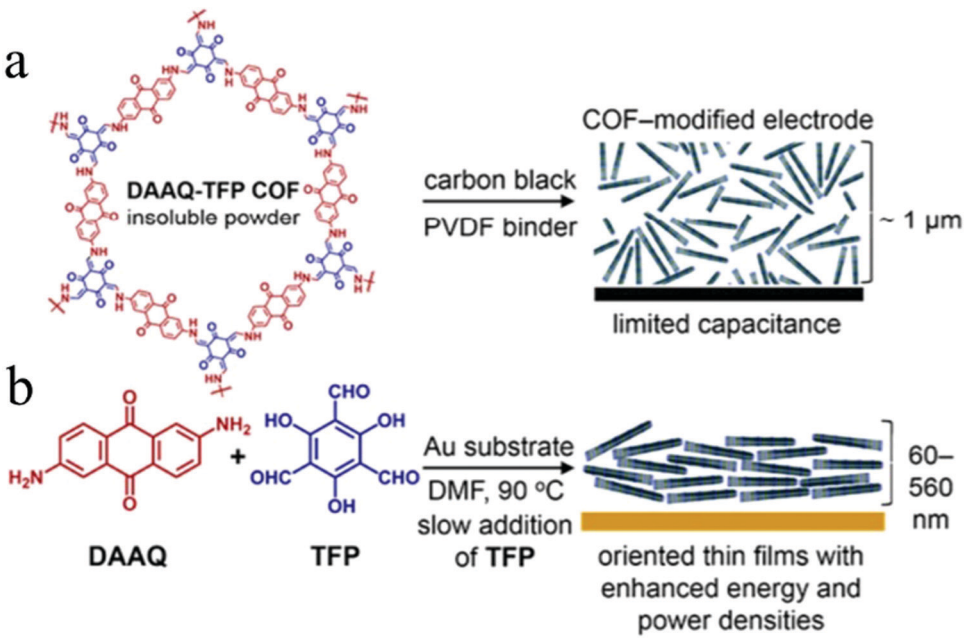

Fig. 14 (a) Structure of DAAQ–TFP COF with random orientation on the electrode; (b) schematic illustration of the DAAQ–TFP COF as an oriented thin film on an electrode surface. Reproduced from ref. 219 with permission from the American Chemical Society, copyright 2015.

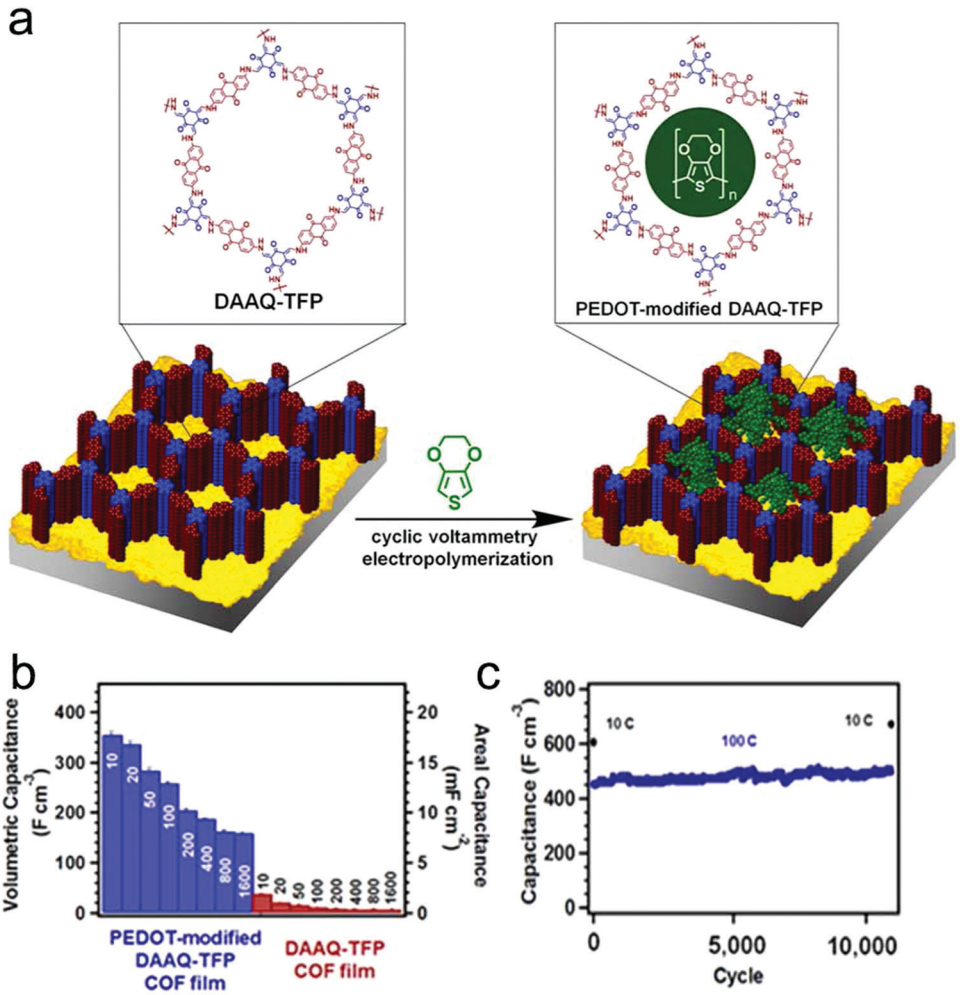

Fig. 15 (a) Schematic representation of the synthesis of PEDOT-modified DAAQ–TFP COF film; (b) average capacitance of PEDOT-modified DAAQ–TFP and DAAQ–TFP at different charging rates; (c) extended cycling of PEDOT-modified DAAQ–TFP film showing stability over 10 000 cycles. Reproduced from ref. 96 with permission from the American Chemical Society, copyright 2016.

displays an areal capacitance of 1600 mF cm^{-2} (gravimetric capacitance 169 F g^{-1}) and good cycling stability (>100 000) with no significant changes in capacitance retention and coulombic efficiency (Fig. 16c and d).

Recently, Banerjee and co-workers reported two kinds of redox-active COFs, that is TpPa–$(OH)_2$ and TpBD–$(OH)_2$, by introducing redox-active hydroquinone moieties into COF backbones through Schiff base condensation of 1,3,5-triformylpholoroglucinol (TFP) with 2,5-dihydroxy-1,4-phenyldiamine [Pa-$(OH)_2$] and 3,3′-dihydroxybenzidine [BD-$(OH)_2$], respectively.[218] The reversible proton-coupled electron transfer ($2H^+/2e^-$) of hydroquinone/benzoquinone moieties are responsible for the specific capacitance of these redox-active COFs.

The hybridization of COFs with conducting materials has been developed to further improve the electrical conductivity and subsequently the electron transport during the charge–discharge process. For example, Sun's group reported a COF/NH_2-rGO composite as a supercapacitor electrode through the condensation of 1,3,5-triformylbenzene and 1,4-diaminobenzene, and a further composite with amine-modified reduced graphene oxide (NH_2-rGO).[220] It was described that the synergistic effect of the active COFs and conductive graphene supports increased the electrochemical performance. Similarly, 3D graphene was modified by growing COFs on its surfaces through an interfacial polymerization method, where redox-active moieties (anthraquinone) were deliberately chosen to increase the electrochemical activities.[221] The as-prepared electrode material had a good conductivity and provided more accessible electrochemically active moieties. As a result, the COF/graphene composite displays improved specific capacitance in alkaline media in comparison to that of the powder 2D COFs.

Very recently, ultralight COF/rGO aerogels with hierarchical porosity were reported. The COFs were produced in the presence of graphene oxide using hydrothermal treatment. Notably, during this treatment, the COF is not only formed as a thin layer on the graphene sheets, but GO is also reduced to rGO, which additionally stacks up in a 3D fashion to finally form a COF/rGO gel. This gel can be transformed into an ultralow density COF/rGO aerogel by freeze-drying (Fig. 17a).[57] Diaminoanthraquinone (Dq) was selected as a redox-active unit,

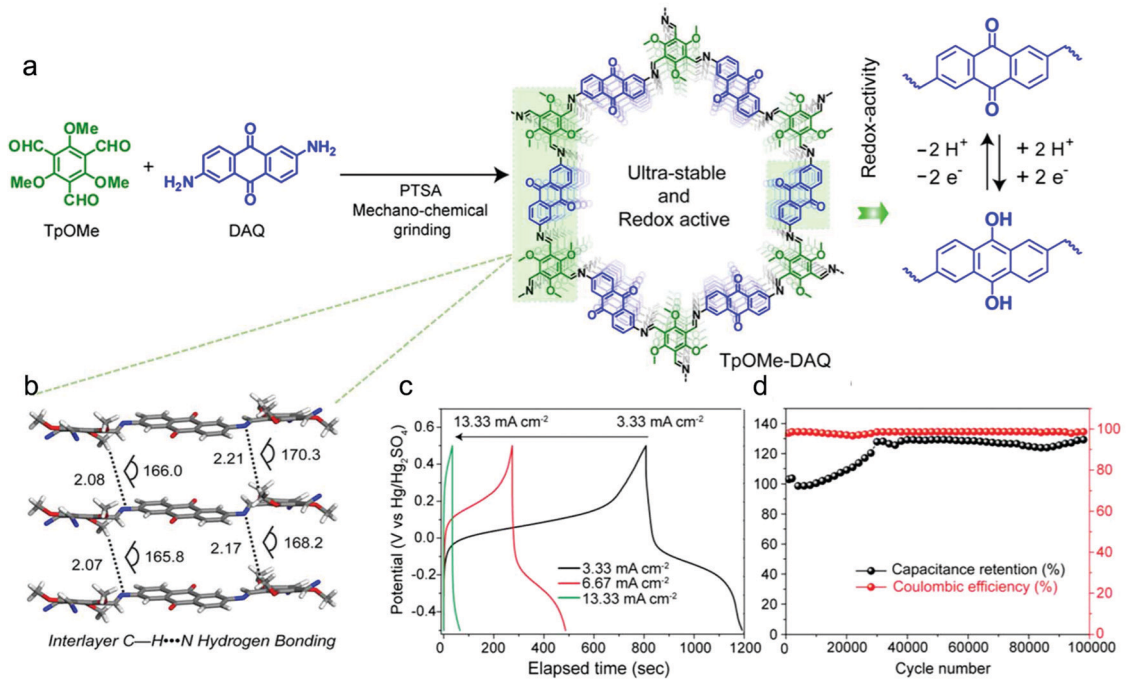

Fig. 16 (a) Schematic representation of the synthesis of TpOMe–DAQ, and the reversible transformation between quinone and hydroquinone; (b) structural illustration of the interlayer C–H···NH-bonding in TpOMe–DAQ; (c) galvanostatic charge–discharge and (d) cycling stability performance (10 mA cm^{-2}) of TpOMe–DAQ thin sheets. Reproduced from ref. 41 with permission from the American Chemical Society, copyright 2018.

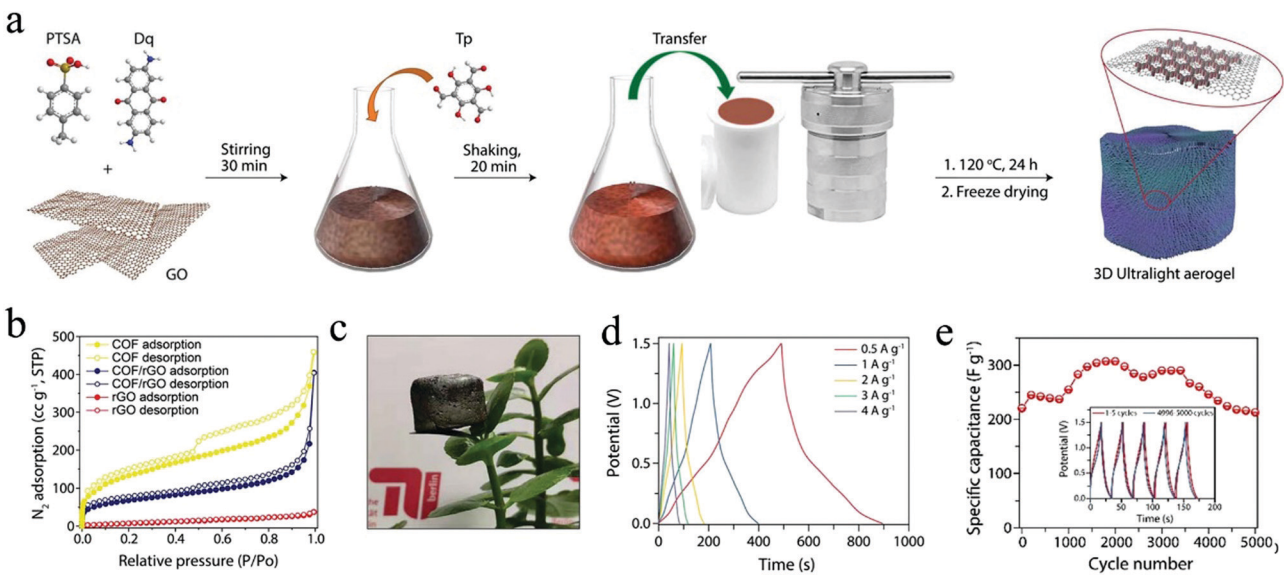

Fig. 17 (a) Schematic illustration of the fabrication of COF/rGO aerogels; (b) N_2 sorption isotherms of COF/rGO, COF and rGO; (c) a photograph of a COF/rGO aerogel held by a leaf; (d) the galvanostatic charge–discharge curves of COF/rGO in 0.5 M H_2SO_4 at 0.5, 1, 2, 3 and 4 A g^{-1}; (e) the cycling stability of COF/rGO at 8 A g^{-1}. The inset image shows the charge/discharge profiles for 1–5 and 4996–5000 cycles. Reproduced from ref. 57 with permission from Springer Nature, copyright 2020.

enabling COFs with pseudocapacitive performance. The obtained COF/rGO provides a specific surface area of ~246 m^2 g^{-1}, lower than that of the pure COF (498 m^2 g^{-1}) due to the existence of rGO (Fig. 17b). By taking advantage of the morphology of the rGO aerogel and the surface-grown COFs, the COF/rGO aerogel exhibits a low density of ~7.0 mg cm^{-3}, which is light enough to be held by a leaf (Fig. 17c). In addition, the COF/rGO composite shows good mechanical strength without breaking when undergoing repeated compression and expansion. As a result of the good electron transport within graphene networks, the COF/rGO aerogel could be applied as an electrode directly for supercapacitors without the addition of conducting binders or additives.

In comparison to rGO and pristine COFs, the COF/rGO showed a superior capacitance (269 F g^{-1} at 0.5 A g^{-1}) and enhanced cycling stability (Fig. 17d and e), which were higher than most of the reported COF-based electrodes.

Similar to graphene, CNTs have also been used to fabricate hybrid composites with COF materials.[222] Very recently, Zhang's group has reported an olefin-linked COF by introducing 1,3,5-triazine units and 3,5-dicyano-2,4,6-trimethylpyridine into the molecular framework.[223] The obtained conjugated COF was assembled with CNTs to form a flexible thin-film as the supercapacitor electrode, which exhibited an areal capacitance of ~15.2 mF cm^{-2} and an energy density of ~7.3 mW h cm^{-3}. It was demonstrated that the synergetic effect of the electron delocalization of olefin-linkages as well as the conductive CNTs could facilitate the electron transport *via* a strong π–π affinity between them, leading to an improved supercapacitor performance. Furthermore, the introduction of CNTs enabled the construction of free-standing COF/CNT thin films, which possess good capability and flexibility, showing promising application in the development of flexible and wearable devices as electrode materials.

As mentioned before, carbon-based materials with suitable pore size distribution and high specific surface area have been applied as electrode materials for supercapacitors. COF-derived carbons have also been investigated for this application as heteroatom-doped carbons,[114,224–227] hierarchically porous carbons,[228] porous carbon with a core–shell structure[115] and carbon nanoparticles.[229] It is supposed that the regular arrangement of heteroatoms and ordered structures make COF materials promising precursors to construct heteroatom-doped carbons with tuneable porosities, controllable morphologies and high surface areas. Xu and co-workers reported a hierarchically porous B-doped carbon with meso/microporous structures using COFs as precursors, where improved porosities were achieved by applying $ZnCl_2$ as a template *via* a molten-salt approach.[228] The obtained hierarchically porous carbons exhibited a specific surface area of 1828 m^2 g^{-1} and supercapacitive performance with specific capacitance of 160 F g^{-1}. However, it can be of course questioned if COF-derived carbons are really competitive electrode materials compared to traditional carbons (*e.g.* activated carbons) considering their sophisticated synthesis and consequently higher cost.

3.2.2 Rechargeable batteries. Rechargeable batteries (including Li-ion batteries, Li–S batteries, Na-ion batteries, *etc.*) are currently intensively discussed and applied to enable emission free electric vehicles.[6,230] In rechargeable batteries, the metal ions transfer between an anode and cathode during the charging/discharging process. Currently, a significant challenge in rechargeable batteries is to design high energy electrode materials, with high electrochemical performance without scarifying their chemical and mechanical stability during long-term cycles. The close relationship between electrode materials and battery performances including specific capacity, charge–discharge ability and recycle stability could provide insight into the design principle of efficient electrode materials. In this section, we concentrate on the COF-based electrode materials and discuss their potential applications in Li-ion batteries, Li–S batteries and Na-ion batteries.

As the most widely utilized member in the rechargeable battery family, Li-ion batteries (LIBs) have many advantages regarding their high energy density, low self-discharge and large voltage window, and are therefore applied successfully in many everyday applications. However, the slow kinetics, poor power density, concerns of safety, cost, Li scarcity and low longevity create major challenges to their practical applications in electric vehicles.[231] Currently, the rational design of advanced electrode materials is applied to address the above concerns. In particular, the performance of anodes provide large room for improvement in terms of higher power density and better cycling stability.[232–234] Currently, commercial LIB anodes are built from carbon materials because of the good electric conductivity, hierarchical structures for lithium ion intercalation and low cost.[235,236] However, the graphite anodes generally face the problems of low specific capacity and safety issues. Thus, a vast amount of research work is being conducted to study alternatives, including metal anodes (such as Sn, Sb, Al, Mg, Ag and their alloys),[232,237,238] transition metal oxides[239–241] and silicon.[242,243]

Recently, COF-based materials have also been explored as potential anode materials in LIBs due to their layered and porous structures, which should allow facile charge carrier transport. In particular, the 2D structures of COFs provide sufficient internal channels for lithium atom insertion/adsorption and short-ended paths for fast lithium ion diffusion. It was demonstrated by theoretical calculations that 2D COFs preferred to adsorb lithium atoms in a regular symmetry, and lithium atoms tended to cross the 1D pores efficiently due to the low energy barrier, enhancing Li storage capacity.[244] Zhao's group reported two conjugated COFs as anodes for Li-ion batteries by the condensation of aldehydes and amines under solvothermal conditions (N2-COF and N3-COF),[245] where the numbers indicate the amino groups in the amino derivatives (Fig. 18a and b). When applied to a Li-ion battery as an anode material, the as-fabricated N2-COF exhibited a charge capacity of 600 mA h g^{-1} with a capacity retention of 82% after 500 cycles. For the battery with N3-COF as the anode, a similar performance was observed (593 mA h g^{-1}) with a capacity retention of 81% (Fig. 18c and d). Moreover, the cycling stability of N2-COF and N3-COF were conducted at different current densities (0.2–5 A g^{-1}) (Fig. 18e). The charge capacity of N2-COF shows a slight decrease from ~806 to 497 mA h g^{-1} with increase of the current density from 0.2 to 5C. When the current density decreased from 5 to 2C, the N2-COF exhibits a recovered capacity of 607 mA h g^{-1}, proving its stability over multiple cycles and various current densities. A similar result can be observed with the N3-COF (Fig. 18f). The performance of N-COFs in LIBs was attributed to the uniform porosity, conjugated structures and considerable chemical stability, showing the promising application of COFs for Li-ion batteries.

Liu and co-workers have designed a conductive 2D COF (TThPP), where polyporphyrin moieties were connected by 4-thiophenephenyl groups *via in situ* oxidative polymerization

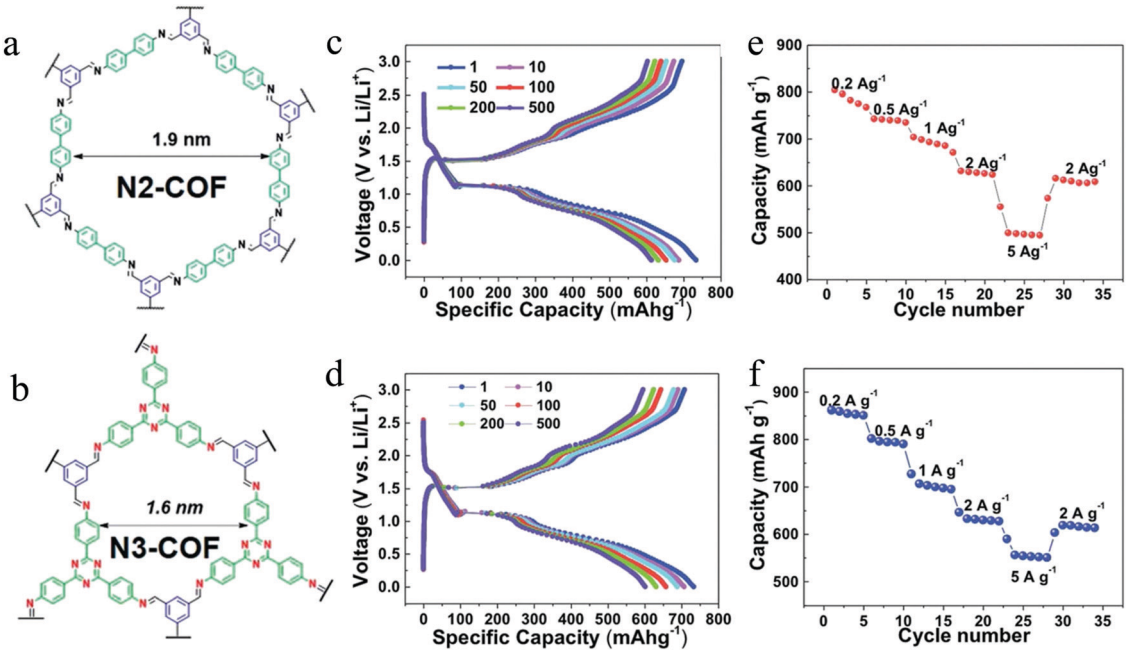

Fig. 18 Structures of (a) N2-COF and (b) N3-COF; charge–discharge cycles at 1 A g^{-1} of (c) N2-COF and (d) N3-COF; chemical stability tests at different current densities (0.2–5 A g^{-1}) of (e) N2-COF and (f) N3-COF. Reproduced from ref. 245 with permission from the Royal Society of Chemistry, copyright 2016.

where porphyrin and thiophene serve as the core and linking bridge, respectively.[246] When the TThPP was grown on the surface of a copper foil to be used as an anode material in a LIB, the COF-based polyporphyrin film exhibits good electrical conductivity with a reversible capacity of ~666 mA h g^{-1}. The high conductivity and capacity of TThPP was attributed to an eclipsed alignment of the polyporphyrin sheets, which can promote the process of charge transfer within the frameworks. To further increase the conductivity and stability, carbon-based conductive materials such as CNTs and graphene were also utilized for the preparation of composites with COFs, forming hybrid electrode materials for Li-ion batteries. For instance, Wang and co-workers synthesized a hybrid COF@CNT composite as the anode material. It was observed that the CNTs could affect the growth process of COFs, and consequently were coated by few-layered COFs *via* π–π interaction (Fig. 19).[42] The as-fabricated COF@CNT composite exhibits a high reversible capacity of 1536 mA h g^{-1} with good retention after 500 cycles at 100 mA g^{-1}. The long-term stability can be ascribed to the few-layered morphology of the COFs and the good conductivity of CNTs within the hybrid composite.

Recently, Li–S batteries have received much attention due to their high theoretical energy density, gravimetric capacity and low production costs.[247] Compared with traditional cathode materials such as $LiFePO_4$ and $LiCoO_2$, the usage of a sulfur cathode endows Li–S batteries with a relatively high theoretical gravimetric capacity of 1672 mA h g^{-1}.[248] However, before applying it into practical applications, some issues need to be considered, including the formation of soluble lithium polysulfides (Li_2S_x, $3 \leq x \leq 8$) and insoluble sulfides (Li_2S_2/Li_2S) in the charge–discharge process.[248] It is supposed that the dissolved polysulfides could lead to the low efficiency and poor stability of Li–S batteries due to the shuttle effect in the charging process between cathode and anode. Thus, development of advanced materials as a sulfur cathode, which can effectively inhibit the loss of soluble intermediates, would have a significant impact in this field. Since COF materials possess high porosity, low density and robustness, and their open pores and rigid networks can promote the transport of electrolyte ions, it is proposed that COFs could become potential cathode materials for hosting sulphur in Li–S batteries.[249–251] In this regard, CTFs, a distinct class of nitrogen-rich COF materials, were applied for the first time as a novel host material for the insertion of sulphur to capture dissolved polysulfides, thus enhancing the stability of Li–S batteries.[122] This work paved the way to applying COF materials as cathode materials for Li–S batteries, but it should be noticed that more advanced methods and strategies still need to be developed to improve the performance of the COF-based sulfur cathodes.

For utilizing the long-range ordering and high porosity present in COFs, the same group further explored the applications of COFs for Li–S batteries by designing a 2D porphyrin-based COF (Por-COF) with large pore volume and narrow pore size distribution, which was used as a host for sulphur storage (Fig. 20a and b).[252] The galvanostatic charge/discharge test of Por-COF/S was conducted at a current rate of 0.5C in the voltage range of 1.8–2.7 V (Fig. 20c). Two plateaus were found both in discharge curves and charge curves (2.1 and 2.3 V for discharge curves; 2.25 and 2.37 V for charge curves), indicating the reversible redox reaction between sulfur and lithium polysulfides (Li_2S_x, $2 < x < 8$). The discharge capacity of the Por-COF/S was calculated after three cycles, which was almost

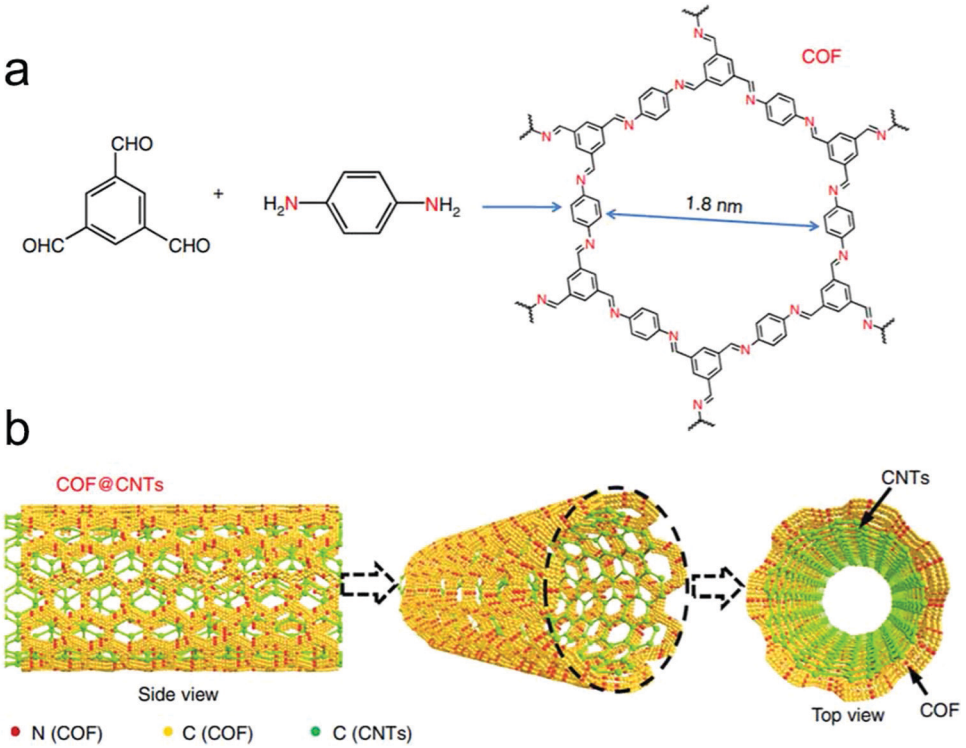

Fig. 19 (a) Synthesis and structure of COFs; (b) schematic illustration of COF@CNTs with few-layered COFs on the CNT surface. Reproduced from ref. 42 with permission from Springer Nature, copyright 2018.

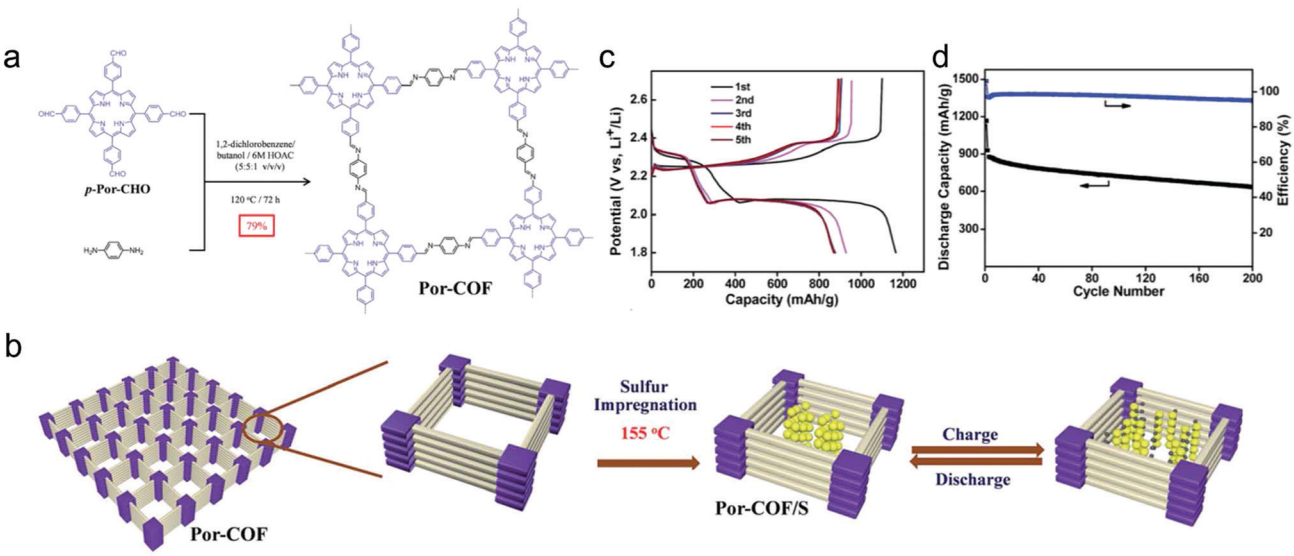

Fig. 20 (a) Synthesis and structure of Por-COF; (b) schematic representation of the charge and discharge process of the Por-COF/S; (c) galvanostatic charge and discharge profiles of the Por-COF/S at a rate of 0.5C; (d) cycling stability and coulombic efficiency of the Por-COF/S at a rate of 0.5C. Reproduced from ref. 252 with permission from the Royal Society of Chemistry, copyright 2016.

unchanged and maintained at 870 mA h g^{-1}. In addition, the cycling performance was evaluated at a charge/discharge rate of 0.5C where the Por-COF/S possessed a capacity of 633 mA h g^{-1} after 200 cycles, with a capacity decay rate of 0.16% per cycle, indicating its stable cycling performance. Moreover, the coulombic efficiency of the Por-COF/S was calculated to be 96% in the cycling process, demonstrating the alleviation of the shuttle effect from dissolved polysulfides (Fig. 20d). In comparison to their previous study, the loaded sulphur within the large pore volume of Por-COF is responsible for the improved cycling performance.

It is supposed that physically isolated sulphur in the COF channels cannot satisfy the prevention of the shuttle effect

from Li–S intermediates, thus leading to an unsatisfactory energy storage performance. To suppress the shuttle effect, recently, the immobilization of polysulfide chains on the pore walls of COFs was demonstrated, and a series of functionalized COFs has been designed by grafting polysulfide chains on the pore walls through covalent coupling.[69,253,254] For example, Jiang's group designed an imine-linked COF by the condensation of 1,3,6,8-tetrakis(4-formylphenyl) pyrene (TFPPy) and 4,4′,4″,4‴-(ethene-1,1,2,2-tetrayl)tetraaniline (ETTA) *via* a solvothermal method (Fig. 21a).[254] The imine linkages (C═N) present in the COF (TFPPy–ETTA-COF) can induce the polymerization of sulphur to form polysulfide chains at elevated temperatures, which can be anchored covalently on the channel walls *via* C–S bonds. As the impact of polysulfide chains grow within COF channels, the as-synthesized polysulfide@TFPPy–ETTA-COF exhibits a capacity of 1069 mA h g^{-1} with a long discharge/charge plateau, which is much higher than that of S@TFPPY–ETTA-COF (723 mA h g^{-1}), where sulfur is just incorporated in the pores (Fig. 21b). Considering the remarkable enhancement of performance, it has been confirmed that the polysulfide chains can both promote the capacity and the efficiency of sulfur utilization. In addition, the cycling performances conducted at 0.1C showed the superior capacity of polysulfide@TFPPy–ETTA-COF to S@TFPPy–ETTA-COF, while the coulombic efficiency did not change during cycling (Fig. 21c). It is supposed that the anchored polysulfide chains are the redox-active sites and suppress the shuttle effect. Apart from the immobilization of polysulfide chains, morphology-controlled engineering was developed for the preparation of porphyrin COFs with hollow spherical structures (POF-HSs).[255] The POF-HSs show two effects, namely physical confinement and chemical adsorption of polysulfides, thus alleviating the shuttle effect of polysulfides.

In addition to LIBs and Li–S batteries, all-solid-state Li-ion batteries, as next-generation energy storage devices, have attracted much attention in recent years. To achieve high-performance of

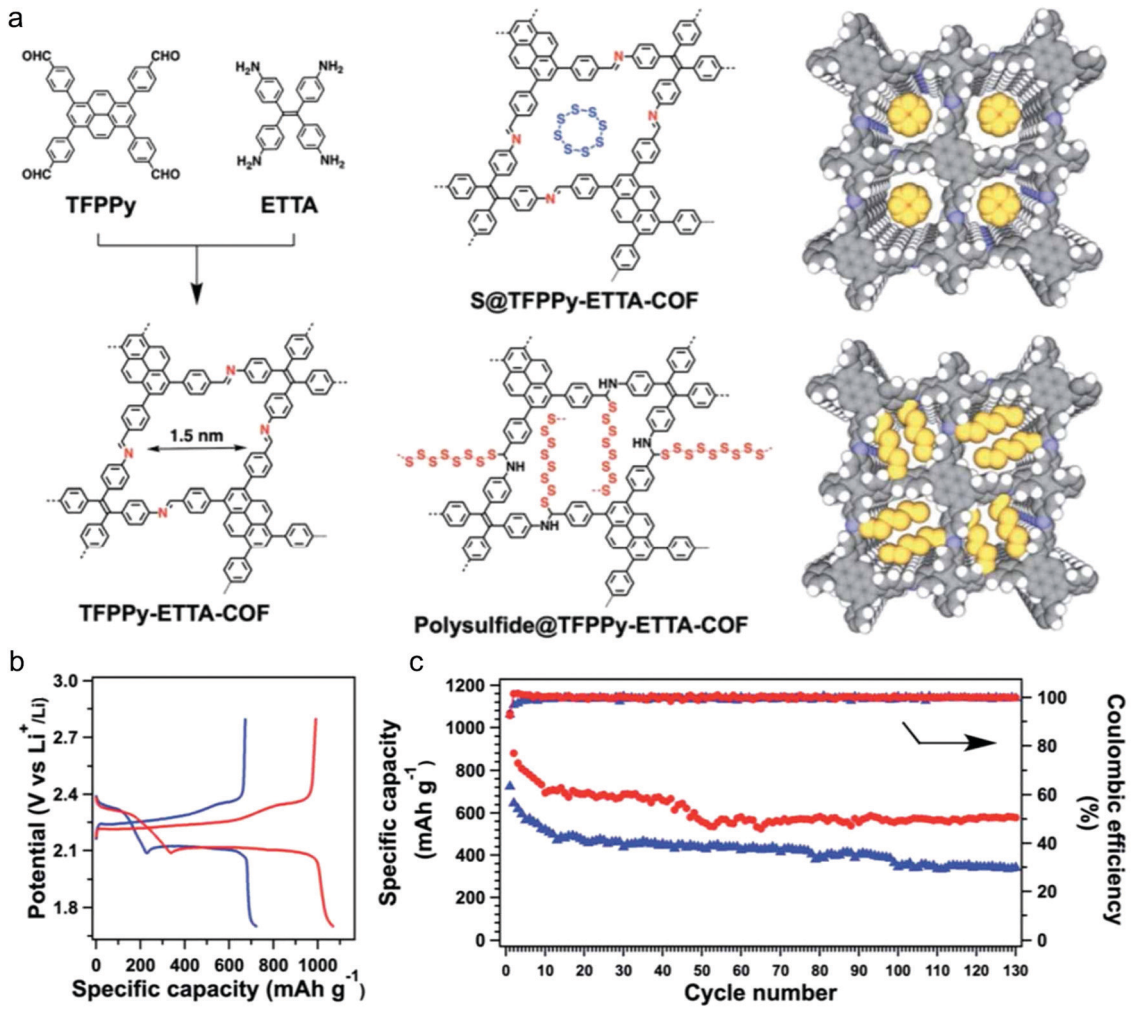

Fig. 21 (a) Structure of TFPPy–ETTA-COF and schematic representation of polysulfide@TFPPy–ETTA-COF; (b) galvanostatic charge–discharge tests of polysulfide@TFPPy–ETTA-COF (red) and S@TFPPy–ETTA-COF (blue) at a rate of 0.1C; (c) chemical stability and coulombic efficiency of polysulfide@TFPPy–ETTA-COF (red) and S@TFPPy–ETTA-COF (blue) at a rate of 0.1C. Reproduced from ref. 254 with permission from the Royal Society of Chemistry, copyright 2019.

an all-solid-state Li-ion batteries, the development of advanced solid electrolytes could be the key determinant. Key materials for the all-solid-state lithium batteries are solid electrolytes, and are generally oxide- and sulfide-based materials. Although several materials have been applied as solid electrolytes such as oxide- and sulfide-based materials, some problems still remain for practical applications.[256] A big challenge could be the formation of an internal short-circuit in the charging–discharging process. To solve this problem, organic materials with good ion conductivity could be an option. In this regard, ionic COFs have been explored as a Li-conducting solid electrolyte in Li-ion batteries due to their high ion conductivity. For example, Zhang's group synthesized a novel type of ionic COFs containing hybridized boron anionic centres and tuneable counter cations [$(NMe_2)^+$ for ICOF-1 and Li^+ for ICOF-2].[257] By taking advantage of the high accessibility of Li ions, ICOF-2 exhibited a high Li-ion conductivity (3.05×10^{-5} S cm^{-1}) and a Li^+ transfer number value of $\sim$0.80, achieving the efficient transportation of Li ion at room-temperature. In similar efforts, a 3D anionic COF was synthesized through the condensation of trimethyl borate and hydroxy groups in γ-cyclodextrin (γ-CD), where the formed tetrakis(spiroborate) tetrahedra needed to balance their negative charge with counterions.[132] Because of the insertion of flexible moieties, the formed COFs (CD-COFs) provide a high Li-ion conductivity of $\sim$2.7 mS cm^{-1} and long-term Li-ion stripping/plating stability. In addition, polyelectrolyte COFs were reported by Jiang's group by introducing flexible oligo(ethylene oxide) chains into the COF pores.[258] When complexed with Li ions, the polyelectrolyte COF shows enhanced ion conductivity, cycle life and thermal stability that extend the potential applications of COF materials as solid-state ion conductors in Li-ion batteries.

Similar to Li-ion batteries, the sodium-ion battery (NIB) is another type of rechargeable battery that uses sodium ions (Na^+) as the charge carriers, which are much more abundant than Li-ions. Considering the larger size of Na^+, COF materials having soft and flexible structures can help in buffering the large volume expansion during sodiation. In addition, the insertion of redox-active sites into COF skeletons, which is desirable to construct COF-based anode materials for Na-ion batteries.[56,259] As mentioned above, DAAQ–TFP COFs with redox-active anthraquinone moieties have been applied as electrode materials for pseudocapacitors (Fig. 14). Recently, Lu and co-workers applied this redox-active COF (DAAQ–TFP COF) also as an anode for Na-ion batteries (Fig. 22a).[56] With different exfoliation processes for the DAAQ-COF, four samples were obtained with thicknesses of 4–12 nm, 50–85 nm, 100–180 nm and 100–250 nm (Fig. 22b). Consequently, the cycling performance of samples with different thicknesses was tested at a rate of 100 mA g^{-1} showing that the 4–12 nm sample exhibit superior capacity (420 mA h g^{-1}) in comparison to the thicker samples. This was attributed to the weak stacking interaction of 2D-COFs which may enhance the capacity and stability by restraining the self-exchange behaviour of the interlayer electrons and creating more accessible active sites. In addition, the 4–12 nm sample also showed a good cycling stability with 99% retention at 5 A g^{-1} over 10 000 cycles (Fig. 22c). Moreover, the authors demonstrated that radical intermediates (C–O$^{\bullet}$ and α-C) are of importance in the sodiation–desodiation

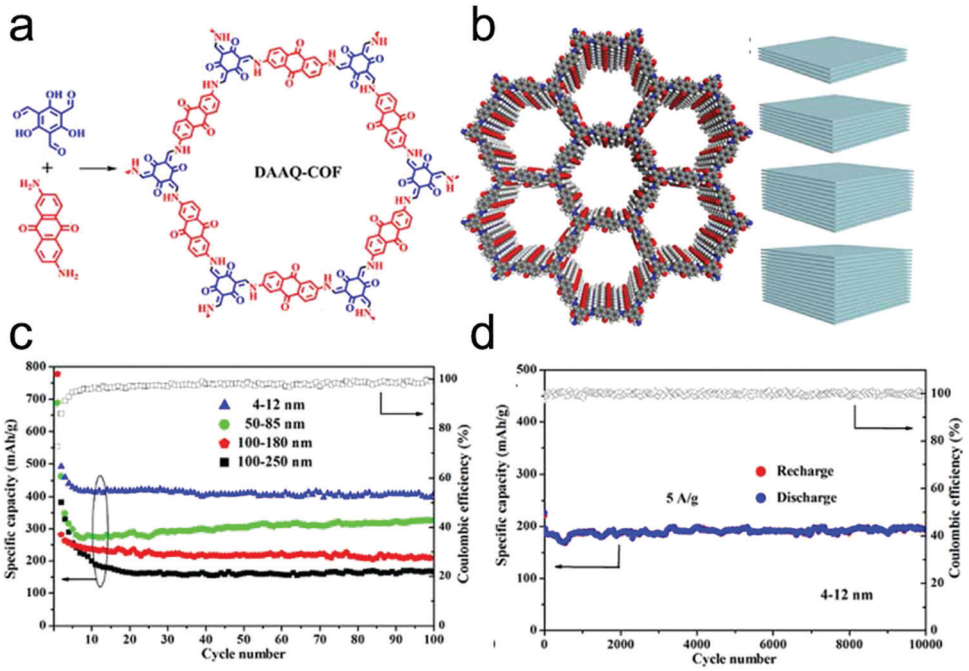

Fig. 22 (a) Synthetic route and structure of DAAQ-COF; (b) simulated structure of DAAQ-COF and the schematic representation of the stacked 2D-COF with different thicknesses; (c) cycling performance of 2D-COFs with different thicknesses and the coulombic efficiency of the 4–12 nm thick COF at 100 mA g^{-1}; (d) cycling performance of the COF with a thickness of 4–12 nm at 5 A g^{-1}. Reproduced from ref. 56 with permission from the American Chemical Society, copyright 2019.

process, and their redox activity and stability could be determined by the stacking behaviour of COFs.

In summary, COFs have shown to efficiently enhance the energy storage capacity in rechargeable batteries as a combined result of the presence of ordered channels, high porosities and possible integration of redox moieties. Even though the application of COFs in this field is still in an initial stage, their comparable performances to those of other reported materials show their promising applications in energy storage devices.

3.2.3 Fuel cells. In comparison to traditional power sources, fuel cells possess many advantages including high conversion efficiency, low maintenance, portability, and environmental friendliness. Among them, proton exchange membrane fuel cells (PEMFCs) are operated at a low temperature range in which COFs can be applied. As a critical component of PEMFCs, the proton exchange membrane (PEM) takes charge of the transport of protons from the anode to cathode, thus recombining with oxygen to form water. Thus, designing the PEMs is referred to as the heart of the PEMFC, and the proton conduction materials have subsequently spurred tremendous interest among researchers. Since the production of the perfluorosulfonic acid membrane with polytetrafluoroethylene as a support, which is called 'Nafion', it soon became a standard for PEMFC and remains so to date.[260] However, the upper operation temperature of Nafion is low (only 80–100 °C) and it has been observed that its proton conductivity significantly drops after 100 °C.[261] Currently, many other types of PEMs have been developed, including polymeric,[262,263] ceramic[264] and inorganic–organic composite membranes, aiming at designing a stable PEM with high proton conductivity.[265]

COF materials are relatively lightweight, provide a variety of functionalities and have membrane processability like polymers through chemical or physical modifications. The high degree of internal ordering within COFs can also facilitate loading and transport of proton conducting substrates.[266] As a proof of concept, Banerjee's group reported an azo (–N=N–)-functionalized COF (Tp–Azo COF) through the reaction between triformylphloroglucinol (Tp) and 4,4′-azodianiline (Azo) (Fig. 23a).[267] The as-synthesized COFs are comprised of β-ketoenamine-linkages that yield enhanced chemical stability against acids, ensuring the sustainability under harsh conditions in fuel cells. Because of the introduction of phosphoric acid (H_3PO_4) into the framework, the azo units were protonated and then formed hydrogen bonds with $H_2PO_4^-$. Consequently, a hydrogen-bonding network was formed in the 1D channels with further interaction with free H_3PO_4 molecules (Fig. 23b). The reported proton conductivity values could reach 6.7×10^{-5} S cm^{-1} under anhydrous conditions and 9.9×10^{-4} S cm^{-1} under 98% relative humidity (Fig. 23d and e). These results indicate the potential of COF-based functional proton conducting materials for applications in fuel cells. As such, in the following years, Banerjee's group reported several proton conductive COF materials based on β-ketoenamine-linkage COFs, such as sulfonic-acid-based COF (TpPa-SO_3H) with intrinsic proton conductivity under anhydrous conditions[79] and mechanochemically synthesized bipyridine-COF with H_3PO_4 incorporation.[268]

Beyond the doping of porous materials with acids, it has been shown that heterocyclic bases can be utilized as proton conducting materials. In this case, the strength of hydrogen bonding interactions could be weak, and the rotation of acid and base molecules could become possible. As expected, a high level of proton conductivity can be achieved *via* the Grotthuss mechanism. In order to achieve this level of proton conductivity in COFs, Jiang's group reported a mesoporous COF (TPB–DMTP-COF) through the reaction between 2,5-dimethoxyterephthalaldehyde (DMTP) and 1,3,5-tri(4-aminophenyl)benzene (TPB) *via* a solvothermal method (Fig. 23f).[65] The authors studied the proton conduction across mesoporous channels in this framework, which could be applied as a host material for loading proton carriers. In this work, triazole and imidazole were chosen as N-heterocyclic proton carriers, providing trz@TPB–DMTP-COF and im@TPB–DMTP-COF with high loading capacities of 180 and 155 wt%, respectively. The frameworks can achieve satisfying proton conductivities (4.37×10^{-3} S cm^{-1} at 130 °C) that are 2–4 orders of magnitude higher than those of microporous and non-porous polymers, implying the importance of doping N-heterocyclic proton carriers for enhanced proton conductivity. Another work about proton conductive COF was reported by Zhu's group, who introduced a cationic COF that was synthesized by combining a cationic monomer, ethidium bromide (EB) (3,8-diamino-5-ethyl-6-phenylphenanthridinium bromide), with 1,3,5-triformylphloroglucinol (TFP) *via* Schiff base reactions. By immobilizing $PW_{12}O_{40}^{3-}$ into this porous cationic framework, the proton conductivity was found to be enhanced to 3.32×10^{-3} S cm^{-1} at 97% relative humidity. These contributions have shown the promising applications of COF materials in fuel cells and will probably encourage researchers to further design functional COF-based proton conducting materials. Although moderate values have been achieved using COFs as a proton conductor, most of the reported materials show conductivities only after doping with acids or N-heterocyclic proton carriers, limiting the utility of COFs for real time applications. On the other hand, because of their robust covalent backbone structures, COFs are generally synthesized as fluffy microcrystalline powders with low processability. It is practically difficult to post-fabricate COF powders for the demands of membrane separation technology. Even though additives and binders are generally used to achieve the fabrication of COF membranes, the possible pore blocking effect from the additives can decrease the accessibility of well-defined pores and functional ligands.[269]

3.3 Electrochemical sensors

Electrochemical sensors have gained extensive attention for the analysis of species of biological, environmental and industrial interest.[270] Typically, an electrochemical sensor consists of a working electrode and a counter electrode connected by a certain electrolyte. Through the reaction between working electrode and analytes, electric signals can be recorded, which are proportional to the analyte concentrations. In comparison with the applications in electrocatalysis and energy storage, just a few COFs have been applied as electrochemical sensors.

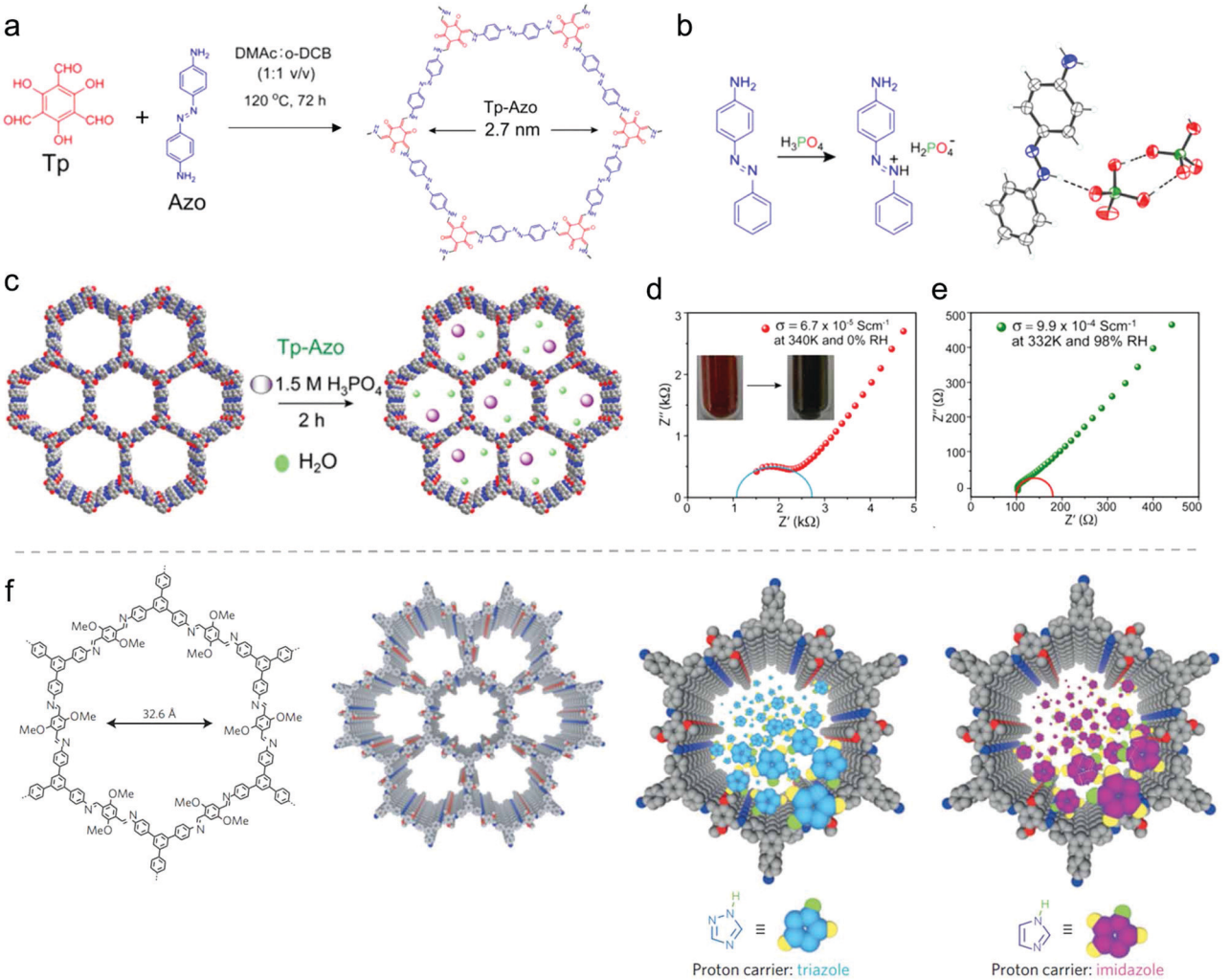

Fig. 23 (a) Synthesis and structure of Tp–Azo; (b) the formation of hydrogen bonding between $H_2PO_4^-$ anion and azo units; (c) schematic illustration of H_3PO_4 doping in COFs; (d) proton conductivities of PA@Tp–Azo under anhydrous conditions. Inset image shows a distinct color change (red to black) in Tp-Azo COF powder upon H_3PO_4 treatment; (e) proton conductivities of PA@Tp–Azo under hydrous conditions; (f) proton conduction across 1D mesopores of crystalline COFs with different proton carriers. Reproduced from ref. 267 with permission from the American Chemical Society, copyright 2014; and ref. 65 with permission from Springer Nature, copyright 2016.

The low density and high surface areas of COFs can be considered as an ideal platform for adsorption/separation and detection/sensing.[271,272] In addition, depending on the modular nature of COFs, their pore structures and functional groups can be tailored independently, thus enabling the introduction of electroactive sites/groups into COF channels to potentially bind and detect the specific species. For example, Zhu and co-workers have recently applied DAAQ–TFP COF (DQ-COF) as a substrate to study its capability for the removal and electrochemical detection of hydrazine from water solutions.[273] By virtue of the high surface area and the presence of abundant anthraquinone sites, DQ-COF exhibits a hydrazine removal capability as high as 1108 mg g^{-1}. Consequently, the DQ-COF was dropped onto a nickel matrix to form the DQ-COF/Ni composite (DQ-COF/Ni), which was further applied for the detection of hydrazine by using an amperometry technique.[274] As revealed, DQ-COF/Ni presents a wider linear range (0.5–1223 μM) and lower detection limit (0.07 μM) towards hydrazine detection than those of reported hydrazine sensors (*e.g.* $NiCo_2O_4$[275] and MnO_2[276]). Its high detection performance was attributed to the synergistic effect of the electroactive DQ-COF and Ni matrix accompanied by the enhanced electron transfer. Apart from hydrazine, environmental pollutants, such as heavy metals (*e.g.* lead[277]), nitrophenol[278] and bisphenol A[279] have also been studied as detection species by using COF-based electrochemical sensors.

Biomedical analysis is another prominent area for COF applications *via* electrochemical sensing. Analytes such as dopamine,[280] glucose,[281] H_2O_2,[282] ascorbic acid (AA)[283] and prostate specific antigen (PSA)[284] have shown positive electrochemical responses to COF-based materials. To further improve the detection performance, COFs are generally constructed with other functional materials to form COF-based composites, to enhance their selectivity or sensitivity for detection molecules. For example, metal nanoparticles (NPs) are widely applied in

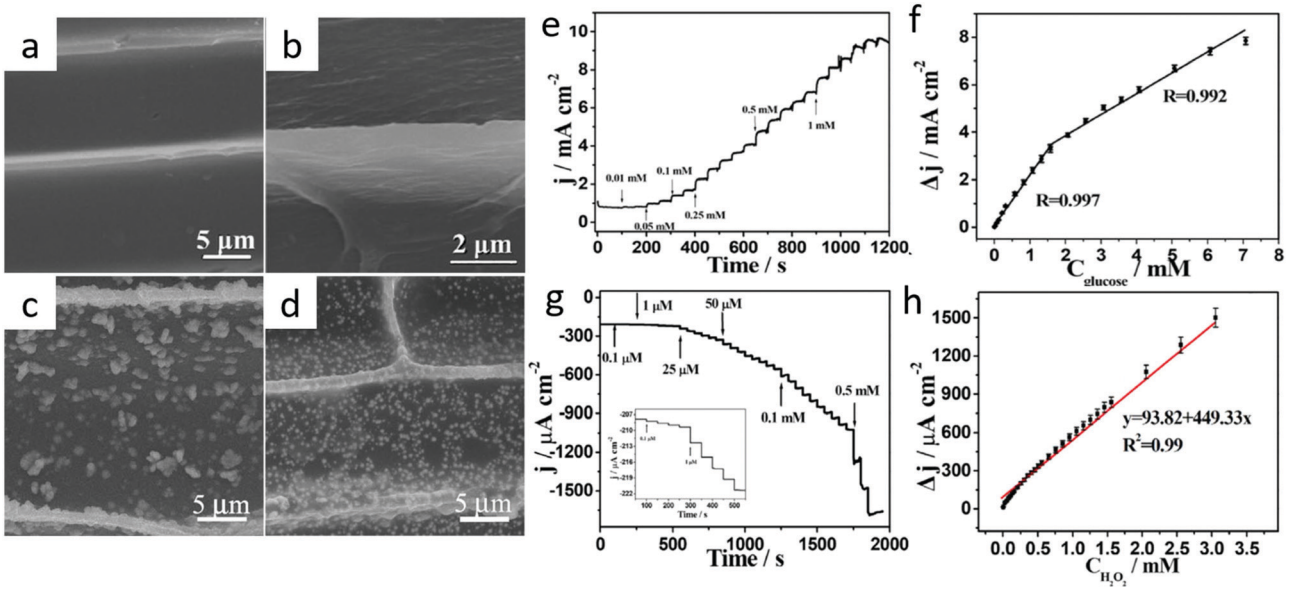

Fig. 24 SEM images of (a) 3D-KSC; (b) 3D-KSC/COFTAPB–PDA; (c) 3D-KSC/COFTAPB–PDA/CuNPs and (d) 3D-KSC/COFTAPB–PDA/PtNPs; (e) amperometric response of 3D-KSC/COFTAPB–PDA/CuNPs under stirring in 0.1 M NaOH solution with continuous addition of glucose; (f) linear relationship between current density and glucose concentration; (g) amperometric response of 3D-KSC/COFTAPB–PDA/PtNPs under stirring in 0.2 M PBS (pH = 7.0) solution with continuous addition of H_2O_2. Inset: Magnification part of the curve; (h) linear relationship between current density and H_2O_2 concentration. Reproduced from ref. 281 with permission from Elsevier Inc, copyright 2019.

detecting targeted compounds such as glucose (Cu NPs) and H_2O_2 (Pt NPs). To avoid the aggregation of metal NPs during the deposition process, Wang and co-workers designed a functionalized 3D porous carbon–COF hybrid (3D-KSC/$COF_{TAPB-PDA}$), by growing a COF thin film ($COF_{TAPB-PDA}$, TAPB: 1,3,5-tris(4-aminophenyl)benzene, PDA: 1,4-phthalaldehyde) on pore walls of 3D-KSC.[281] By taking advantage of the exposed active sites in the COF film, the spherical Cu and Pt nanoparticles were deposited uniformly on the 3D-KSC/$COF_{TAPB-PDA}$ electrode by electrostatic potential deposition, named 3D-KSC/$COF_{TAPB-PDA}$/CuNPs and 3D-KSC/$COF_{TAPB-PDA}$/PtNPs, respectively (Fig. 24a–d). After optimization, the amperometric response of 3D-KSC/$COF_{TAPB-PDA}$/CuNPs was recorded by continuously adding glucose solution at 0.5 V (Fig. 24e). As shown in Fig. 24f, the linear range of glucose detection by 3D-KSC/$COF_{TAPB-PDA}$/CuNPs was 4.69 μM–1.57 mM and 1.57–7.07 mM with a detection limit of 1.54 μM. The result was much better than those of 3D-KSC/CuNPs (6.33 μM–4.07 mM, and detection limit of 2.08 μM) as well as some of the Cu/Cu_xO related electrochemical sensors.[285] Similarly, the 3D-KSC/$COF_{TAPB-PDA}$/PtNPs also provided a comparable performance in the detection of H_2O_2 (Fig. 24g and h).

4. Chemical stability of COFs and their impact on electrochemical operations

The periodicity in COF structures is achieved *via* dynamic covalent chemistry. In this regard, a high crystallinity in COFs is always then observed when good reversibility of the newly formed covalent bonds is ensured. This naturally means that the bonds can be easily opened again, consequently resulting in limited chemical stability. Indeed, crystallinity and stability seem to be contradictory properties of COFs. Thus, the first reported boroxine and boronate-ester COFs have been found to be unstable in water and even under humid conditions, as the linkages are susceptible to attack by nucleophiles (*e.g.*, water molecules) at the electron-deficient boron sites.[16] As such, boroxine and boronate-ester COFs have several limitations for real applications, especially those involving aqueous solutions for electrocatalysis (HER, OER, ORR, *etc.*). To circumvent these limitations, various novel linkages have been explored for the construction of COFs in recent years (Fig. 25). Covalent triazine frameworks (CTFs) synthesized by the cyano-trimerization are found to be extremely robust towards strong acid or base environments as well as in the presence of strong oxidizing and reducing agents, and thus were considered as promising candidates for a range of electrochemical applications.[286,287] Nevertheless, to ensure reversibility, the triazine formation was carried out under harsh conditions in salt melts, which limits the amount of applicable monomers and also yielded defect-rich materials with lower crystallinity.[269]

Imine,[288] azine[289] and hydrazone[290] COFs linked by C=N bonds exhibit superior hydrolytic stability compared to that of the first reported boron-based COFs. The chemical stability of most imine, azine and hydrazone COFs is however still unsatisfactory since they undergo hydrolysis under acidic conditions, resulting in some limitations for their electrochemical applications in acidic media.[291] Notably, β-ketoenamine-linked COFs offer a much enhanced stability in aqueous, acidic and basic media, due to the irreversible tautomerization of their initially formed imines. Indeed β-ketoenamine-linked COFs with

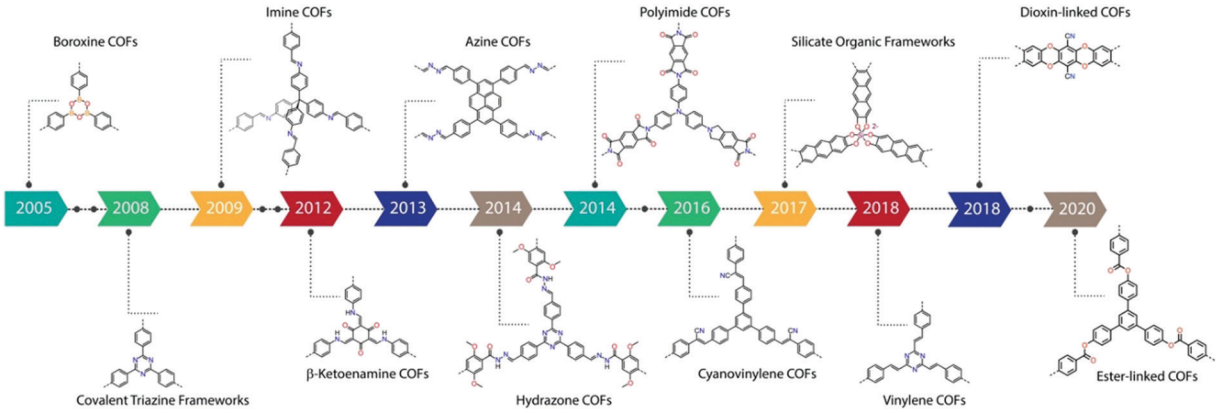

Fig. 25 Synthetic approaches and accompanying linkages used for the synthesis of two- and three-dimensional COFs.

varying porosity and diverse functionalities have been tested for various electrochemical applications such as OER, ORR, supercapacitors, batteries and proton conductivity.[41,55,269]

Polyimide COFs show good framework retention in pure water and acid solutions; however, alkali aqueous solutions significantly affect the framework stability due to the nucleophilic substitution in the presence of a base.[292] Due to their limited chemical stability, silicate organic frameworks (Si-COFs) have not been explored for electrocatalysis.[33] However, cyanovinylene and vinylene-linked COFs possessing fully conjugated backbones are very promising, and are significantly less prone to hydrolysis compared to boroxine,[16] boronate ester,[293] or imine[288] linkages, while still showing high crystallinity. Indeed, shortly after their discovery, cyanovinylene and vinylene-linked COFs have already been used for electrocatalytic applications.[294–296] Similarly, dioxin(polyarylether)- and ester-linked COFs show considerable chemical stability, which might be useful for exploring their electrochemical applications.[297]

Nonetheless, beside the increasing stability of COFs in acid or basic media, there are still some other issues, which have to be considered before applying the COFs for practical applications, especially when a voltage is applied over a long-term operation. Concerns regarding COFs in long-term applications are the evolution of morphology/structure of COFs and of initially well-defined active sites in electrolytes under applied voltages. For example, when a Co-bipyridine-based COF was applied as an electrocatalyst for oxygen production, the conversion of Co(II) to Co(III) was detected, to form cobalt hydroxide/oxyhydroxide on the surface after long-term OER operation, both of which are also OER active.[36]

Besides, attributing electrochemical performance to the morphology/structure of COFs is valid only if the COF structure remains intact throughout the electrochemical process. So, it is crucial to analyse and discuss their structures before and after long-term operation, to identify the real active sites as well as the operational stability of constructed COF-based electrodes. Generally, *ex situ* characterizations of spent catalysts (*e.g.*, XRD, XPS, XANES, SEM and TEM) are a facile solution to illustrate structural changes of COFs. However, this can be problematic if an additive (Nafion, carbon, *etc.*) has to be added to the COF for the electrochemical testing. Furthermore, *in situ* techniques can be applied to detect formed intermediates and conversion of active centres during operation. Indeed, techniques like operando ambient pressure XPS,[158] *in situ* Raman spectroscopy[298] and *in situ* TEM[299] are commonly used nowadays in electrocatalytic/chemical processes and have enabled a detailed insight into reaction mechanisms and evolution of active sites.

5. Summary and outlook

Since the discovery of covalent organic frameworks in 2005 by Yaghi and co-workers, a series of COFs has been designed and synthesized targeting versatile applications. Given their controllable and well-defined structure, high porosity and surface area, COFs are promising materials for energy conversion and storage applications. Indeed, COFs feature certain advantages, which distinguish them from other typical materials used in this field. Compared to carbon- and graphene-based materials, there is at first very good structural control. By selection of appropriate linkage motifs and building blocks, materials with defined chemical structures, tuneable pore sizes and structures and low densities can be prepared, which are not seen in other typical carbon-based electrode materials. For example, metal-coordinating moieties in COFs can act as well-defined active sites for electrocatalysis or redox-active sites can enable an enhanced pseudocapacitive performance in supercapacitors or reversable processes in rechargeable batteries. On the other hand, the exclusive covalent connections can yield fully π-conjugated COFs enabling enhanced charge transport, which is often problematic in MOFs.

To achieve high and robust electrocatalytic performance, increasing the number of active sites and intrinsic activity of each individual active site is required, which is enabled by the high surface area of COFs. Meanwhile, as the redox reactions in electrocatalysis generally happen between electrolyte and electrodes along with ion transport and electron exchange, novel synthetic approaches of COF-based electrocatalysts focus on facilitating mass transport and promoting the electric conductivity during electrocatalytic processes. The introduction of

hierarchically porous structures and conducting materials into COFs is thus a promising option to create more advanced electrocatalysts.

In general, to design and fabricate efficient COF-based materials for electrochemical applications, different strategies have been developed, including:

(i) Chemical modifications: depending on the desired application in electrocatalysis, COF structures can be controlled by developing different strategies including backbone modification, functional group modifications and post-synthetic modifications.

(ii) Controlling COF structures on all length scales: COFs at the macroscopic length scale can combine their crystalline structures with the possibility to design architectures with well-defined morphologies and hybrid components, endowing them with good mass transfer and high conductivity.

COF-based materials have been applied as electrocatalysts, for HER, OER, ORR and CO_2RR, as electrodes in supercapacitors and rechargeable batteries and as solid electrolytes or proton conducting membranes in batteries and fuel cells. However, several challenges for COFs in energy applications still exist. Primarily, the low stability or limited durability largely limits the practical realization of COF materials in energy-related devices. Under strong aqueous acidic/alkaline electrolytes, the collapse of COF structures could cause that active centres are getting inaccessible and that mass as well as charge transport is impaired. In addition, the poor processability of COFs could be another main issue for their applications in electrocatalysis as most synthetic methods for COFs involve solvothermal reactions of precursors in sealed glass tubes at elevated temperatures, yielding completely insoluble powders comprised of randomly aggregated crystallites. This makes the integration of COF materials into energy-related devices challenging.

Therefore, it is desirable to develop synthetic and processing methodologies for construction of COFs with enhanced stability and processability that allow shaping, placing and orienting COFs as per necessity, while integrating them with other components of the devices for stable operation. For improving the electrocatalytic performance and energy storage performance in COFs, it seems furthermore necessary to improve their electrical conductivity. Growing of oriented COF thin films on a conducting support or the preparation of composites has been described as an option to achieve the same. Finally, using the new stable and fully conjugated COFs composed of cyanovinylene- or olefin-linkages will not only be advantageous for enhancing the recyclability (robustness), but also for improving charge transport properties that are mandatory for electrochemical applications.

Diverse building units and flexible molecular design are available for scientists to design COF-based electrocatalysts at the molecular level with precisely controllable active sites. COFs with their defined structures indeed offer the possibility to study optimal structures of active sites, and to understand the underlying chemical and electrochemical reactions. The combination of advanced *in situ*/*in operando* characterization techniques and computational tools, both of which can be more suitably applied to a crystalline material than to an amorphous or a rather ill-defined material, can indeed yield novel insight into structure–function relationships in electrochemical devices.

Conflicts of interest

There are no conflicts to declare.

Acknowledgements

This work was supported by the Natural Science Foundation of Hebei Province (E2020205004). The funding by the Deutsche Forschungsgemeinschaft (DFG, German Research Foundation) under Germany's Excellence Strategy – EXC 2008 – 390540038 – UniSysCat and Project TH 1463/12-1 and the Science Foundation of Hebei Normal University (L2020B13) is acknowledged.

References

1 W. Li, J. Liu and D. Y. Zhao, Mesoporous materials for energy conversion and storage devices, *Nat. Rev. Mater.*, 2016, **1**, 16023.
2 A. S. Arico, P. Bruce, B. Scrosati, J. M. Tarascon and W. Van Schalkwijk, Nanostructured materials for advanced energy conversion and storage devices, *Nat. Mater.*, 2005, **4**, 366–377.
3 X. X. Zou and Y. Zhang, Noble metal-free hydrogen evolution catalysts for water splitting, *Chem. Soc. Rev.*, 2015, **44**, 5148–5180.
4 H. Y. Jin, C. X. Guo, X. Liu, J. L. Liu, A. Vasileff, Y. Jiao, Y. Zheng and S. Z. Qiao, Emerging Two-Dimensional Nanomaterials for Electrocatalysis, *Chem. Rev.*, 2018, **118**, 6337–6408.
5 J. Wang, F. Xu, H. Y. Jin, Y. Q. Chen and Y. Wang, Non-Noble Metal-based Carbon Composites in Hydrogen Evolution Reaction: Fundamentals to Applications, *Adv. Mater.*, 2017, **29**, 1605838.
6 S. W. Lee, N. Yabuuchi, B. M. Gallant, S. Chen, B. S. Kim, P. T. Hammond and Y. Shao-Horn, High-power lithium batteries from functionalized carbon-nanotube electrodes, *Nat. Nanotechnol.*, 2010, **5**, 531–537.
7 P. F. Zhang, J. S. Zhang and S. Dai, Mesoporous Carbon Materials with Functional Compositions, *Chem. – Eur. J.*, 2017, **23**, 1986–1998.
8 M. R. Benzigar, S. N. Talapaneni, S. Joseph, K. Ramadass, G. Singh, J. Scaranto, U. Ravon, K. Al-Bahily and A. Vinu, Recent advances in functionalized micro and mesoporous carbon materials: synthesis and applications, *Chem. Soc. Rev.*, 2018, **47**, 2680–2721.
9 N. Chaoui, M. Trunk, R. Dawson, J. Schmidt and A. Thomas, Trends and challenges for microporous polymers, *Chem. Soc. Rev.*, 2017, **46**, 3302–3321.

10 J. T. Zhang, Z. H. Xia and L. M. Dai, Carbon-based electrocatalysts for advanced energy conversion and storage, *Sci. Adv.*, 2015, **1**, e1500564.
11 C. Y. Lin, D. T. Zhang, Z. H. Zhao and Z. H. Xia, Covalent Organic Framework Electrocatalysts for Clean Energy Conversion, *Adv. Mater.*, 2018, **30**, 1703646.
12 H. C. Zhou, J. R. Long and O. M. Yaghi, Introduction to Metal-Organic Frameworks, *Chem. Rev.*, 2012, **112**, 673–674.
13 L. Jiao and H.-L. Jiang, Metal-Organic-Framework-Based Single-Atom Catalysts for Energy Applications, *Chem*, 2019, **5**, 786–804.
14 C. S. Diercks and O. M. Yaghi, The atom, the molecule, and the covalent organic framework, *Science*, 2017, **355**, eaal1585.
15 S. Y. Ding and W. Wang, Covalent organic frameworks (COFs): from design to applications, *Chem. Soc. Rev.*, 2013, **42**, 548–568.
16 A. P. Cote, A. I. Benin, N. W. Ockwig, M. O'Keeffe, A. J. Matzger and O. M. Yaghi, Porous, crystalline, covalent organic frameworks, *Science*, 2005, **310**, 1166–1170.
17 A. Thomas, P. Kuhn, J. Weber, M. M. Titirici and M. Antonietti, Porous Polymers: Enabling Solutions for Energy Applications, *Macromol. Rapid Commun.*, 2009, **30**, 221–236.
18 H. C. Zhou and S. Kitagawa, Metal-Organic Frameworks (MOFs), *Chem. Soc. Rev.*, 2014, **43**, 5415.
19 T. Kitao, Y. Zhang, S. Kitagawa, B. Wang and T. Uemura, Hybridization of MOFs and polymers, *Chem. Soc. Rev.*, 2017, **46**, 3108–3133.
20 L. J. Murray, M. Dinca and J. R. Long, Hydrogen storage in metal-organic frameworks, *Chem. Soc. Rev.*, 2009, **38**, 1294–1314.
21 S. Q. Ma, D. F. Sun, J. M. Simmons, C. D. Collier, D. Q. Yuan and H. C. Zhou, Metal-Organic Framework from an Anthracene Derivative Containing Nanoscopic Cages Exhibiting High Methane Uptake, *J. Am. Chem. Soc.*, 2007, **130**, 1012–1016.
22 L. Bastin, P. S. Barcia, E. J. Hurtado, J. A. C. Silva, A. E. Rodrigues and B. L. Chen, A Microporous Metal-Organic Framework for Separation of CO_2/N_2 and CO_2/CH_4 by Fixed-Bed Adsorption, *J. Phys. Chem. C*, 2008, **112**, 1575–1581.
23 S. S. Nagarkar, B. Joarder, A. K. Chaudhari, S. Mukherjee and S. K. Ghosh, Highly selective detection of nitro explosives by a luminescent metal-organic framework, *Angew. Chem., Int. Ed.*, 2013, **52**, 2881–2885.
24 J. W. Zhou, R. Li, X. X. Fan, Y. F. Chen, R. D. Han, W. Li, J. Zheng, B. Wang and X. G. Li, Rational design of a metal-organic framework host for sulfur storage in fast, long-cycle Li-S batteries, *Energy Environ. Sci.*, 2014, **7**, 2715–2724.
25 P. Pachfule, A. Acharjya, J. Roeser, T. Langenhahn, M. Schwarze, R. Schomacker, A. Thomas and J. Schmidt, Diacetylene Functionalized Covalent Organic Framework (COF) for Photocatalytic Hydrogen Generation, *J. Am. Chem. Soc.*, 2018, **140**, 1423–1427.
26 M. S. Lohse and T. Bein, Covalent Organic Frameworks: Structures, Synthesis, and Applications, *Adv. Funct. Mater.*, 2018, **28**, 1705553.
27 E. L. Spitler, M. R. Giovino, S. L. White and W. R. Dichtel, A mechanistic study of Lewis acid-catalyzed covalent organic framework formation, *Chem. Sci.*, 2011, **2**, 1588–1593.
28 H. Furukawa and O. M. Yaghi, Storage of Hydrogen, Methane, and Carbon Dioxide in Highly Porous Covalent Organic Frameworks for Clean Energy Applications, *J. Am. Chem. Soc.*, 2009, **131**, 8875–8883.
29 S. Y. Ding, J. Gao, Q. Wang, Y. Zhang, W. G. Song, C. Y. Su and W. Wang, Construction of covalent organic framework for catalysis: Pd/COF-LZU1 in Suzuki-Miyaura coupling reaction, *J. Am. Chem. Soc.*, 2011, **133**, 19816–19822.
30 X. Han, J. Zhang, J. J. Huang, X. W. Wu, D. Q. Yuan, Y. Liu and Y. Cui, Chiral induction in covalent organic frameworks, *Nat. Commun.*, 2018, **9**, 1294.
31 A. Nagai, Z. Q. Guo, X. Feng, S. B. Jin, X. Chen, X. S. Ding and D. L. Jiang, Pore surface engineering in covalent organic frameworks, *Nat. Commun.*, 2011, **2**, 536.
32 L. Ma, S. Wang, X. Feng and B. Wang, Recent advances of covalent organic frameworks in electronic and optical applications, *Chin. Chem. Lett.*, 2016, **27**, 1383–1394.
33 J. Roeser, D. Prill, M. J. Bojdys, P. Fayon, A. Trewin, A. N. Fitch, M. U. Schmidt and A. Thomas, Anionic silicate organic frameworks constructed from hexacoordinate silicon centres, *Nat. Chem.*, 2017, **9**, 977–982.
34 X. L. Jiang, H. H. Wu, S. J. Chang, R. Si, S. Miao, W. X. Huang, Y. H. Li, G. X. Wang and X. H. Bao, Boosting CO_2 electroreduction over layered zeolitic imidazolate frameworks decorated with Ag_2O nanoparticles, *J. Mater. Chem. A*, 2017, **5**, 19371–19377.
35 N. Kornienko, Y. B. Zhao, C. S. Kiley, C. H. Zhu, D. Kim, S. Lin, C. J. Chang, O. M. Yaghi and P. D. Yang, Metal-Organic Frameworks for Electrocatalytic Reduction of Carbon Dioxide, *J. Am. Chem. Soc.*, 2015, **137**, 14129–14135.
36 X. J. Zhao, P. Pachfule, S. Li, T. Langenhahn, M. Y. Ye, C. Schlesiger, S. Praetz, J. Schmidt and A. Thomas, Macro/Microporous Covalent Organic Frameworks for Efficient Electrocatalysis, *J. Am. Chem. Soc.*, 2019, **141**, 6623–6630.
37 H. M. El-Kaderi, J. R. Hunt, J. L. Mendoza-Cortes, A. P. Cote, R. E. Taylor, M. O'Keeffe and O. M. Yaghi, Designed synthesis of 3D covalent organic frameworks, *Science*, 2007, **316**, 268–272.
38 X. Feng, X. S. Ding and D. L. Jiang, Covalent organic frameworks, *Chem. Soc. Rev.*, 2012, **41**, 6010–6022.
39 O. Yahiaoui, A. N. Fitch, F. Hoffman, M. Froba, A. Thomas and J. Roeser, 3D Anionic Silicate Covalent Organic Framework with srs Topology, *J. Am. Chem. Soc.*, 2018, **140**, 5330–5333.
40 S. Kandambeth, A. Mallick, B. Lukose, M. V. Mane, T. Heine and R. Banerjee, Construction of crystalline 2D covalent organic frameworks with remarkable chemical (acid/base) stability *via* a combined reversible and irreversible route, *J. Am. Chem. Soc.*, 2012, **134**, 19524–19527.
41 A. Halder, M. Ghosh, M. A. Khayum, S. Bera, M. Addicoat, H. S. Sasmal, S. Karak, S. Kurungot and R. Banerjee, Interlayer Hydrogen-Bonded Covalent Organic Frameworks as High-Performance Supercapacitors, *J. Am. Chem. Soc.*, 2018, **140**, 10941–10945.

42 Z. D. Lei, Q. S. Yang, Y. Xu, S. Y. Guo, W. W. Sun, H. Liu, L. P. Lv, Y. Zhang and Y. Wang, Boosting lithium storage in covalent organic framework *via* activation of 14-electron redox chemistry, *Nat. Commun.*, 2018, **9**, 576.

43 S. Lin, S. D. Christian, Y. B. Zhang, N. Kornienko, E. M. Nichols, Y. B. Zhao, A. R. Paris, D. Kim, P. D. Yang, O. M. Yaghi and C. J. Chang, Covalent organic frameworks comprising cobalt porphyrins for catalytic CO_2 reduction in water, *Science*, 2015, **349**, 1208–1213.

44 H. J. Zhu, M. Lu, Y. R. Wang, S. J. Yao, M. Kan, Y. H. Zhang, J. Liu, Y. Chen, S. L. Li and Y. Q. Lan, Efficient electron transmission in covalent organic framework nanosheets for highly active electrocatalytic carbon dioxide reduction, *Nat. Commun.*, 2020, **11**, 497.

45 M. H. Shao, Q. W. Chang, J. P. Dodelet and R. Chenitz, Recent Advances in Electrocatalysts for Oxygen Reduction Reaction, *Chem. Rev.*, 2016, **116**, 3594–3657.

46 J. K. Norskov, J. Rossmeisl, A. Logadottir, L. Lindqvist, J. R. Kitchin, T. Bligaard and H. Jonsson, Origin of the overpotential for oxygen reduction at a fuel-cell cathode, *J. Phys. Chem. B*, 2004, **108**, 17886–17892.

47 C. C. L. McCrory, S. H. Jung, J. C. Peters and T. F. Jaramillo, Benchmarking Heterogeneous Electrocatalysts for the Oxygen Evolution Reaction, *J. Am. Chem. Soc.*, 2013, **135**, 16977–16987.

48 B. Zhang, X. L. Zheng, O. Voznyy, R. Comin, M. Bajdich, M. Garcia-Melchor, L. L. Han, J. X. Xu, M. Liu, L. R. Zheng, F. P. G. de Arquer, C. T. Dinh, F. J. Fan, M. J. Yuan, E. Yassitepe, N. Chen, T. Regier, P. F. Liu, Y. H. Li, P. De Luna, A. Janmohamed, H. L. L. Xin, H. G. Yang, A. Vojvodic and E. H. Sargent, Homogeneously dispersed multimetal oxygen-evolving catalysts, *Science*, 2016, **352**, 333–337.

49 N. Mahmood, Y. D. Yao, J. W. Zhang, L. Pan, X. W. Zhang and J. J. Zou, Electrocatalysts for Hydrogen Evolution in Alkaline Electrolytes: Mechanisms, Challenges, and Prospective Solutions, *Adv. Sci.*, 2018, **5**, 1700464.

50 S. Zhang, Q. Fan, R. Xia and T. J. Meyer, CO_2 Reduction: From Homogeneous to Heterogeneous Electrocatalysis, *Acc. Chem. Res.*, 2020, **53**, 255–264.

51 X. L. Wang, J. F. de Araujo, W. Ju, A. Bagger, H. Schmies, S. Kuhl, J. Rossmeisl and P. Strasser, Mechanistic reaction pathways of enhanced ethylene yields during electroreduction of CO_2-CO co-feeds on Cu and Cu-tandem electrocatalysts, *Nat. Nanotechnol.*, 2019, **14**, 1063–1070.

52 G. P. Wang, L. Zhang and J. J. Zhang, A review of electrode materials for electrochemical supercapacitors, *Chem. Soc. Rev.*, 2012, **41**, 797–828.

53 C. Zhong, Y. D. Deng, W. B. Hu, J. L. Qiao, L. Zhang and J. J. Zhang, A review of electrolyte materials and compositions for electrochemical supercapacitors, *Chem. Soc. Rev.*, 2015, **44**, 7484–7539.

54 P. Peng, Z. Zhou, J. Guo and Z. Xiang, Well-Defined 2D Covalent Organic Polymers for Energy Electrocatalysis, *ACS Energy Lett.*, 2017, **2**, 1308–1314.

55 H. B. Aiyappa, J. Thote, D. B. Shinde, R. Banerjee and S. Kurungot, Cobalt-Modified Covalent Organic Framework as a Robust Water Oxidation Electrocatalyst, *Chem. Mater.*, 2016, **28**, 4375–4379.

56 S. Gu, S. F. Wu, L. J. Cao, M. C. Li, N. Qin, J. Zhu, Z. Q. Wang, Y. Z. Li, Z. Q. Li, J. J. Chen and Z. G. Lu, Tunable Redox Chemistry and Stability of Radical Intermediates in 2D Covalent Organic Frameworks for High Performance Sodium Ion Batteries, *J. Am. Chem. Soc.*, 2019, **141**, 9623–9628.

57 C. Li, J. Yang, P. Pachfule, S. Li, M. Y. Ye, J. Schmidt and A. Thomas, Ultralight covalent organic framework/graphene aerogels with hierarchical porosity, *Nat. Commun.*, 2020, **11**, 4712.

58 P. Kuhn, M. Antonietti and A. Thomas, Porous, covalent triazine-based frameworks prepared by ionothermal synthesis, *Angew. Chem., Int. Ed.*, 2008, **47**, 3450–3453.

59 F. J. Uribe-Romo, J. R. Hunt, H. Furukawa, C. Klock, M. O'Keeffe and O. M. Yaghi, A Crystalline Imine-Linked 3-D Porous Covalent Organic Framework, *J. Am. Chem. Soc.*, 2009, **131**, 4570–4571.

60 F. Haase, E. Troschke, G. Savasci, T. Banerjee, V. Duppel, S. Dorfler, M. M. J. Grundei, A. M. Burow, C. Ochsenfeld, S. Kaskel and B. V. Lotsch, Topochemical conversion of an imine-into a thiazole-linked covalent organic framework enabling real structure analysis, *Nat. Commun.*, 2018, **9**, 2600.

61 P. J. Waller, S. J. Lyle, T. M. O. Popp, C. S. Diercks, J. A. Reimer and O. M. Yaghi, Chemical Conversion of Linkages in Covalent Organic Frameworks, *J. Am. Chem. Soc.*, 2016, **138**, 15519–15522.

62 C. Qian, Q. Y. Qi, G. F. Jiang, F. Z. Cui, Y. Tian and X. Zhao, Toward Covalent Organic Frameworks Bearing Three Different Kinds of Pores: The Strategy for Construction and COF-to-COF Transformation *via* Heterogeneous Linker Exchange, *J. Am. Chem. Soc.*, 2017, **139**, 6736–6743.

63 C. R. DeBlase, K. E. Silberstein, T. T. Truong, H. D. Abruna and W. R. Dichtel, beta-Ketoenamine-Linked Covalent Organic Frameworks Capable of Pseudocapacitive Energy Storage, *J. Am. Chem. Soc.*, 2013, **135**, 16821–16824.

64 K. Jeong, S. Park, G. Y. Jung, S. H. Kim, Y. H. Lee, S. K. Kwak and S. Y. Lee, Solvent-Free, Single Lithium-Ion Conducting Covalent Organic Frameworks, *J. Am. Chem. Soc.*, 2019, **141**, 5880–5885.

65 H. Xu, S. S. Tao and D. L. Jiang, Proton conduction in crystalline and porous covalent organic frameworks, *Nat. Mater.*, 2016, **15**, 722–726.

66 X. L. Li, C. L. Zhang, S. L. Cai, X. H. Lei, V. Altoe, F. Hong, J. J. Urban, J. Ciston, E. M. Chan and Y. Liu, Facile transformation of imine covalent organic frameworks into ultrastable crystalline porous aromatic frameworks, *Nat. Commun.*, 2018, **9**, 2998.

67 M. S. Lohse, T. Stassin, G. Naudin, S. Wuttke, R. Ameloot, D. De Vos, D. D. Medina and T. Bein, Sequential Pore Wall Modification in a Covalent Organic Framework for Application in Lactic Acid Adsorption, *Chem. Mater.*, 2016, **28**, 626–631.

68 Y. Wu, Z. Y. Zhang, S. Bandow and K. Awaga, A Novel Strategy to Functionalize Covalent Organic Frameworks for

High-Energy Rechargeable Lithium Organic Batteries *via* Graft Polymerization in Nano-Channels, *Bull. Chem. Soc. Jpn.*, 2017, **90**, 1382–1387.

69 S. Royuela, J. Almarza, M. J. Mancheno, J. C. Perez-Flores, E. G. Michel, M. M. Ramos, F. Zamora, P. Occon and J. L. Segura, Synergistic Effect of Covalent Bonding and Physical Encapsulation of Sulfur in the Pores of a Microporous COF to Improve Cycling Performance in Li-S Batteries, *Chem. – Eur. J.*, 2019, **25**, 12394–12404.

70 L. Chen, K. Furukawa, J. Gao, A. Nagai, T. Nakamura, Y. P. Dong and D. L. Jiang, Photoelectric Covalent Organic Frameworks: Converting Open Lattices into Ordered Donor-Acceptor Heterojunctions, *J. Am. Chem. Soc.*, 2014, **136**, 9806–9809.

71 J. L. Segura, S. Royuela and M. M. Ramos, Post-synthetic modification of covalent organic frameworks, *Chem. Soc. Rev.*, 2019, **48**, 3903–3945.

72 M. Y. Ye, S. Li, X. J. Zhao, N. V. Tarakina, C. Teutloff, W. Y. Chow, R. Bittl and A. Thomas, Cobalt-Exchanged Poly(Heptazine Imides) as Transition Metal-N-x Electrocatalysts for the Oxygen Evolution Reaction, *Adv. Mater.*, 2020, **32**, 1903942.

73 D. A. Popov, J. M. Luna, N. M. Orchanian, R. Haiges, C. A. Downes and S. C. Marinescu, A 2,2-bipyridine-containing covalent organic framework bearing rhenium(i) tricarbonyl moieties for CO_2 reduction, *Dalton Trans.*, 2018, **47**, 17450–17460.

74 B. Q. Li, S. Y. Zhang, B. Wang, Z. J. Xia, C. Tang and Q. Zhang, A porphyrin covalent organic framework cathode for flexible Zn-air batteries, *Energy Environ. Sci.*, 2018, **11**, 1723–1729.

75 S. Wannakao, T. Maihom, K. Kongpatpanich, J. Limtrakul and V. Promarak, Halogen substitutions leading to enhanced oxygen evolution and oxygen reduction reactions in metalloporphyrin frameworks, *Phys. Chem. Chem. Phys.*, 2017, **19**, 29540–29548.

76 E. M. Johnson, R. Haiges and S. C. Marinescu, Covalent-Organic Frameworks Composed of Rhenium Bipyridine and Metal Porphyrins: Designing Heterobimetallic Frameworks with Two Distinct Metal Sites, *ACS Appl. Mater. Interfaces*, 2018, **10**, 37919–37927.

77 S. S. Yuan, X. Li, J. Y. Zhu, G. Zhang, P. Van Puyvelde and B. Van der Bruggen, Covalent organic frameworks for membrane separation, *Chem. Soc. Rev.*, 2019, **48**, 2665–2681.

78 H. Wang, Z. T. Zeng, P. Xu, L. S. Li, G. M. Zeng, R. Xiao, Z. Y. Tang, D. L. Huang, L. Tang, C. Lai, D. N. Jiang, Y. Liu, H. Yi, L. Qin, S. J. Ye, X. Y. Ren and W. W. Tang, Recent progress in covalent organic framework thin films: fabrications, applications and perspectives, *Chem. Soc. Rev.*, 2019, **48**, 488–516.

79 S. Chandra, T. Kundu, K. Dey, M. Addicoat, T. Heine and R. Banerjee, Interplaying Intrinsic and Extrinsic Proton Conductivities in Covalent Organic Frameworks, *Chem. Mater.*, 2016, **28**, 1489–1494.

80 Z. X. Kang, Y. W. Peng, Y. H. Qian, D. Q. Yuan, M. A. Addicoat, T. Heine, Z. G. Hu, L. Tee, Z. G. Guo and D. Zhao, Mixed Matrix Membranes (MMMs) Comprising Exfoliated 2D Covalent Organic Frameworks (COFs) for Efficient CO_2 Separation, *Chem. Mater.*, 2016, **28**, 1277–1285.

81 H. S. Sasmal, H. B. Aiyappa, S. N. Bhange, S. Karak, A. Halder, S. Kurungot and R. Banerjee, Superprotonic Conductivity in Flexible Porous Covalent Organic Framework Membranes, *Angew. Chem., Int. Ed.*, 2018, **57**, 10894–10898.

82 S. Kandambeth, B. P. Biswal, H. D. Chaudhari, K. C. Rout, H. S. Kunjattu, S. Mitra, S. Karak, A. Das, R. Mukherjee, U. K. Kharul and R. Banerjee, Selective Molecular Sieving in Self-Standing Porous Covalent-Organic-Framework Membranes, *Adv. Mater.*, 2017, **29**, 1603945.

83 G. Li, K. Zhang and T. Tsuru, Two-Dimensional Covalent Organic Framework (COF) Membranes Fabricated *via* the Assembly of Exfoliated COF Nanosheets, *ACS Appl. Mater. Interfaces*, 2017, **9**, 8433–8436.

84 K. Dey, M. Pal, K. C. Rout, H. S. Kunjattu, A. Das, R. Mukherjee, U. K. Kharul and R. Banerjee, Selective Molecular Separation by lnterfacially Crystallized Covalent Organic Framework Thin Films, *J. Am. Chem. Soc.*, 2017, **139**, 13083–13091.

85 J. Wang, J. Tang, B. Ding, V. Malgras, Z. Chang, X. D. Hao, Y. Wang, H. Dou, X. G. Zhang and Y. Yamauchi, Hierarchical porous carbons with layer-by-layer motif architectures from confined soft-template self-assembly in layered materials, *Nat. Commun.*, 2017, **8**, 15717.

86 H. W. Liang, X. D. Zhuang, S. Bruller, X. L. Feng and K. Mullen, Hierarchically porous carbons with optimized nitrogen doping as highly active electrocatalysts for oxygen reduction, *Nat. Commun.*, 2014, **5**, 4973.

87 P. Pachfule, S. Kandmabeth, A. Mallick and R. Banerjee, Hollow tubular porous covalent organic framework (COF) nanostructures, *Chem. Commun.*, 2015, **51**, 11717–11720.

88 B. Gole, V. Stepanenko, S. Rager, M. Grune, D. D. Medina, T. Bein, F. Wurthner and F. Beuerle, Microtubular Self-Assembly of Covalent Organic Frameworks, *Angew. Chem., Int. Ed.*, 2018, **57**, 846–850.

89 S. Kandambeth, V. Venkatesh, D. B. Shinde, S. Kumari, A. Halder, S. Verma and R. Banerjee, Self-templated chemically stable hollow spherical covalent organic framework, *Nat. Commun.*, 2015, **6**, 6786.

90 Y. Li, Z. Y. Fu and B. L. Su, Hierarchically Structured Porous Materials for Energy Conversion and Storage, *Adv. Funct. Mater.*, 2012, **22**, 4634–4667.

91 J. Guo, Y. Xu, S. Jin, L. Chen, T. Kaji, Y. Honsho, M. A. Addicoat, J. Kim, A. Saeki, H. Ihee, S. Seki, S. Irle, M. Hiramoto, J. Gao and D. Jiang, Conjugated organic framework with three-dimensionally ordered stable structure and delocalized pi clouds, *Nat. Commun.*, 2013, **4**, 2736.

92 S. Wan, F. Gándara, A. Asano, H. Furukawa, A. Saeki, S. K. Dey, L. Liao, M. W. Ambrogio, Y. Y. Botros, X. Duan, S. Seki, J. F. Stoddart and O. M. Yaghi, Covalent Organic Frameworks with High Charge Carrier Mobility, *Chem. Mater.*, 2011, **23**, 4094–4097.

93 Z. Meng, R. M. Stolz and K. A. Mirica, Two-Dimensional Chemiresistive Covalent Organic Framework with High

Intrinsic Conductivity, *J. Am. Chem. Soc.*, 2019, **141**, 11929–11937.

94 H. Li, J. Chang, S. Li, X. Guan, D. Li, C. Li, L. Tang, M. Xue, Y. Yan, V. Valtchev, S. Qiu and Q. Fang, Three-Dimensional Tetrathiafulvalene-Based Covalent Organic Frameworks for Tunable Electrical Conductivity, *J. Am. Chem. Soc.*, 2019, **141**, 13324–13329.

95 J. N. Guo, C. Y. Lin, Z. H. Xia and Z. H. Xiang, A Pyrolysis-Free Covalent Organic Polymer for Oxygen Reduction, *Angew. Chem., Int. Ed.*, 2018, **57**, 12567–12572.

96 C. R. Mulzer, L. X. Shen, R. P. Bisbey, J. R. McKone, N. Zhang, H. D. Abruna and W. R. Dichtel, Superior Charge Storage and Power Density of a Conducting Polymer-Modified Covalent Organic Framework, *ACS Cent. Sci.*, 2016, **2**, 667–673.

97 S. Karak, S. Kandambeth, B. P. Biswal, H. S. Sasmal, S. Kumar, P. Pachfule and R. Banerjee, Constructing Ultraporous Covalent Organic Frameworks in Seconds *via* an Organic Terracotta Process, *J. Am. Chem. Soc.*, 2017, **139**, 1856–1862.

98 S. Karak, K. Dey, A. Torris, A. Halder, S. Bera, F. Kanheerampockil and R. Banerjee, Inducing Disorder in Order: Hierarchically Porous Covalent Organic Framework Nanostructures for Rapid Removal of Persistent Organic Pollutants, *J. Am. Chem. Soc.*, 2019, **141**, 7572–7581.

99 M. S. Zhang, L. Y. Li, Q. M. Lin, M. Tang, Y. Y. Wu and C. F. Ke, Hierarchical-Coassembly-Enabled 3D-Printing of Homogeneous and Heterogeneous Covalent Organic Frameworks, *J. Am. Chem. Soc.*, 2019, **141**, 5154–5158.

100 A. K. Mohammed, S. Usgaonkar, F. Kanheerampockil, S. Karak, A. Halder, M. Tharkar, M. Addicoat, T. G. Ajithkumar and R. Banerjee, Connecting Microscopic Structures, Mesoscale Assemblies, and Macroscopic Architectures in 3D-Printed Hierarchical Porous Covalent Organic Framework Foams, *J. Am. Chem. Soc.*, 2020, **142**, 8252–8261.

101 S. Bhunia, S. K. Das, R. Jana, S. C. Peter, S. Bhattacharya, M. Addicoat, A. Bhaumik and A. Pradhan, Electrochemical Stimuli-Driven Facile Metal-Free Hydrogen Evolution from Pyrene-Porphyrin-Based Crystalline Covalent Organic Framework, *ACS Appl. Mater. Interfaces*, 2017, **9**, 23843–23851.

102 J. M. Rotter, S. Weinberger, J. Kampmann, T. Sick, M. Shalom, T. Bein and D. D. Medina, Covalent Organic Framework Films through Electrophoretic Deposition-Creating Efficient Morphologies for Catalysis, *Chem. Mater.*, 2019, **31**, 10008–10016.

103 Z. L. Huang, Q. Xu and X. Y. Hu, Covalent organic frameworks functionalized carbon fiber paper for the capture and detection of hydroxyl radical in the atmosphere, *Chin. Chem. Lett.*, 2020, **31**, 2495–2498.

104 J. P. Paraknowitsch and A. Thomas, Doping carbons beyond nitrogen: an overview of advanced heteroatom doped carbons with boron, sulphur and phosphorus for energy applications, *Energy Environ. Sci.*, 2013, **6**, 2839–2855.

105 S. Li, C. Cheng, H. W. Liang, X. Feng and A. Thomas, 2D Porous Carbons prepared from Layered Organic-Inorganic Hybrids and their Use as Oxygen-Reduction Electrocatalysts, *Adv. Mater.*, 2017, **29**, 1700707.

106 S. Li, C. Cheng, X. J. Zhao, J. Schmidt and A. Thomas, Active Salt/Silica-Templated 2D Mesoporous FeCo-N-x-Carbon as Bifunctional Oxygen Electrodes for Zinc-Air Batteries, *Angew. Chem., Int. Ed.*, 2018, **57**, 1856–1862.

107 X. J. Zhao, S. Li, H. F. Cheng, J. Schmidt and A. Thomas, Ionic Liquid-Assisted Synthesis of Mesoporous Carbons with Surface-Enriched Nitrogen for the Hydrogen Evolution Reaction, *ACS Appl. Mater. Interfaces*, 2018, **10**, 3912–3920.

108 X. J. Zhao, P. Pachfule, S. Li, J. R. J. Simke, J. Schmidt and A. Thomas, Bifunctional Electrocatalysts for Overall Water Splitting from an Iron/Nickel-Based Bimetallic Metal-Organic Framework/Dicyandiamide composite, *Angew. Chem., Int. Ed.*, 2018, **130**, 9059–9064.

109 P. Pachfule, D. Shinde, M. Majumder and Q. Xu, Fabrication of carbon nanorods and graphene nanoribbons from a metal-organic framework, *Nat. Chem.*, 2016, **8**, 718–724.

110 X. J. Zhao, P. Pachfule, S. Li, T. Langenhahn, M. Y. Ye, G. Y. Tian, J. Schmidt and A. Thomas, Silica-Templated Covalent Organic Framework-Derived Fe-N-Doped Mesoporous Carbon as Oxygen Reduction Electrocatalyst, *Chem. Mater.*, 2019, **31**, 3274–3280.

111 S. Li, C. Cheng, A. Sagaltchik, P. Pachfule, C. S. Zhao and A. Thomas, Metal-Organic Precursor-Derived Mesoporous Carbon Spheres with Homogeneously Distributed Molybdenum Carbide/Nitride Nanoparticles for Efficient Hydrogen Evolution in Alkaline Media, *Adv. Funct. Mater.*, 2019, **29**, 1807419.

112 Q. Xu, Y. P. Tang, X. B. Zhang, Y. Oshima, Q. H. Chen and D. L. Jiang, Template Conversion of Covalent Organic Frameworks into 2D Conducting Nanocarbons for Catalyzing Oxygen Reduction Reaction, *Adv. Mater.*, 2018, **30**, 1706330.

113 L. Y. Chen, L. Zhang, Z. J. Chen, H. J. Liu, R. Luque and Y. W. Li, A covalent organic framework-based route to the in situ encapsulation of metal nanoparticles in N-rich hollow carbon spheres, *Chem. Sci.*, 2016, **7**, 6015–6020.

114 M. Zhou, X. Y. Li, H. Zhao, J. Wang, Y. P. Zhao, F. Y. Ge and Z. S. Cai, Combined effect of nitrogen and oxygen heteroatoms and micropores of porous carbon frameworks from Schiff-base networks on their high supercapacitance, *J. Mater. Chem. A*, 2018, **6**, 1621–1629.

115 Q. Xu, Y. P. Tang, L. P. Zhai, Q. H. Chen and D. L. Jiang, Pyrolysis of covalent organic frameworks: a general strategy for template converting conventional skeletons into conducting microporous carbons for high-performance energy storage, *Chem. Commun.*, 2017, **53**, 11690–11693.

116 A. Thomas, F. Goettmann and M. Antonietti, Hard templates for soft materials: Creating nanostructured organic materials, *Chem. Mater.*, 2008, **20**, 738–755.

117 Y. Yan, T. He, B. Zhao, K. Qi, H. F. Liu and B. Y. Xia, Metal/covalent-organic frameworks-based electrocatalysts for water splitting, *J. Mater. Chem. A*, 2018, **6**, 15905–15926.

118 K. Q. Zhang, K. O. Kirlikovali, R. S. Varma, Z. Jin, H. W. Jang, O. K. Farha and M. Shokouhimehr, Covalent

Organic Frameworks: Emerging Organic Solid Materials for Energy and Electrochemical Applications, *ACS Appl. Mater. Interfaces*, 2020, **12**, 27821–27852.

119 J. Li, X. C. Jing, Q. Q. Li, S. W. Li, X. Gao, X. Feng and B. Wang, Bulk COFs and COF nanosheets for electrochemical energy storage and conversion, *Chem. Soc. Rev.*, 2020, **49**, 3565–3604.

120 H. X. Jia, Z. J. Sun, D. C. Jiang and P. W. Du, Covalent Cobalt Porphyrin Framework on Multiwalled Carbon Nanotubes for Efficient Water Oxidation at Low Overpotential, *Chem. Mater.*, 2015, **27**, 4586–4593.

121 K. Kamiya, R. Kamai, K. Hashimoto and S. Nakanishi, Platinum-modified covalent triazine frameworks hybridized with carbon nanoparticles as methanol-tolerant oxygen reduction electrocatalysts, *Nat. Commun.*, 2014, **5**, 5040.

122 H. P. Liao, H. M. Ding, B. J. Li, X. P. Ai and C. Wang, Covalent-organic frameworks: potential host materials for sulfur impregnation in lithium-sulfur batteries, *J. Mater. Chem. A*, 2014, **2**, 8854–8858.

123 M. A. Khayum, V. Vijayakumar, S. Karak, S. Kandambeth, M. Bhadra, K. Suresh, N. Acharambath, S. Kurungot and R. Banerjee, Convergent Covalent Organic Framework Thin Sheets as Flexible Supercapacitor Electrodes, *ACS Appl. Mater. Interfaces*, 2018, **10**, 28139–28146.

124 Y. Y. Liu, X. C. Li, S. Wang, T. Cheng, H. Yang, C. Liu, Y. Gong, W. Y. Lai and W. Huang, Self-templated synthesis of uniform hollow spheres based on highly conjugated three-dimensional covalent organic frameworks, *Nat. Commun.*, 2020, **11**, 5561.

125 P. Peng, L. Shi, F. Huo, S. J. Zhang, C. X. Mi, Y. H. Cheng and Z. H. Xiang, In Situ Charge Exfoliated Soluble Covalent Organic Framework Directly Used for Zn-Air Flow Battery, *ACS Nano*, 2019, **13**, 878–884.

126 H. Huang, F. M. Li, Y. Zhang and Y. Chen, Two-dimensional graphdiyne analogue Co-coordinated porphyrin covalent organic framework nanosheets as a stable electrocatalyst for the oxygen evolution reaction, *J. Mater. Chem. A*, 2019, **7**, 5575–5582.

127 S. L. Qiao, B. Y. Zhang, Q. Li, Z. Li, W. B. Wang, J. Zhao, X. J. Zhang and Y. Q. Hu, Pore Surface Engineering of Covalent Triazine Frameworks@MoS_2 Electrocatalyst for the Hydrogen Evolution Reaction, *ChemSusChem*, 2019, **12**, 5032–5040.

128 H. Y. Liu, J. Chu, Z. L. Yin, X. Cai, L. Zhuang and H. X. Deng, Covalent Organic Frameworks Linked by Amine Bonding for Concerted Electrochemical Reduction of CO_2, *Chem*, 2018, **4**, 1696–1709.

129 Z. A. Ghazi, L. Y. Zhu, H. Wang, A. Naeem, A. M. Khattak, B. Liang, N. A. Khan, Z. X. Wei, L. S. Li and Z. Y. Tang, Efficient Polysulfide Chemisorption in Covalent Organic Frameworks for High-Performance Lithium-Sulfur Batteries, *Adv. Energy Mater.*, 2016, **6**, 1601250.

130 Z. Y. Yang, C. X. Peng, R. J. Meng, L. H. Zu, Y. T. Feng, B. J. Chen, Y. L. Mi, C. Zhang and J. H. Yang, Hybrid Anatase/Rutile Nanodots-Embedded Covalent Organic Frameworks with Complementary Polysulfide Adsorption for High-Performance Lithium-Sulfur Batteries, *ACS Cent. Sci.*, 2019, **5**, 1876–1883.

131 E. Vitaku, C. N. Gannett, K. L. Carpenter, L. X. Shen, H. D. Abruna and W. R. Dichtel, Phenazine-Based Covalent Organic Framework Cathode Materials with High Energy and Power Densities, *J. Am. Chem. Soc.*, 2020, **142**, 16–20.

132 Y. Y. Zhang, J. Y. Duan, D. Ma, P. F. Li, S. W. Li, H. W. Li, J. W. Zhou, X. J. Ma, X. Feng and B. Wang, Three-Dimensional Anionic Cyclodextrin-Based Covalent Organic Frameworks, *Angew. Chem., Int. Ed.*, 2017, **56**, 16313–16317.

133 V. Artero, M. Chavarot-Kerlidou and M. Fontecave, Splitting Water with Cobalt, *Angew. Chem., Int. Ed.*, 2011, **50**, 7238–7266.

134 D. Merki and X. L. Hu, Recent developments of molybdenum and tungsten sulfides as hydrogen evolution catalysts, *Energy Environ. Sci.*, 2011, **4**, 3878–3888.

135 Y. Jiao, Y. Zheng, M. T. Jaroniec and S. Z. Qiao, Design of electrocatalysts for oxygen- and hydrogen-involving energy conversion reactions, *Chem. Soc. Rev.*, 2015, **44**, 2060–2086.

136 D. Y. Wang, M. Gong, H. L. Chou, C. J. Pan, H. A. Chen, Y. P. Wu, M. C. Lin, M. Y. Guan, J. Yang, C. W. Chen, Y. L. Wang, B. J. Hwang, C. C. Chen and H. J. Dai, Highly Active and Stable Hybrid Catalyst of Cobalt-Doped FeS_2 Nanosheets-Carbon Nanotubes for Hydrogen Evolution Reaction, *J. Am. Chem. Soc.*, 2015, **137**, 1587–1592.

137 X. Long, G. X. Li, Z. L. Wang, H. Y. Zhu, T. Zhang, S. Xiao, W. Y. Guo and S. H. Yang, Metallic Iron-Nickel Sulfide Ultrathin Nanosheets As a Highly Active Electrocatalyst for Hydrogen Evolution Reaction in Acidic Media, *J. Am. Chem. Soc.*, 2015, **137**, 11900–11903.

138 J. Yang, D. Voiry, S. J. Ahn, D. Kang, A. Y. Kim, M. Chhowalla and H. S. Shin, Two-Dimensional Hybrid Nanosheets of Tungsten Disulfide and Reduced Graphene Oxide as Catalysts for Enhanced Hydrogen Evolution, *Angew. Chem., Int. Ed.*, 2013, **52**, 13751–13754.

139 Y. Jiao, Y. Zheng, K. Davey and S. Z. Qiao, Activity origin and catalyst design principles for electrocatalytic hydrogen evolution on heteroatom-doped graphene, *Nat. Energy*, 2016, **1**, 16130.

140 H. W. Liang, S. Bruller, R. H. Dong, J. Zhang, X. L. Feng and K. Mullen, Molecular metal-N-x centres in porous carbon for electrocatalytic hydrogen evolution, *Nat. Commun.*, 2015, **6**, 7992.

141 Y. Peng, B. Z. Lu and S. W. Chen, Carbon-Supported Single Atom Catalysts for Electrochemical Energy Conversion and Storage, *Adv. Mater.*, 2018, **30**, 1801995.

142 W. X. Chen, J. J. Pei, C. T. He, J. W. Wan, H. L. Ren, Y. Q. Zhu, Y. Wang, J. C. Dong, S. B. Tian, W. C. Cheong, S. Q. Lu, L. R. Zheng, X. S. Zheng, W. S. Yan, Z. B. Zhuang, C. Chen, Q. Peng, D. S. Wang and Y. D. Li, Rational Design of Single Molybdenum Atoms Anchored on N-Doped Carbon for Effective Hydrogen Evolution Reaction, *Angew. Chem., Int. Ed.*, 2017, **56**, 16086–16090.

143 W. X. Chen, J. J. Pei, C. T. He, J. W. Wan, H. L. Ren, Y. Wang, J. C. Dong, K. L. Wu, W. C. Cheong, J. J. Mao, X. S. Zheng, W. S. Yan, Z. B. Zhuang, C. Chen, Q. Peng,

D. S. Wang and Y. D. Li, Single Tungsten Atoms Supported on MOF-Derived N-Doped Carbon for Robust Electrochemical Hydrogen Evolution, *Adv. Mater.*, 2018, **30**, 1800396.

144 B. C. Patra, S. Khilari, R. N. Manna, S. Mondal, D. Pradhan, A. Pradhan and A. Bhaumik, A Metal-Free Covalent Organic Polymer for Electrocatalytic Hydrogen Evolution, *ACS Catal.*, 2017, **7**, 6120–6127.

145 J. J. Duan, S. Chen and C. Zhao, Ultrathin metal-organic framework array for efficient electrocatalytic water splitting, *Nat. Commun.*, 2017, **8**, 15341.

146 W. Y. Gao, M. Chrzanowski and S. Q. Ma, Metal-metalloporphyrin frameworks: a resurging class of functional materials, *Chem. Soc. Rev.*, 2014, **43**, 5841–5866.

147 Y. Chen, T. Hoang and S. Q. Ma, Biomimetic Catalysis of a Porous Iron-Based Metal-Metalloporphyrin Framework, *Inorg. Chem.*, 2012, **51**, 12600–12602.

148 Y. Y. Wu, J. M. Veleta, D. Y. Tang, A. D. Price, C. E. Botez and D. Villagran, Efficient electrocatalytic hydrogen gas evolution by a cobalt-porphyrin-based crystalline polymer, *Dalton Trans.*, 2018, **47**, 8801–8806.

149 S. Maiti, A. R. Chowdhury and A. K. Das, Electrochemically Facile Hydrogen Evolution Using Ruthenium Encapsulated Two Dimensional Covalent Organic Framework (2D COF), *ChemNanoMat*, 2020, **6**, 99–106.

150 S. Hug, L. Stegbauer, H. Oh, M. Hirscher and B. V. Lotsch, Nitrogen-Rich Covalent Triazine Frameworks as High-Performance Platforms for Selective Carbon Capture and Storage, *Chem. Mater.*, 2015, **27**, 8001–8010.

151 A. Thomas, A. Fischer, F. Goettmann, M. Antonietti, J. O. Muller, R. Schlogl and J. M. Carlsson, Graphitic carbon nitride materials: variation of structure and morphology and their use as metal-free catalysts, *J. Mater. Chem.*, 2008, **18**, 4893–4908.

152 K. Kamiya, Selective single-atom electrocatalysts: a review with a focus on metal-doped covalent triazine frameworks, *Chem. Sci.*, 2020, **11**, 8339–8349.

153 N. T. Suen, S. F. Hung, Q. Quan, N. Zhang, Y. J. Xu and H. M. Chen, Electrocatalysis for the oxygen evolution reaction: recent development and future perspectives, *Chem. Soc. Rev.*, 2017, **46**, 337–365.

154 D. Friebel, M. W. Louie, M. Bajdich, K. E. Sanwald, Y. Cai, A. M. Wise, M. J. Cheng, D. Sokaras, T. C. Weng, R. Alonso-Mori, R. C. Davis, J. R. Bargar, J. K. Norskov, A. Nilsson and A. T. Bell, Identification of Highly Active Fe Sites in (Ni, Fe) OOH for Electrocatalytic Water Splitting, *J. Am. Chem. Soc.*, 2015, **137**, 1305–1313.

155 M. Gong, Y. G. Li, H. L. Wang, Y. Y. Liang, J. Z. Wu, J. G. Zhou, J. Wang, T. Regier, F. Wei and H. J. Dai, An Advanced Ni-Fe Layered Double Hydroxide Electrocatalyst for Water Oxidation, *J. Am. Chem. Soc.*, 2013, **135**, 8452–8455.

156 F. Song and X. L. Hu, Exfoliation of layered double hydroxides for enhanced oxygen evolution catalysis, *Nat. Commun.*, 2014, **5**, 4477.

157 R. Subbaraman, D. Tripkovic, K. C. Chang, D. Strmcnik, A. P. Paulikas, P. Hirunsit, M. Chan, J. Greeley, V. Stamenkovic and N. M. Markovic, Trends in activity for the water electrolyser reactions on 3d M(Ni, Co, Fe, Mn) hydr(oxy)oxide catalysts, *Nat. Mater.*, 2012, **11**, 550–557.

158 M. Favaro, J. H. Yang, S. Nappini, E. Magnano, F. M. Toma, E. J. Crumlin, J. Yano and I. D. Sharp, Understanding the Oxygen Evolution Reaction Mechanism on CoOx using Operando Ambient-Pressure X-ray Photoelectron Spectroscopy, *J. Am. Chem. Soc.*, 2017, **139**, 8960–8970.

159 H. B. Yang, J. W. Miao, S. F. Hung, J. Z. Chen, H. B. Tao, X. Z. Wang, L. P. Zhang, R. Chen, J. J. Gao, H. M. Chen, L. M. Dai and B. Liu, Identification of catalytic sites for oxygen reduction and oxygen evolution in N-doped graphene materials: Development of highly efficient metal-free bifunctional electrocatalyst, *Sci. Adv.*, 2016, **2**, e1501122.

160 K. G. Qu, Y. Zheng, S. Dai and S. Z. Qiao, Graphene oxide-polydopamine derived N, S-codoped carbon nanosheets as superior bifunctional electrocatalysts for oxygen reduction and evolution, *Nano Energy*, 2016, **19**, 373–381.

161 H. L. Fei, J. C. Dong, Y. X. Feng, C. S. Allen, C. Z. Wan, B. Volosskiy, M. F. Li, Z. P. Zhao, Y. L. Wang, H. T. Sun, P. F. An, W. X. Chen, Z. Y. Guo, C. Lee, D. L. Chen, I. Shakir, M. J. Liu, T. D. Hu, Y. D. Li, A. I. Kirkland, X. F. Duan and Y. Huang, General synthesis and definitive structural identification of Mn_4C_4 single-atom catalysts with tunable electrocatalytic activities, *Nat. Catal.*, 2018, **1**, 63–72.

162 Y. Pan, S. J. Liu, K. A. Sun, X. Chen, B. Wang, K. L. Wu, X. Cao, W. C. Cheong, R. G. Shen, A. J. Han, Z. Chen, L. R. Zheng, J. Luo, Y. Lin, Y. Q. Liu, D. S. Wang, Q. Peng, Q. Zhang, C. Chen and Y. D. Li, A Bimetallic Zn/Fe Polyphthalocyanine-Derived Single-Atom Fe-N-4 Catalytic Site:A Superior Trifunctional Catalyst for Overall Water Splitting and Zn-Air Batteries, *Angew. Chem., Int. Ed.*, 2018, **57**, 8614–8618.

163 S. M. Barnett, K. I. Goldberg and J. M. Mayer, A soluble copper-bipyridine water-oxidation electrocatalyst, *Nat. Chem.*, 2012, **4**, 498–502.

164 N. Elgrishi, M. B. Chambers, X. Wang and M. Fontecave, Molecular polypyridine-based metal complexes as catalysts for the reduction of CO_2, *Chem. Soc. Rev.*, 2017, **46**, 761–796.

165 B. Wurster, D. Grumelli, D. Hotger, R. Gutzler and K. Kern, Driving the Oxygen Evolution Reaction by Nonlinear Cooperativity in Bimetallic Coordination Catalysts, *J. Am. Chem. Soc.*, 2016, **138**, 3623–3626.

166 N. Yoshinori, M. Sasayama and T. Sasaki, Oxygen Evolution by Oxidation of Water with Manganese Porphyrin Dimers, *Angew. Chem., Int. Ed. Engl.*, 1994, **33**, 1839–1841.

167 S. Shaik, H. Hirao and D. Kumar, Reactivity of high-valent iron-oxo species in enzymes and synthetic reagents: A tale of many states, *Acc. Chem. Res.*, 2007, **40**, 532–542.

168 C. Y. Lin, L. P. Zhang, Z. H. Zhao and Z. H. Xia, Design Principles for Covalent Organic Frameworks as Efficient Electrocatalysts in Clean Energy Conversion and Green Oxidizer Production, *Adv. Mater.*, 2017, **29**, 1606635.

169 C. S. Huang, Y. J. Li, N. Wang, Y. R. Xue, Z. C. Zuo, H. B. Liu and Y. L. Li, Progress in Research into 2D Graphdiyne-Based Materials, *Chem. Rev.*, 2018, **118**, 7744–7803.

170 D. Malko, C. Neiss and A. Gorling, Two-dimensional materials with Dirac cones: Graphynes containing heteroatoms, *Phys. Rev. B: Condens. Matter Mater. Phys.*, 2012, **86**, 045443.

171 F. Y. Cheng and J. Chen, Metal-air batteries: from oxygen reduction electrochemistry to cathode catalysts, *Chem. Soc. Rev.*, 2012, **41**, 2172–2192.

172 I. E. L. Stephens, A. S. Bondarenko, U. Gronbjerg, J. Rossmeisl and I. Chorkendorff, Understanding the electrocatalysis of oxygen reduction on platinum and its alloys, *Energy Environ. Sci.*, 2012, **5**, 6744–6762.

173 J. T. Zhang, Z. H. Zhao, Z. H. Xia and L. M. Dai, A metal-free bifunctional electrocatalyst for oxygen reduction and oxygen evolution reactions, *Nat. Nanotechnol.*, 2015, **10**, 444–452.

174 H.-W. Liang, W. Wei, Z.-S. Wu, X. Feng and K. Müllen, Mesoporous Metal–Nitrogen-Doped Carbon Electrocatalysts for Highly Efficient Oxygen Reduction Reaction, *J. Am. Chem. Soc.*, 2013, **135**, 16002–16005.

175 Y. H. Qian, I. A. Khan and D. Zhao, Electrocatalysts Derived from Metal-Organic Frameworks for Oxygen Reduction and Evolution Reactions in Aqueous Media, *Small*, 2017, **13**, 1701143.

176 W. Xia, A. Mahmood, R. Q. Zou and Q. Xu, Metal-organic frameworks and their derived nanostructures for electrochemical energy storage and conversion, *Energy Environ. Sci.*, 2015, **8**, 1837–1866.

177 Y. Y. Liang, Y. G. Li, H. L. Wang, J. G. Zhou, J. Wang, T. Regier and H. J. Dai, Co_3O_4 nanocrystals on graphene as a synergistic catalyst for oxygen reduction reaction, *Nat. Mater.*, 2011, **10**, 780–786.

178 S. F. Wu, M. C. Li, H. Phan, D. G. Wang, T. S. Herng, J. Ding, Z. G. Lu and J. S. Wu, Toward Two-Dimensional Pi-Conjugated Covalent Organic Radical Frameworks, *Angew. Chem., Int. Ed.*, 2018, **57**, 8007–8011.

179 K. Iwase, K. Kamiya, M. Miyayama, K. Hashimoto and S. Nakanishi, Sulfur-Linked Covalent Triazine Frameworks Doped with Coordinatively Unsaturated Cu(I) as Electrocatalysts for Oxygen Reduction, *ChemElectroChem*, 2018, **5**, 805–810.

180 C. Krishnaraj, H. Sekhar Jena, L. Bourda, A. Laemont, P. Pachfule, J. Roeser, C. V. Chandran, S. Borgmans, S. M. J. Rogge, K. Leus, C. V. Stevens, J. A. Martens, V. Van Speybroeck, E. Breynaert, A. Thomas and P. Van Der Voort, Strongly Reducing (Diarylamino)benzene-Based Covalent Organic Framework for Metal-Free Visible Light Photocatalytic H_2O_2 Generation, *J. Am. Chem. Soc.*, 2020, **142**, 20107–20116.

181 Y. M. Zhao, G. Q. Yu, F. F. Wang, P. J. Wei and J. G. Liu, Bioinspired Transition-Metal Complexes as Electrocatalysts for the Oxygen Reduction Reaction, *Chem. – Eur. J.*, 2019, **25**, 3726–3739.

182 Q. Li, W. Chen, H. Xiao, Y. Gong, Z. Li, L. Zheng, X. Zheng, W. Yan, W. C. Cheong, R. Shen, N. Fu, L. Gu, Z. Zhuang, C. Chen, D. Wang, Q. Peng, J. Li and Y. Li, Fe Isolated Single Atoms on S, N Co doped Carbon by Copolymer Pyrolysis Strategy for Highly Efficient Oxygen Reduction Reaction, *Adv. Mater.*, 2018, e1800588.

183 Q. Zuo, G. Z. Cheng and W. Luo, A reduced graphene oxide/covalent cobalt porphyrin framework for efficient oxygen reduction reaction, *Dalton Trans.*, 2017, **46**, 9344–9348.

184 X. H. Fan, F. T. Kong, A. G. Kong, A. L. Chen, Z. Q. Zhou and Y. K. Shan, Covalent Porphyrin Framework-Derived Fe_2P@Fe_4N-Coupled Nanoparticles Embedded in N-Doped Carbons as Efficient Trifunctional Electrocatalysts, *ACS Appl. Mater. Interfaces*, 2017, **9**, 32840–32850.

185 D. K. Wu, Q. Xu, J. Qian, X. P. Li and Y. H. Sun, Bimetallic Covalent Organic Frameworks for Constructing Multifunctional Electrocatalyst, *Chem. – Eur. J.*, 2019, **25**, 3105–3111.

186 F. T. Kong, X. H. Fan, A. G. Kong, Z. Q. Zhou, X. Y. Zhang and Y. K. Shan, Covalent Phenanthroline Framework Derived FeS@Fe_3C Composite Nanoparticles Embedding in N-S-Co doped Carbons as Highly Efficient Trifunctional Electrocatalysts, *Adv. Funct. Mater.*, 2018, **28**, 1803973.

187 J. N. Guo, T. T. Li, Q. L. Wang, N. Y. Zhang, Y. H. Cheng and Z. H. Xiang, Superior oxygen electrocatalysts derived from predesigned covalent organic polymers for zinc-air flow batteries, *Nanoscale*, 2019, **11**, 211–218.

188 X. Y. Cai, L. F. Lai, J. Y. Lin and Z. X. Shen, Recent advances in air electrodes for Zn-air batteries: electrocatalysis and structural design, *Mater. Horiz.*, 2017, **4**, 945–976.

189 Z. L. Wang, D. Xu, J. J. Xu and X. B. Zhang, Oxygen electrocatalysts in metal-air batteries: from aqueous to nonaqueous electrolytes, *Chem. Soc. Rev.*, 2014, **43**, 7746–7786.

190 B. Q. Li, S. Y. Zhang, X. Chen, C. Y. Chen, Z. J. Xia and Q. Zhang, One-Pot Synthesis of Framework Porphyrin Materials and Their Applications in Bifunctional Oxygen Electrocatalysis, *Adv. Funct. Mater.*, 2019, **29**, 1901301.

191 N. S. Spinner, J. A. Vega and W. E. Mustain, Recent progress in the electrochemical conversion and utilization of CO_2, *Catal. Sci. Technol.*, 2012, **2**, 19–28.

192 J. L. Qiao, Y. Y. Liu, F. Hong and J. J. Zhang, A review of catalysts for the electroreduction of carbon dioxide to produce low-carbon fuels, *Chem. Soc. Rev.*, 2014, **43**, 631–675.

193 E. V. Kondratenko, G. Mul, J. Baltrusaitis, G. O. Larrazabal and J. Perez-Ramirez, Status and perspectives of CO_2 conversion into fuels and chemicals by catalytic, photocatalytic and electrocatalytic processes, *Energy Environ. Sci.*, 2013, **6**, 3112–3135.

194 A. Loiudice, P. Lobaccaro, E. A. Kamali, T. Thao, B. H. Huang, J. W. Ager and R. Buonsanti, Tailoring Copper Nanocrystals towards C-2 Products in Electrochemical CO_2 Reduction, *Angew. Chem., Int. Ed.*, 2016, **55**, 5789–5792.

195 Q. Tang, Y. J. Lee, D. Y. Li, W. Choi, C. W. Liu, D. Lee and D. E. Jiang, Lattice-Hydride Mechanism in Electrocatalytic CO_2 Reduction by Structurally Precise Copper-Hydride Nanoclusters, *J. Am. Chem. Soc.*, 2017, **139**, 9728–9736.

196 Z.-L. Wang, C. Li and Y. Yamauchi, Nanostructured nonprecious metal catalysts for electrochemical reduction of carbon dioxide, *Nano Today*, 2016, **11**, 373–391.

197 T. Möller, W. Ju, A. Bagger, X. Wang, F. Luo, T. Ngo Thanh, A. S. Varela, J. Rossmeisl and P. Strasser, Efficient CO_2 to CO electrolysis on solid Ni–N–C catalysts at industrial current densities, *Energy Environ. Sci.*, 2019, **12**, 640–647.

198 Y. H. Chen, C. W. Li and M. W. Kanan, Aqueous CO_2 Reduction at Very Low Overpotential on Oxide-Derived Au Nanoparticles, *J. Am. Chem. Soc.*, 2012, **134**, 19969–19972.

199 C. W. Li and M. W. Kanan, CO_2 Reduction at Low Overpotential on Cu Electrodes Resulting from the Reduction of Thick Cu_2O Films, *J. Am. Chem. Soc.*, 2012, **134**, 7231–7234.

200 P. L. Cheung, S. K. Lee and C. P. Kubiak, Facile Solvent-Free Synthesis of Thin Iron Porphyrin COFs on Carbon Cloth Electrodes for CO_2 Reduction, *Chem. Mater.*, 2019, **31**, 1908–1919.

201 C. L. Yao, J. C. Li, W. Gao and Q. Jiang, An Integrated Design with new Metal-Functionalized Covalent Organic Frameworks for the Effective Electroreduction of CO_2, *Chem. – Eur. J.*, 2018, **24**, 11051–11058.

202 Y. S. Wang, J. X. Chen, G. X. Wang, Y. Li and Z. H. Wen, Perfluorinated Covalent Triazine Framework Derived Hybrids for the Highly Selective Electroconversion of Carbon Dioxide into Methane, *Angew. Chem., Int. Ed.*, 2018, **57**, 13120–13124.

203 C. B. Lu, J. Yang, S. Wei, S. Bi, Y. Xia, M. X. Chen, Y. Hou, M. Qiu, C. Yuan, Y. Z. Su, F. Zhang, H. W. Liang and X. D. Zhuang, Atomic Ni Anchored Covalent Triazine Framework as High Efficient Electrocatalyst for Carbon Dioxide Conversion, *Adv. Funct. Mater.*, 2019, **29**, 1806884.

204 P. P. Su, K. Iwase, T. Harada, K. Kamiya and S. Nakanishi, Covalent triazine framework modified with coordinatively-unsaturated Co or Ni atoms for CO_2 electrochemical reduction, *Chem. Sci.*, 2018, **9**, 3941–3947.

205 C. Merlet, B. Rotenberg, P. A. Madden, P. L. Taberna, P. Simon, Y. Gogotsi and M. Salanne, On the molecular origin of supercapacitance in nanoporous carbon electrodes, *Nat. Mater.*, 2012, **11**, 306–310.

206 I. E. Rauda, V. Augustyn, B. Dunn and S. H. Tolbert, Enhancing Pseudocapacitive Charge Storage in Polymer Templated Mesoporous Materials, *Acc. Chem. Res.*, 2013, **46**, 1113–1124.

207 L. F. Chen, X. D. Zhang, H. W. Liang, M. G. Kong, Q. F. Guan, P. Chen, Z. Y. Wu and S. H. Yu, Synthesis of nitrogen-doped porous carbon nanofibers as an efficient electrode materials for supercapacitors, *ACS Nano*, 2012, **6**, 7092–7102.

208 L. Qie, W. Chen, H. Xu, X. Xiong, Y. Jiang, F. Zou, X. Hu, Y. Xin, Z. Zhang and Y. Huang, Synthesis of functionalized 3D hierarchical porous carbon for high-performance supercapacitors, *Energy Environ. Sci.*, 2013, **6**, 2497–2504.

209 S. L. Zhang and N. Pan, Supercapacitors Performance Evaluation, *Adv. Energy Mater.*, 2015, **5**, 1401401.

210 R. Xue, H. Guo, L. G. Yue, T. Wang, M. Y. Wang, Q. Li, H. Liu and W. Yang, Preparation and energy storage application of a long-life and high rate performance pseudocapacitive COF material linked with -NH- bonds, *New J. Chem.*, 2018, **42**, 13726–13731.

211 S. Liu, L. Yao, Y. Lu, X. L. Hua, J. Q. Liu, Z. Yang, H. Wei and Y. Y. Mai, All-organic covalent organic framework/polyaniline composites as stable electrode for high-performance supercapacitors, *Mater. Lett.*, 2019, **236**, 354–357.

212 F. Xu, H. Xu, X. Chen, D. C. Wu, Y. Wu, H. Liu, C. Gu, R. W. Fu and D. L. Jiang, Radical Covalent Organic Frameworks: A General Strategy to Immobilize Open-Accessible Polyradicals for High-Performance Capacitive Energy Storage, *Angew. Chem., Int. Ed.*, 2015, **54**, 6814–6818.

213 P. Bhanja, K. Bhunia, S. K. Das, D. Pradhan, R. Kimura, Y. Hijikata, S. Irle and A. Bhaumik, New Triazine-Based Covalent Organic Framework for High-Performance Capacitive Energy Storage, *ChemSusChem*, 2017, **10**, 921–929.

214 S. B. Alahakoon, C. M. Thompson, G. Occhialini and R. A. Smaldone, Design Principles for Covalent Organic Frameworks in Energy Storage Applications, *ChemSusChem*, 2017, **10**, 2116–2129.

215 S. Feng, H. Xu, C. Zhang, Y. Chen, J. H. Zeng, D. L. Jiang and J. X. Jiang, Bicarbazole-based redox-active covalent organic frameworks for ultrahigh-performance energy storage, *Chem. Commun.*, 2017, **53**, 11334–11337.

216 M. Y. Wang, H. Guo, R. Xue, Q. Li, H. Liu, N. Wu, W. Q. Yao and W. Yang, Covalent Organic Frameworks: A New Class of Porous Organic Frameworks for Supercapacitor Electrodes, *ChemElectroChem*, 2019, **6**, 2984–2997.

217 A. M. Khattak, Z. A. Ghazi, B. Liang, N. A. Khan, A. Iqbal, L. S. Li and Z. Y. Tang, A redox-active 2D covalent organic framework with pyridine moieties capable of faradaic energy storage, *J. Mater. Chem. A*, 2016, **4**, 16312–16317.

218 S. Chandra, D. R. Chowdhury, M. Addicoat, T. Heine, A. Paul and R. Banerjee, Molecular Level Control of the Capacitance of Two-Dimensional Covalent Organic Frameworks: Role of Hydrogen Bonding in Energy Storage Materials, *Chem. Mater.*, 2017, **29**, 2074–2080.

219 C. R. DeBlase, K. Hernandez-Burgos, K. E. Silberstein, G. G. Rodriguez-Calero, R. P. Bisbey, H. D. Abruna and W. R. Dichtel, Rapid and Efficient Redox Processes within 2D Covalent Organic Framework Thin Films, *ACS Nano*, 2015, **9**, 3178–3183.

220 P. Y. Wang, Q. Wu, L. F. Han, S. Wang, S. M. Fang, Z. H. Zhang and S. M. Sun, Synthesis of conjugated covalent organic frameworks/graphene composite for supercapacitor electrodes, *RSC Adv.*, 2015, **5**, 27290–27294.

221 Z. Q. Zha, L. R. Xu, Z. K. Wang, X. G. Li, Q. M. Pan, P. G. Hu and S. B. Lei, 3D Graphene Functionalized by Covalent Organic Framework Thin Film as Capacitive Electrode in Alkaline Media, *ACS Appl. Mater. Interfaces*, 2015, **7**, 17837–17843.

222 B. Sun, J. Liu, A. M. Cao, W. G. Song and D. Wang, Interfacial synthesis of ordered and stable covalent organic frameworks on amino-functionalized carbon nanotubes with enhanced electrochemical performance, *Chem. Commun.*, 2017, **53**, 6303–6306.

223 J. S. Xu, Y. F. He, S. Bi, M. Wang, P. Yang, D. Q. Wu, J. J. Wang and F. Zhang, An Olefin-Linked Covalent Organic Framework as a Flexible Thin-Film Electrode for

a High-Performance Micro-Supercapacitor, *Angew. Chem., Int. Ed.*, 2019, **58**, 12065–12069.

224 G. Kim, J. Yang, N. Nakashima and T. Shiraki, Highly Microporous Nitrogen-doped Carbon Synthesized from Azine-linked Covalent Organic Framework and its Supercapacitor Function, *Chem. – Eur. J.*, 2017, **23**, 17504–17510.

225 J. Romero, D. Rodriguez-San-Miguel, A. Ribera, R. Mas-Balleste, T. F. Otero, I. Manet, F. Liscio, G. Abellan, F. Zamora and E. Coronado, Metal-functionalized covalent organic frameworks as precursors of super capacitive porous N-doped graphene, *J. Mater. Chem. A*, 2017, **5**, 4343–4351.

226 H. M. Li, J. H. Li, A. Thomas and Y. Z. Liao, Ultra-High Surface Area Nitrogen-Doped Carbon Aerogels Derived From a Schiff-Base Porous Organic Polymer Aerogel for CO_2 Storage and Supercapacitors, *Adv. Funct. Mater.*, 2019, **29**, 1904785.

227 Y. Z. Liao, H. G. Wang, M. F. Zhu and A. Thomas, Efficient Supercapacitor Energy Storage Using Conjugated Microporous Polymer Networks Synthesized from Buchwald-Hartwig Coupling, *Adv. Mater.*, 2018, **30**, 1705710.

228 Y. B. Huang, P. Pachfule, J. K. Sun and Q. Xu, From covalent-organic frameworks to hierarchically porous B-doped carbons: a molten-salt approach, *J. Mater. Chem. A*, 2016, **4**, 4273–4279.

229 D. J. Kim, J. W. Yoon, C. S. Lee, Y. S. Bae and J. H. Kim, Covalent organic framework-derived microporous carbon nanoparticles coated with conducting polypyrrole as an electrochemical capacitor, *Appl. Surf. Sci.*, 2018, **439**, 833–838.

230 M. Armand, S. Grugeon, H. Vezin, S. Laruelle, P. Ribiere, P. Poizot and J. M. Tarascon, Conjugated dicarboxylate anodes for Li-ion batteries, *Nat. Mater.*, 2009, **8**, 120–125.

231 P. Simon, Y. Gogotsi and B. Dunn, Where Do Batteries End and Supercapacitors Begin?, *Science*, 2014, **343**, 1210–1211.

232 M. N. Obrovac and V. L. Chevrier, Alloy Negative Electrodes for Li-Ion Batteries, *Chem. Rev.*, 2014, **114**, 11444–11502.

233 H. J. Lin, W. Weng, J. Ren, L. B. Qiu, Z. T. Zhang, P. N. Chen, X. L. Chen, J. Deng, Y. G. Wang and H. S. Peng, Twisted Aligned Carbon Nanotube/Silicon Composite Fiber Anode for Flexible Wire-Shaped Lithium-Ion Battery, *Adv. Mater.*, 2014, **26**, 1217–1222.

234 N. Mahmood, T. Y. Tang and Y. L. Hou, Nanostructured Anode Materials for Lithium Ion Batteries: Progress, Challenge and Perspective, *Adv. Energy Mater.*, 2016, **6**, 1600374.

235 K. H. Park, D. Lee, J. Kim, J. Song, Y. M. Lee, H. T. Kim and J. K. Park, Defect-Free, Size-Tunable Graphene for High-Performance Lithium Ion Battery, *Nano Lett.*, 2014, **14**, 4306–4313.

236 X. H. Cao, B. Zheng, X. H. Rui, W. H. Shi, Q. Y. Yan and H. Zhang, Metal Oxide-Coated Three-Dimensional Graphene Prepared by the Use of Metal-Organic Frameworks as Precursors, *Angew. Chem., Int. Ed.*, 2014, **53**, 1404–1409.

237 Y. H. Hu and X. L. Sun, Flexible rechargeable lithium ion batteries: advances and challenges in materials and process technologies, *J. Mater. Chem. A*, 2014, **2**, 10712–10738.

238 M. N. Obrovac, L. Christensen, D. B. Le and J. R. Dahn, Alloy Design for Lithium-Ion Battery Anodes, *J. Electrochem. Soc.*, 2007, **154**, A849.

239 Y. F. Wang and L. J. Zhang, Simple synthesis of CoO-NiO-C anode materials for lithium-ion batteries and investigation on its electrochemical performance, *J. Power Sources*, 2012, **209**, 20–29.

240 S. Zhu, J. Li, X. Deng, C. He, E. Liu, F. He, C. Shi and N. Zhao, Ultrathin-Nanosheet-Induced Synthesis of 3D Transition Metal Oxides Networks for Lithium Ion Battery Anodes, *Adv. Funct. Mater.*, 2017, **27**, 1605017.

241 M. Zheng, H. Tang, L. Li, Q. Hu, L. Zhang, H. Xue and H. Pang, Hierarchically Nanostructured Transition Metal Oxides for Lithium-Ion Batteries, *Adv. Sci.*, 2018, **5**, 1700592.

242 J. S. Bridel, T. Azais, M. Morcrette, J. M. Tarascon and D. Larcher, Key Parameters Governing the Reversibility of Si/Carbon/CMC Electrodes for Li-Ion Batteries, *Chem. Mater.*, 2010, **22**, 1229–1241.

243 X. Zuo, J. Zhu, P. Müller-Buschbaum and Y.-J. Cheng, Silicon based lithium-ion battery anodes: A chronicle perspective review, *Nano Energy*, 2017, **31**, 113–143.

244 L. Huang and G. Cao, 2D Squaraine-Linked Polymers with High Lithium Storage Capacity Using the First Principle Methods, *ChemistrySelect*, 2017, **2**, 1728–1733.

245 L. Y. Bai, Q. Gao and Y. L. Zhao, Two fully conjugated covalent organic frameworks as anode materials for lithium ion batteries, *J. Mater. Chem. A*, 2016, **4**, 14106–14110.

246 H. Yang, S. L. Zhang, L. H. Han, Z. Zhang, Z. Xue, J. Gao, Y. J. Li, C. S. Huang, Y. P. Yi, H. B. Liu and Y. L. Li, High Conductive Two-Dimensional Covalent Organic Framework for Lithium Storage with Large Capacity, *ACS Appl. Mater. Interfaces*, 2016, **8**, 5366–5375.

247 Y. Yang, G. Y. Zheng and Y. Cui, Nanostructured sulfur cathodes, *Chem. Soc. Rev.*, 2013, **42**, 3018–3032.

248 A. Manthiram, Y. Z. Fu and Y. S. Su, Challenges and Prospects of Lithium-Sulfur Batteries, *Acc. Chem. Res.*, 2013, **46**, 1125–1134.

249 F. Xu, S. H. Yang, G. S. Jiang, Q. Ye, B. Q. Wei and H. Q. Wang, Fluorinated, Sulfur-Rich, Covalent Triazine Frameworks for Enhanced Confinement of Polysulfides in Lithium-Sulfur Batteries, *ACS Appl. Mater. Interfaces*, 2017, **9**, 37731–37738.

250 X. H. Hu, J. H. Jian, Z. S. Fang, L. F. Zhong, Z. K. Yuan, M. J. Yang, S. J. Ren, Q. Zhang, X. D. Chen and D. S. Yu, Hierarchical assemblies of conjugated ultrathin COF nanosheets for high-sulfur-loading and long-lifespan lithium-sulfur batteries: Fully-exposed porphyrin matters, *Energy Storage Mater.*, 2019, **22**, 40–47.

251 J. Y. Wang, L. P. Si, Q. Wei, X. J. Hong, S. L. Cai and Y. P. Cai, Covalent Organic Frameworks as the Coating Layer of Ceramic Separator for High-Efficiency Lithium–Sulfur Batteries, *ACS Appl. Nano Mater.*, 2018, **1**, 132–138.

252 H. P. Liao, H. M. Wang, H. M. Ding, X. S. Meng, H. Xu, B. S. Wang, X. P. Ai and C. Wang, A 2D porous porphyrin-

based covalent organic framework for sulfur storage in lithium sulfur batteries, *J. Mater. Chem. A*, 2016, **4**, 7416–7421.

253 Q. Jiang, Y. S. Li, X. X. Zhao, P. X. Xiong, X. Yu, Y. H. Xu and L. Chen, Inverse-vulcanization of vinyl functionalized covalent organic frameworks as efficient cathode materials for Li-S batteries, *J. Mater. Chem. A*, 2018, **6**, 17977–17981.

254 F. Xu, S. H. Yang, X. Chen, Q. H. Liu, H. J. Li, H. Q. Wang, B. Q. Wei and D. L. Jiang, Energy-storage covalent organic frameworks: improving performance *via* engineering polysulfide chains on walls, *Chem. Sci.*, 2019, **10**, 6001–6006.

255 B. Q. Li, S. Y. Zhang, L. Kong, H. J. Peng and Q. Zhang, Porphyrin Organic Framework Hollow Spheres and Their Applications in Lithium-Sulfur Batteries, *Adv. Mater.*, 2018, **30**, 1707483.

256 K. Kataoka, H. Nagata and J. Akimoto, Lithium-ion conducting oxide single crystal as solid electrolyte for advanced lithium battery application, *Sci. Rep.*, 2018, **8**, 9965.

257 Y. Du, H. S. Yang, J. M. Whiteley, S. Wan, Y. H. Jin, S. H. Lee and W. Zhang, Ionic Covalent Organic Frameworks with Spiroborate Linkage, *Angew. Chem., Int. Ed.*, 2016, **55**, 1737–1741.

258 Q. Xu, S. S. Tao, Q. H. Jiang and D. L. Jiang, Ion Conduction in Polyelectrolyte Covalent Organic Frameworks, *J. Am. Chem. Soc.*, 2018, **140**, 7429–7432.

259 B. C. Patra, S. K. Das, A. Ghosh, K. A. Raj, P. Moitra, M. Addicoat, S. Mitra, A. Bhaumik, S. Bhattacharya and A. Pradhan, Covalent organic framework based microspheres as an anode material for rechargeable sodium batteries, *J. Mater. Chem. A*, 2018, **6**, 16655–16663.

260 S. J. Peighambardoust, S. Rowshanzamir and M. Amjadi, Review of the proton exchange membranes for fuel cell applications, *Int. J. Hydrogen Energy*, 2010, **35**, 9349–9384.

261 M. Casciola, G. Alberti, M. Sganappa and R. Narducci, On the decay of Nafion proton conductivity at high temperature and relative humidity, *J. Power Sources*, 2006, **162**, 141–145.

262 S. J. Paddison and J. A. Elliott, Molecular Modeling of the short-side-chain perfluorosulfonic acid membrane, *J. Phys. Chem. A*, 2005, **109**, 7583–7593.

263 M. M. Guo, B. J. Liu, Z. Liu, L. F. Wang and Z. H. Jiang, Novel acid-base molecule-enhanced blends/copolymers for fuel cell applications, *J. Power Sources*, 2009, **189**, 894–901.

264 E. A. Tsui and M. R. Wiesner, Fast proton-conducting ceramic membranes derived from ferroxane nanoparticle-precursors as fuel cell electrolytes, *J. Membr. Sci.*, 2008, **318**, 79–83.

265 R. K. Nagarale, W. Shin and P. K. Singh, Progress in ionic organic-inorganic composite membranes for fuel cell applications, *Polym. Chem.*, 2010, **1**, 388–408.

266 C. Montoro, D. Rodriguez-San-Miguel, E. Polo, R. Escudero-Cid, M. L. Ruiz-Gonzalez, J. A. R. Navarro, P. Ocon and F. Zamora, Ionic Conductivity and Potential Application for Fuel Cell of a Modified Imine-Based Covalent Organic Framework, *J. Am. Chem. Soc.*, 2017, **139**, 10079–10086.

267 S. Chandra, T. Kundu, S. Kandambeth, R. BabaRao, Y. Marathe, S. M. Kunjir and R. Banerjee, Phosphoric Acid Loaded Azo (–N=N–) Based Covalent Organic Framework for Proton Conduction, *J. Am. Chem. Soc.*, 2014, **136**, 6570–6573.

268 D. B. Shinde, H. B. Aiyappa, M. Bhadra, B. P. Biswal, P. Wadge, S. Kandambeth, B. Garai, T. Kundu, S. Kurungot and R. Banerjee, A mechanochemically synthesized covalent organic framework as a proton-conducting solid electrolyte, *J. Mater. Chem. A*, 2016, **4**, 2682–2690.

269 S. Kandambeth, K. Dey and R. Banerjee, Covalent Organic Frameworks: Chemistry beyond the Structure, *J. Am. Chem. Soc.*, 2018, **141**, 1807–1822.

270 S. Chen, B. Yuan, G. Liu and D. Zhang, Electrochemical Sensors Based on Covalent Organic Frameworks: A Critical Review, *Front. Chem.*, 2020, **8**, 601044.

271 R. Wen, Y. Li, M. Zhang, X. Guo, X. Li, X. Li, J. Han, S. Hu, W. Tan, L. Ma and S. Li, Graphene-synergized 2D covalent organic framework for adsorption: A mutual promotion strategy to achieve stabilization and functionalization simultaneously, *J. Hazard. Mater.*, 2018, **358**, 273–285.

272 L. Chen, Q. Wu, J. Gao, H. Li, S. Dong, X. Shi and L. Zhao, Applications of covalent organic frameworks in analytical chemistry, *Trends Anal. Chem.*, 2019, **113**, 182–193.

273 C. Liang, H. Lin, Q. Wang, E. Shi, S. Zhou, F. Zhang, F. Qu and G. Zhu, A redox-active covalent organic framework for the efficient detection and removal of hydrazine, *J. Hazard. Mater.*, 2020, **381**, 120983.

274 C. Karuppiah, S. Palanisamy, S.-M. Chen, S. K. Ramaraj and P. Periakaruppan, A novel and sensitive amperometric hydrazine sensor based on gold nanoparticles decorated graphite nanosheets modified screen printed carbon electrode, *Electrochim. Acta*, 2014, **139**, 157–164.

275 X. Zhang, Y. Wang, X. Ning, L. Li, J. Chen, D. Shan, R. Gao and X. Lu, Three-dimensional porous self-assembled chestnut-like nickel-cobalt oxide structure as an electrochemical sensor for sensitive detection of hydrazine in water samples, *Anal. Chim. Acta*, 2018, **1022**, 28–36.

276 J. Wu, T. Zhou, Q. Wang and A. Umar, Morphology and chemical composition dependent synthesis and electrochemical properties of MnO_2-based nanostructures for efficient hydrazine detection, *Sens. Actuators, B*, 2016, **224**, 878–884.

277 T. Zhang, C. Gao, W. Huang, Y. Chen, Y. Wang and J. Wang, Covalent organic framework as a novel electrochemical platform for highly sensitive and stable detection of lead, *Talanta*, 2018, **188**, 578–583.

278 Q. Wang, R. Li, Y. Zhao, T. Zhe, T. Bu, Y. Liu, X. Sun, H. Hu, M. Zhang, X. Zheng and L. Wang, Surface morphology-controllable magnetic covalent organic frameworks: A novel electrocatalyst for simultaneously high-performance detection of p-nitrophenol and o-nitrophenol, *Talanta*, 2020, **219**, 121255.

279 Y.-H. Pang, Y.-Y. Huang, L. Wang, X.-F. Shen and Y.-Y. Wang, Determination of bisphenol A and bisphenol S by a covalent organic framework electrochemical sensor, *Environ. Pollut.*, 2020, **263**, 114616.

280 Z. Lu, Z. Shi, S. Huang, R. Zhang, G. Li and Y. Hu, Covalent organic framework derived Fe_3O_4/N co-doped hollow carbon nanospheres modified electrode for simultaneous

determination of biomolecules in human serum, *Talanta*, 2020, **214**, 120864.

281 Y. Yang, Y. Shen, L. Wang, Y. Song and L. Wang, Three-dimensional porous carbon/covalent-organic framework films integrated electrode for electrochemical sensors, *J. Electroanal. Chem.*, 2019, **855**, 113590.

282 M. Xu, L. Wang, Y. Xie, Y. Song and L. Wang, Ratiometric electrochemical sensing and biosensing based on multiple redox-active state COFDHTA-TTA, *Sens. Actuators, B*, 2019, **281**, 1009–1015.

283 L. Y. Wang, Y. Xie, Y. X. Yang, H. H. Liang, L. Wang and Y. H. Song, Electroactive covalent organic frameworks/carbon nanotubes composites for electrochemical sensing, *ACS Appl. Nano Mater.*, 2020, **3**, 1412–1419.

284 H. Liang, H. Xu, Y. Zhao, J. Zheng, H. Zhao, G. Li and C.-P. Li, Ultrasensitive electrochemical sensor for prostate specific antigen detection with a phosphorene platform and magnetic covalent organic framework signal amplifier, *Biosens. Bioelectron.*, 2019, **144**, 111691.

285 R. Ahmad, N. Tripathy, Y. B. Hahn, A. Umar, A. Ibrahim and S. H. Kim, A robust enzymeless glucose sensor based on CuO nanoseed modified electrodes, *Dalton Trans.*, 2015, **44**, 12488–12492.

286 M. Y. Liu, L. P. Guo, S. B. Jin and B. E. Tian, Covalent triazine frameworks: synthesis and applications, *J. Mater. Chem. A*, 2019, **7**, 5153–5172.

287 R. Palkovits, M. Antonietti, P. Kuhn, A. Thomas and F. Schuth, Solid catalysts for the selective low-temperature oxidation of methane to methanol, *Angew. Chem., Int. Ed.*, 2009, **48**, 6909–6912.

288 F. J. Uribe-Romo, J. R. Hunt, H. Furukawa, C. Klock, M. O'Keeffe and O. M. Yaghi, A crystalline imine-linked 3-D porous covalent organic framework, *J. Am. Chem. Soc.*, 2009, **131**, 4570–4571.

289 S. Dalapati, S. Jin, J. Gao, Y. Xu, A. Nagai and D. Jiang, An Azine-Linked Covalent Organic Framework, *J. Am. Chem. Soc.*, 2013, **135**, 17310–17313.

290 F. J. Uribe-Romo, C. J. Doonan, H. Furukawa, K. Oisaki and O. M. Yaghi, Crystalline covalent organic frameworks with hydrazone linkages, *J. Am. Chem. Soc.*, 2011, **133**, 11478–11481.

291 F. Haase and B. V. Lotsch, Solving the COF trilemma: towards crystalline, stable and functional covalent organic frameworks, *Chem. Soc. Rev.*, 2020, **49**, 8469–8500.

292 R. van der Jagt, A. Vasileiadis, H. Veldhuizen, P. Shao, X. Feng, S. Ganapathy, N. C. Habisreutinger, M. A. van der Veen, C. Wang, M. Wagemaker, S. van der Zwaag and A. Nagai, Synthesis and Structure-Property Relationships of Polyimide Covalent Organic Frameworks for Carbon Dioxide Capture and (Aqueous) Sodium-Ion Batteries, *Chem. Mater.*, 2021, **33**, 818–833.

293 R. W. Tilford, W. R. Gemmill, H.-C. zur Loye and J. J. Lavigne, Facile Synthesis of a Highly Crystalline, Covalently Linked Porous Boronate Network, *Chem. Mater.*, 2006, **18**, 5296–5301.

294 E. Jin, M. Asada, Q. Xu, S. Dalapati, M. A. Addicoat, M. A. Brady, H. Xu, T. Nakamura, T. Heine, Q. H. Chen and D. L. Jiang, Two-dimensional sp2 carbon-conjugated covalent organic frameworks, *Science*, 2017, **357**, 637–676.

295 J. S. Xu, Y. F. He, S. Bi, M. Wang, P. Yang, D. Q. Wu, J. J. Wang and F. Zhang, An olefin-linked covalent organic framework as a flexible thin-film electrode for a high-performance micro-supercapacitor, *Angew. Chem., Int. Ed.*, 2019, **58**, 12065–12069.

296 A. Acharjya, P. Pachfule, J. Roeser, F. J. Schmitt and A. Thomas, Vinylene-Linked Covalent Organic Frameworks by Base-Catalyzed Aldol Condensation, *Angew. Chem., Int. Ed.*, 2019, **58**, 14865–14870.

297 X. Guan, H. Li, Y. Ma, M. Xue, Q. Fang, Y. Yan, V. Valtchev and S. Qiu, Chemically stable polyarylether-based covalent organic frameworks, *Nat. Chem.*, 2019, **11**, 587–594.

298 W. Zheng, M. Liu and L. Y. S. Lee, Electrochemical Instability of Metal–Organic Frameworks: In Situ Spectroelectrochemical Investigation of the Real Active Sites, *ACS Catal.*, 2019, **10**, 81–92.

299 M. Gocyla, S. Kuehl, M. Shviro, H. Heyen, S. Selve, R. E. Dunin-Borkowski, M. Heggen and P. Strasser, Shape Stability of Octahedral PtNi Nanocatalysts for Electrochemical Oxygen Reduction Reaction Studied by in situ Transmission Electron Microscopy, *ACS Nano*, 2018, **12**, 5306–5311.